The identification and delineation of high-yielding wellfield areas in Karoo Aquifers as future water supply options to local authorities

By

Kathleen Victoria Baker

THESIS

Submitted in fulfilment of the requirement for the degree of

Master of Science

Faculty of Natural and Agricultural Science

Institute for Groundwater Studies, Bloemfontein

University of the Free State

2011

Supervisor:

Dr S.R Dennis

Acknowledgements

I would like to thank the following:

- Dr R. Murray for his advice, assistance and contribution throughout the period of study
- Dr R. Dennis, for his work on developing the Wellfield model
- The Council for Geoscience, Bellville, for their role in this project and in particular Dr L. Chevallier and Dr C. Musekiwa for their work on the Geology chapter and Transmissivity chapter
- Prof G van Tonder for his input during the period of study
- Mr A. Woodford and Mr P. Ravenscroft for their work on the Aquifer Assured Yield Model
- Dr S. Adams of the Water Research Commission for his support to the project
- Members of the WRC Project K1763 Reference Group who provided input on the Aquifer Assured Yield Model, and in particular Dr M Basson and Dr J du Plessis
- Mr M. Damhuis and Miss K. Robey for their comments and proof-reading of the script
- The Alfred Nzo District Municipality where the cases studies on Matatiele and Makhoba where undertaken.

Abstract

This Masters thesis forms the capacity development component of the Water Research Commission (WRC) project number K5/1763, entitled "The identification and delineation of high-yielding well-field areas in Karoo aquifers as future water supply options to local authorities". The project was initiated due to the need to place the significant knowledge on groundwater of the Karoo Basin within the realms of water resource planning. The ever growing issues related to water resource planning include not only the challenge of finding groundwater resources, but quantifying the supply of this resource in terms that are readily understood by hydrogeologists and related professions.

In an attempt to address these issues, a method by which groundwater resources can be identified as well as quantified is described in this thesis, which incorporates the concept of assurance of supply. This method involves the use of a number of tools, some of which are existing and are readily available to the public, others may be available in the specific area of interest (e.g. aeromagnetic imagery), and the remaining have been developed as part of the WRC project, and critically reviewed in this thesis.

The development of the Transmissivity Map in this thesis took both existing borehole yields and geology into account, and provides a range of possible transmissivity values presented both in tables and maps. The ranges are provided for each hydrogeological domain (based on lithologies and in some cases, sub-divided lithologies), dolerite dykes and sills, fractured margins of sills and areas of thick alluvium. Woodford's method was used, which can be found in Dondo *et al.*, 2010, which was then extrapolated across the Main Karoo Basin. This map is the most detailed map produced of the Main Karoo Basin and from the case studies presented appears to provide a reasonable estimate of transmissivity values.

The Aquifer Assured Yield Model (AAYM) was run for a large number of quaternary catchments spread across the Karoo Basin to test the model's credibility, as well as to propose parameter values to be used per region or drainage basin. The AAYM compared well with other databases, namely the HP and GRAII AGEP. The work appears to be the first

documented approach to quantifying groundwater with levels of assurance, and thus should be considered "work-in-progress", as is it requires an iterative process of development, testing, modifying and re-testing.

The Wellfield Model was successfully developed on the basis of the Cooper-Jacob equation (Cooper & Jacob, 1946). Through the testing of the model, relationships of borehole spacing with transmissivity values were investigated in an attempt to provide a guideline on the design of a wellfield with certain borehole interference limitations. In addition to this, the distinct nature of groundwater flow in dykes was considered by referring to the Boonstra-Boehmer equation (Kruseman & de Ridder, 1992) whereby a certain increase in borehole spacing is required when a borehole is sited on a dyke. This model enables the designing and manipulation of a wellfield and the effect of groundwater abstraction on drawdown can be evaluated thereby aiding in the most optimum design.

The methodology applied to case studies demonstrates the practical application of these tools and models described above. The purpose of the case studies was to apply the groundwater yield assessment methods in areas with known aquifer parameters and yields. The yield assessment methods were evaluated in terms of their accuracy and practicality by comparing the results with other existing yield assessment tools and with field data. The case studies showed that the newly produced geological maps and the Transmissivity Map can be easily used with satellite imagery to identify new potential borehole and wellfield areas.

Overall, this thesis provides a step by step methodology to identify and delineate high groundwater potential areas in the Main Karoo Basin, and quantify the groundwater that is available in these areas. In order for groundwater resources to be accurately quantified, it must be presented with levels of assurance of supply and from these rates a wellfield can be developed whereby guidelines should be followed to obtain an optimum design in order to avoid over abstraction. Recommendations have been provided regarding further work and expansion to be undertaken in each of these tools and models.

Opsomming

Hierdie Meesters tesis vorm die ontwikkelings komponent van die Waternavorsingskommisie (WNK) projek nommer K5/1763, getiteld "Die identifisering en afbakening van hoë-lewerings grondwater produksieveld gebiede in Karoo akwifere as toekomstige opsies vir water voorsiening aan plaaslike owerhede". Die projek is begin as gevolg van die behoefte om die aansienlike kennis van die grondwater van die Karoo Kom binne die grense van water hulpbron beplanning te plaas. Die steeds groeiende kwessies in verband met water hulpbronbeplanning sluit nie net die uitdaging om die grondwater hulpbronne te vind nie, maar ook die kwantifisering van hierdie hulpbron in terme wat maklik verstaanbaar is deur hidrogeoloeë asook ander verwante beroepe.

In 'n poging om hierdie kwessies aan te spreek, word 'n metode om grondwater hulpbronne te kan identifiseer asook te kwantifiseer in hierdie tesis beskryf en word die konsep van versekering van lewering van water ook ingesluit. Hierdie metode behels die gebruik van verskeie hulpbronne, sommige is reeds bestaande en geredelik aan die publiek beskikbaar, ander mag slegs beskikbaar wees in die spesifieke area van belangstelling (bv. aeromagnetiese beelde), en die res is ontwikkel as deel van die WNK-projek en word krities hersien in hierdie tesis.

Die ontwikkeling van die Grondwater Geleidings Kaart in hierdie tesis het beide bestaande boorgat lewerings asook die geologie in ag geneem, en bied 'n reeks van moontlike grondwater geleidings waardes in beide tabel vorm asook op kaarte. Die reekse is vir elke hidrogeologiese eenheid (gebaseer op litologieë en in sommige gevalle, onderverdeelde litilogieë) doleriet gange en plate, gefraktuurde kantlyne van plate en gebiede van dik alluvium. Woodford se metode was gebruik, gevind in Dondo *et al.,* 2010; wat dan geëkstrapoleer is oor die Hoof Karoo Kom. Hierdie kaart is die mees gedetaileerde kaart van die Hoof Karoo Kom en, afgelei uit die gevallestudies wat voorgelê is, blyk dit asof 'n redelike raming van grondwater geleidings waardes voorgelê word.

Die "Aquifer Assured Yield Model" (AAYM) was vir 'n groot aantal kwaternêre opvangsgebiede, verspreid oor die Karoo Kom, gehardloop om die model se geloofwaardigheid te toets, asook om parameter waardes voor te stel wat per area of

dreinerings-kom gebruik kan word. Die AAYM het goed vergelyk met ander databasisse, naamlik die HP en GRAII AGEP. Dit kom voor asof hierdie werk die eerste gedokumenteerde benadering tot grondwater kwantifisering met vlakke van versekering is en moet dus as 'n "werk-in-ontwikkeling" gesien word omdat dit 'n herhalende proses van ontwikkeling, toetsing, verandering en her-toetsing vereis.

Die Grondwater Produksie Veld Model was suksesvol op die basis van die Cooper-Jacob vergelyking (Cooper & Jacob, 1946) ontwikkel. Deur die toetsing van die model is die verhoudings van boorgat spasiëring met grondwater geleidings waardes ondersoek in 'n poging om 'n riglyn vir die ontwerp van 'n grondwater produksie veld met sekere boorgat interferensie beperkings te vind. Benewens hierdie , is die duidelike aard van grondwater vloei in gange oorweeg deur te verwys na die Boonstra-Boehmer vergelyking (Kruseman & de Ridder, 1992), waarvolgens 'n sekere toename in boorgat spasiëring vereis word wanneer 'n boorgat op 'n gang geleë is. Hierdie model kan mens in staat stel om die ontwerp en manipulasie van 'n grondwater produksie veld voor te stel en die effek van grondwater onttrekking op grondwater aftrekking kan ge-evalueer word en daardeur kan die model help om die mees optimale grondwater produksie veld te ontwerp.

Die metodologie wat toegepas is op di gevallestudies demonstreer die praktiese toepassing van die hulpbronne en modelle soos hierbo beskryf. Die doel van die gevallestudies was om die grondwater lewerings assesserings metodes toe te pas op areas met bekende akwifeer parameters en lewerings. Die lewering assesserings metodes was in terme van hul akkuraatheid en praktiese sin ge-evalueer en die resultate is met ander bestaande lewerings assesserings hulpbronne en veld data vergelyk. Die gevallestudies het gewys dat die nuut geproduseerde geologiese kaarte en die Watergeleidings Kaart baie maklik in samewerking met satellietbeelde gebruik kan word om nuwe potensiële boorgate en grondwater produksie velde te identifiseer.

In die algeheel bied hierdie tesis 'n stap vir stap metodologie om hoë grondwater potensiaal gebiede in die Hoof Karoo Kom te identifiseer en af te baken, en om die grondwater wat beskikbaar is in hierdie areas te kwantifiseer. Ten einde die grondwater hulpbronne akkuraat te kwantifiseer, moet dit voorgestel word met vlakke van versekering van lewering en van

hierdie lewerings kan 'n grondwater produksie veld ontwikkel word waarby riglyne gevolg moet word om optimale ontwerp te verseker wat die oor-onttrekking van grondwater uit die grondwater produksie velde te voorkom. Aanbevelings is ten opsigte van verdere werk en die uitbreidings wat onderneem moet word in elkeen van hierdie hulpbronne en modelle.

Contents

List of Figures

List of Tables

Chapter 1

1 Introduction

1.1 Thesis background

This Masters thesis forms the capacity development component of the Water Research Commission (WRC) project number K5/1763, entitled "The identification and delineation of high-yielding well-field areas in Karoo aquifers as future water supply options to local authorities". The project was initiated due to the need to place the significant knowledge on groundwater of the Karoo Basin within the realms of water resource planning. The ever growing issues related to water resource planning include not only the challenge of finding groundwater resources, but quantifying the supply of this resource in terms that are readily understood by hydrogeologists and related professions, thus attempting to bridge the surface water-groundwater divide.

In an attempt to address these issues, a method by which groundwater resources can be identified as well as quantified is described in this thesis, which incorporates the concept of assurance of supply. This is developed for large-scale assessments using existing national-scale data sets and for smaller scale assessments using localized data sets (if available). This method involves the use of a number of tools, some of which are existing and are readily available to the public, others may be available in the specific area of interest (e.g. aeromagnetic imagery), and the remaining have been developed as part of the WRC project, and critically reviewed in this thesis.

It was ensured that the tools that have been developed both as part of the WRC project and this thesis are user-friendly and practical, aimed primarily at hydrogeologists, but must be understood by hydrologists and engineers, ranging from ground level and upwards in skills. Existing tools and resources like locally developed groundwater software such as the GRDM (DWA, 2010) and maps that describe and quantify groundwater resources, were researched in order to fully understand the processes carried out in their compilation, as well as highlighting limitations, in order to learn from, expand and improve on these methods and resources. In the same sense, methods by which assurance of supply has been provided was investigated and incorporated into the new tools developed. All of these tools can be used

concurrently in an attempt to improve planning and management of groundwater resources, each one potentially becoming more detailed.

1.2 Study area

The study area for the WRC project is the Main Karoo Basin and covers an area of approximately 560 000 km^2 (Figure 1) and includes 1014 quaternary catchments. Excluded from the delineated basin are areas to the north partially covered by Kalahari sediments, as well as folded strata in the south, related to the Cape Supergroup (~500 – 330 Ma). The geology of the Main Karoo Basin is the Karoo Supergroup, which is known for its complex nature regarding groundwater movement and occurrence. Following the deposition and lithification of the Karoo sequence a series of volcanic pulses occurred, which were characterised by dolerite dyke and sill intrusions of the Jurassic Age (~180 Ma) (Vivier, 1996). The dolerite intrusions caused major deformation and fracturing of the intruded Karoo rocks and led to the formation of conduits (fractures) for the efficient movement of groundwater in this Basin (Vivier, 1996).

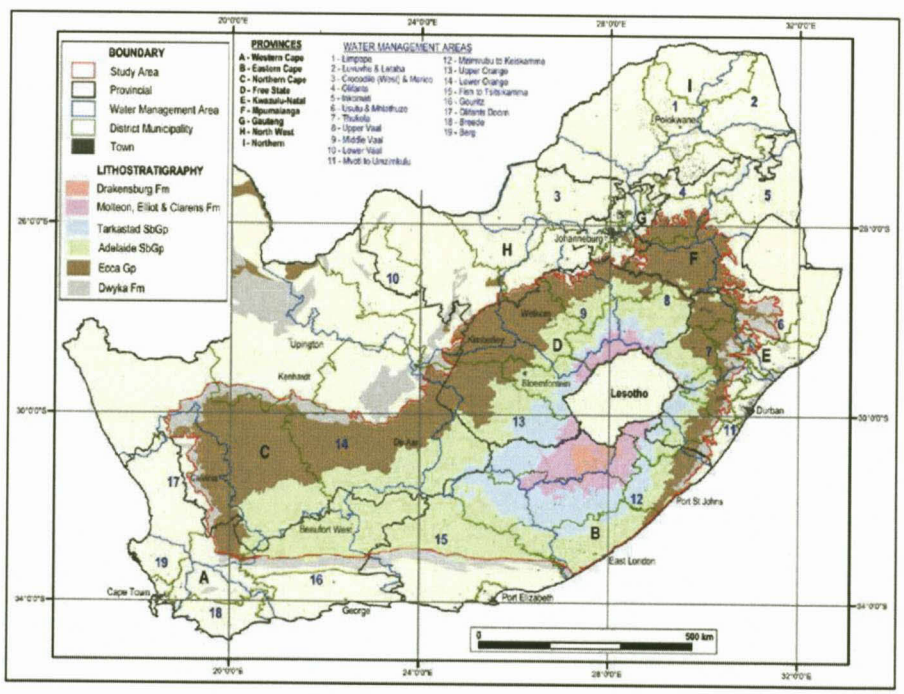

Figure 1. A geological map of South Africa exhibits the different groups of the Karoo Supergroup (Murray *et al.*, 2008, WRC Project K1763, Deliverable 1).

1.3 Main Karoo Basin Hydrogeology

The source of recharge to Karoo (and other) aquifers is predominantly rainfall, with snow contributing in the high-lying areas. A large portion of this water is lost through evaporation, evapotranspiration and surface runoff, and a small portion finds its way into the aquifers through fracture flow where it flows down gradient and ultimately discharges as springs and seeps in lower lying areas (Woodford, 1988).

Aquifers in the Karoo consist of several layers of differing rock types, geometry (e.g. lens vs. sheets), thickness and hydraulic properties (Vivier, 1996). Furthermore, dolerite intrusions resulted in aquifers of the Karoo consisting of two components, fractures and matrix. Flow in these aquifers occurs mainly through discrete fractures, which have a higher transmissivity but a lower storativity compared to matrix settings. Flow through fractures is dependent on the fracture orientation, connectivity and aperture size (Odling, 1993). Due to the large hydraulic conductivity of the fractures their dewatering can occur during pumping, followed by increased flow from the matrix to the fracture, which can change the hydraulic conditions from a confined/semi-confined aquifer system to an unconfined aquifer system resulting in increased rate of drawdown surrounding the borehole. Although the matrix is the primary storage unit able to hold a significant volume of water, its small hydraulic conductivity (due to adhesive forces in small pore spaces) results in limited release of the water (Vivier, 1996). For the reasons given above, it is evident that in quantifying groundwater resources, the whole aquifer, both fractures and matrix, need to be taken into account, whereas to locate high yielding boreholes, or transmissive zones, identifying fracture zones is crucial.

1.4 Aims

The aims of this thesis include:

1. Identify and delineate areas in the Main Karoo Basin with high groundwater yield and development potential

2. Provide relevant groundwater resource information and integrate it into existing water resource planning frameworks.

1.5 Objectives

The project was set out with the following objectives:

- Produce a Transmissivity Map for the Main Karoo Basin to aid in the identification of groundwater development areas
- Describe the process by which tools such as the geological GIS coverages and the Transmissivity Maps are to be used in the identification of these areas
- Test the credibility of the newly developed models Aquifer Assured Yield Model (AAYM) and Wellfield Model
- Develop and recommend a process for the identification of high groundwater potential areas, and the quantification of groundwater in these areas
- Provide case studies demonstrating the functionality of existing and newly developed tools and models

Chapter 2

2 Methodology: A recommended process for identifying high groundwater potential areas

2.1 Introduction

This chapter outlines the methodology behind the process by which high groundwater potential areas can be identified in the Main Karoo Basin and briefly describes the tools, existing and new, to aid in this process. The high groundwater potential areas are identified based upon spatial variability of geology, aquifer transmissivity, and assured aquifer yield which are favourable for groundwater development. When estimating the potential yield of a large area such as a quaternary catchment (which is the standard for surface water yield assessments in South Africa) several types of methods are employed. These include: the use of previously established databases; regional maps of geology and transmissivity; and water balance models. The databases were established using set parameters of a quaternary catchment and include the Harvest Potential (HP) (Baron *et al.,* 1998) and Groundwater Resource Assessment Phase II (GRAII) (DWAF, 2006). Both the regional maps and water balance models, which include the Aquifer Assured Yield Model (AAYM) and Wellfield Model, were developed as part of the WRC project K1763 entitled "The identification and delineation of high-yielding well-field areas in Karoo aquifers as future water supply options to local authorities". The regional maps were produced using various GIS coverages, whereby broad areas can be identified and then investigated in more detail; and the models are based on adjustable aquifer parameters which can be modified and adapted to better represent the study area. The different methods can provide a large range of detail from a quaternary catchment scale all the way down to parameter estimation of a single borehole.

The overall intention of this process is to present an approach to identifying wellfields and their potential yields that can be used for water supply planning purposes. The recommended process has been outlined below in a series of six steps, which includes a brief overview of the developed maps and models and their implementation in the methodology. These maps and models are later described in further detail in the thesis.

2.2 Step 1: Identifying the area

GIS shape files were developed from the 1:1 000 000 Geological Map, producing a regional coverage of high groundwater yield potential zones, which can be used to initially identify your area of interest. These GIS spacial techniques were developed by the Council for Geoscience (Dondo *et al.,* 2010) as part of the WRC project, and include layers of lithostratigraphy, quaternary deposits, dolerite intrusions, and faults. A good understanding of the subsurface geology and geological structures present in the study areas provides a good indication of the type of aquifers present, as well, as the nature of the targets for borehole siting, such as zones of extensive fracturing associated with contact zones of dolerite intrusions. Furthermore, the geology provides an initial idea of the expected aquifer parameters (transmissivity and storativity) and yields.

In collaboration with the GIS Geological maps developed by Dondo *et al.,* 2010, the Transmissivity Map can be used, which was developed in this thesis and is a guide on potential borehole yields. The map provides ranges of transmissivity values for each hydrogeological domain, which are based on lithologies and in some cases, sub-divided lithologies, dolerite intrusions (i.e. dykes and sills), fractured margins of dolerite sills and areas of thick alluvium. Locating areas with high transmissivity can then be investigated in more detail in the design of a sustainable wellfield.

2.3 Step 2: Delineating the area

Once an area of interest has been identified, it can be looked at in more detail and the smaller study area delineated. Collated data-sets used to delineate the study area include: Geological maps, scale of 1:250 000, Arcview GIS (Geological map 1:250 000, Topographical maps, 1:50 000, aerial photography) and satellite imagery. The aerial photography and satellite imagery provide the most detail by making topographical boundaries and geological structures such as major dykes visible and thus aiding significantly in the delineation of the study area.

The delineated aquifer needs to include the area from which water will be drawn into a potential wellfield. In situations of undulating topography, this typically matches topographical divides, since groundwater levels are generally considered to mirror topography (Vegter, 1995). However, in many areas, such as flat-lying areas of the Central Karoo Basin or where permeable geological structures transcend topographical boundaries, the area over which groundwater can be drawn into a wellfield can extend beyond the topographical divide. For example, high-potential abstraction boreholes are likely to be sited either on or in proximity to major dykes, and water can be expected to be drawn along the extent of the dyke (Baker & Murray, WRC Project K1763, Deliverable 21, 2010).

Hydrogeological expertise and judgment is thus required to delineate the aquifer boundaries. Once the area is delineated as a polygon, it can be converted into a KML file to be imported into Google Earth where the area size can be calculated.

2.4 Step 3: Determining aquifer yields

Once the study area has been delineated, the quaternary catchment in which the area lies can be established, thus allowing the determination of a range of aquifer yields from existing databases, such as the Harvest Potential (HP) and GRAII (AGEP drought and normal), and the groundwater balance model AAYM (98% assured yield) and Wellfield Model. The existing databases provide approximate figures which the AAYM and Wellfield Model can be measured against and evaluated.

The AAYM is a simple groundwater balance model that reproduces storage dynamics based on variable volumes of inflow and outflow, and produces groundwater yields with increasing levels of assurance. It is run on a quaternary catchment scale whereby inflow and outflow parameters have default values, or alternatively can be set according to the user. This yield, like the GRAII and HP yields, provides a rough estimate of the catchment's groundwater potential – a yield to bear in mind (and generally not exceed) when undertaking more detailed, localised estimates with tools such as the Wellfield Model.

The Wellfield Model enables the designing and manipulation of a wellfield, while evaluating the effect of groundwater abstraction on drawdown. Any boreholes already present in the area must be noted and can be placed in the wellfield model, using their coordinates, yield and aquifer parameter values (if available). From this, existing abstraction in the area can be established, which will give an indication of groundwater still available for further borehole development.

Two volumes for the study area will thus be obtained, an assured yield from the AAYM and the volume of available groundwater for further abstraction from the Wellfield Model. These volumes must then be proportioned according to the ratio of the size of the delineated area to the total quaternary catchment size.

2.5 Step 4: Siting new boreholes in the Wellfield Model

From Step 3 an approximate *available volume* of groundwater will be obtained using the AAYM model, as well as the *existing abstraction* in the Wellfield Model. Further potential for groundwater development in the wellfield area can therefore be calculated (available groundwater minus groundwater abstracted) and, if a sufficient volume is available, additional boreholes may be sited. The design of the Wellfield Model enables the reproduction of the existing environment in which your investigation is taking place. GIS shape files can be imported such as the background geology, outline of the study area, dykes within the study area and the positions of the existing boreholes. The reproduction of your existing environment can aid in siting of additional boreholes whereby geological features associated with high groundwater potential can be easily identified, such as dolerite dykes and rings, inclined dolerite sheets, suspected deep alluvial deposits and folded or faulted formations.

2.6 Step 5: Establishing borehole sites

Before additional borehole sites can be finalised, the drilling accessibility must be determined using resources such as aerial photography and satellite imagery. The aerial and satellite layers provide detail on the most important considerations when determining site accessibility which include: elevation and presence of steep cliffs and roads. If the site

cannot be accessed, the borehole cannot be sited. Once your final borehole sites have been established, parameter values can be assigned to each borehole in order to run the Wellfield Model. Parameter values will either be based on existing data of boreholes in the near proximity (if available), or on theoretical values taken from the Transmissivity Map and various other general data sets. Once the Model has been run, it will determine the various rates of abstraction taking place from these new boreholes, and subsequent drawdown that occurs, the latter of which is a limiting factor and is governed by the nature of the area.

2.7 Step 6: Comparison of various yields

Once finalised, all yields must be compared. In reality, an aquifer's yield is greater than a wellfield's yield, which in turn is greater than an individual borehole's yield. These yields need to be compared and where this is found not to be the case, the assumptions that governed the estimates need to be re-examined and modified.

Chapter 3

3 Delineation of the Study Area

3.1 Introduction

(Adapted from WRC Project K1763, Deliverables 3 & 8, Council for Geoscience, 2010)

The delineation of the study area and the development of the geological data sets were done by the Dr L. Chevallier and Dr C. Musekiwa (Council for Geoscience) with input from Dr R. Murray (Groundwater Africa) and Mr A. Woodford (Specialist Groundwater Solutions). The bulk of the work in this chapter has been taken from Dr. Chevalier and Dr C. Musekiwa, WRC Project K1763, Deliverables 3 & 8, and is incorporated in this thesis as it played a vital role in the development of the Transmissivity Map and in delineating groundwater target areas, both of which are described later in the thesis.

The study area for this project is the Main Karoo Basin which was delineated and defined using outcrop of the Karoo Supergroup. GIS shape files were derived from the 1 : 1 000 000 Geological map. Outliers of the Basin were excluded from the study area. An example of such an area is the southern margin of the Basin where the Karoo Supergroup meets the Table Mountain Supergroup (TMG) south of Prince Albert. It is an extensively folded outcrop of Karoo rocks which are isolated and lens like in nature, and thus been left out of the study area.

The Main Karoo Basin can be divided into three subgroups based on hydrogeological properties. These subgroups include the Karoo Supergroup, Quaternary deposits and Karoo dolerites.

1) The Karoo Supergroup: This comprises the Permo-Triassic sediment succession and forms primary and secondary aquifers. Groundwater occurs in the matrix porosity of primary aquifers and in fractures associated with secondary, hard-rock aquifers.

2) The Quaternary deposits: These are characterised by primary aquifers (granular porosity) and includes alluvium, eluvium and calcrete.

3) The Karoo dolerites: These are characterised by fractured rock aquifers formed by intrusive dykes, sills and saucer shape sill-ring systems during the Jurassic period.

3.2 The Karoo Supergroup Lithostratigraphic Map

A polygon coverage of the Karoo Supergroup Lithology was completed through a series of steps (Figure 2). Each formation had to be extracted and saved as a separate file. The dolerite sills and quaternary geology were then clipped to each formation. Due to sedimentological characteristics of the Katberg Formation present in the 1 : 250 000 geological map, it was merged into the 1 : 1 000 000 lithostratigraphic map.

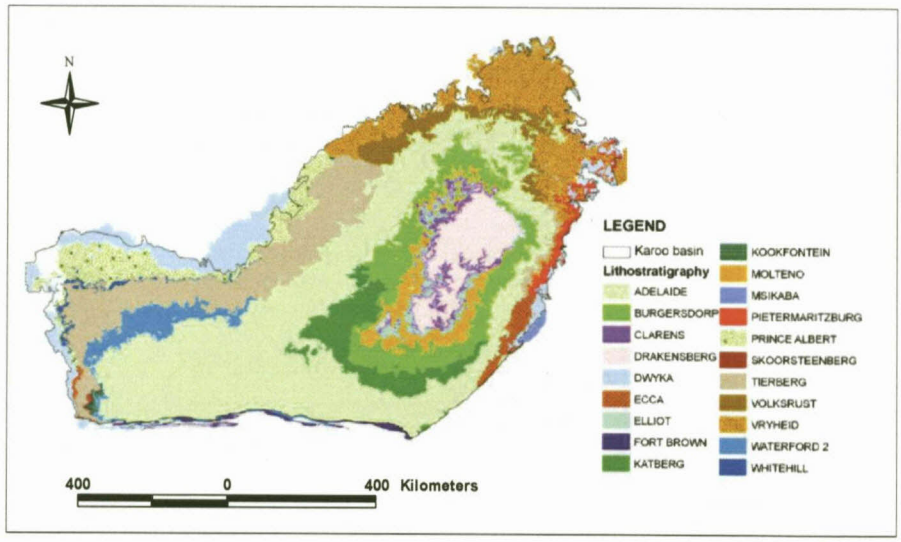

Figure 2. The study area of the Main Karoo Basin showing the lithostratigraphy from the 1 : 1000 000 Geological map where dolerites and quaternary have been removed with the Katberg Formation merged from the 1: 250 000 scale geology.

The lithological units display regional variations, which have an influence on groundwater occurrence. Factors defining this variation include the following:

- Distance from the source (distal or proximal) and direction of transport. The grain size of the deposited material decreases with distance from the source (the ratio of sandstone/mudstone generally decreases).

- Deposition environment (continental, delta, shore). Environmental deposition of a unit can change from fluvial, deltaic, to prodeltaic to shoreline with consequences for lithology and grain size (coarse sandstone, siltstone, mudstone, shale).
- Lateral variation. Interfingering with another unit. Numerous diachronous formations are present in the Karoo with specific consequence for the mudstone/sandstone/shale ratio and the thickness.
- Degree of metamorphism. The Karoo can be subdivided into separate metamorphic and digenetic zones. Firstly, the Cape Fold Belt generated a tectono-metamorphic front that affected the southern part of the Karoo basin with low grade metamorphism in the zeolite field. Secondly, sediment burial beneath the Drakensberg Group created low calcite metamorphism conditions. Thirdly, dolerite intrusions caused regional thermal metamorphism.
- Porosity. The Karoo sandstone and siltstone porosities were established by Rowsell and de Swardt (1976) from tests carried out on drill cores from SOEKOR. North of latitude 29° higher porosity and permeability are encountered. These figures should, however, be taken with caution since they were determined by average tests done on samples taken at different depths along the boreholes and do not entirely reflect sub-surface conditions.

The following domains were identified in the Karoo Basin (Figure 3).

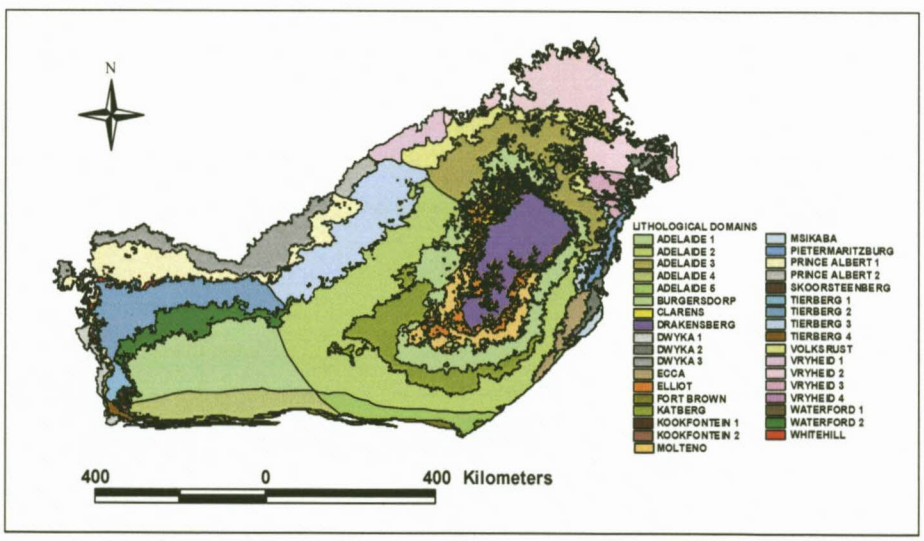

Figure 3. The Karoo basin divided into lithological – metamorphic and depositional domains.

3.3 Lithologies

3.3.1 Dwyka Group

The Dwyka can be subdivided into three domains according to their lithology and the influence of the tectono-metamorphic front of the Cape Fault. These domains include an eastern domain, a southwestern domain and a northern domain (Visser *et al.*, 1990).

The Eastern domain, also referred to as Dwyka 1, is characterized by a fairly uniform lithology and massive diamectite (70%). It corresponds to a plateform facies.

The Western Domain, or Dwyka 2, is characterized by a uniform lithology with massive diamectite (80%). This domain underwent low grade tectono-metaporhism.

The Northern Domain, or Dwyka 3, is characterized by a highly variable lithology, low massive diamectite (20%) and high mudrock/sandstone ratio. This domain reflects a valley and inlet depositional environment.

3.3.2 Prince Albert Formation

This formation can be subdivided into two domains, a southwestern and a northeastern domain (Cole, 2005).

The south west domain, or Prince Albert 1, consists of mainly dark grey shale (95%) where deep marine conditions prevailed (phosphate deposits).

The north east domain, or Prince Albert 2, is present around Boshof and consists of rythmite and sandstone comprising 50% of the rock. The domain characterises a shallow deltaic depositional environment with no phosphate deposits.

3.3.3 White Hill Formation

This formation is not subdivided. It consists of thinly laminated shale and contains up to 14% carbonaceous material. Siltstone occurs in the north east at the base of the Formation. The shales are thought to represent suspension-settling of mud under reducing conditions. The salinity conditions of deposition remain unsolved.

3.3.4 Fort Brown Formation

This formation consists of rhytmites (50%) and mudrock (50%) with minor sandstone intercalation. These lithologies were deposited in a prodelta environment.

3.3.5 Undifferentiated Ecca Group

This group has not been subdivided and is dominated by mudrock (95%). The unit may possibly display duplication of the succession due to faulting.

3.3.6 Pietermaritzburg Formation

This formation is not subdivided and consists of dark, upward coarsening, silty mudrock. It was deposited in a prodelta environment.

3.3.7 Vryheid Formation

This formation consists of sandstone (75%) and mudrock (25%). It has good average porosity (> 2%) and good permeability. It can be subdivided upon the following criteria (Van Vuuren and Cole, 1979):

- Depositional environment: shore line; deltaic or fluvial

- Source: N; NW or W

- Porosity

Based on these criteria, four domains are defined.

In the west, the domain referred to as Vryheid 1 is present. This lithology was deposited in a deltaic-shore line environment with beach deposits and heavy mineral sands. The porosity ranges from 3 to 20 % and the permeability reaches up to 250 m/d in certain areas.

In the north, the domain Vryheid 2 is present. This was deposited in a fluviodeltaic environment with many sedimentary cycles. The porosity ranges from 2 to 28%.

In the east, Vryheid 3 is present. The depositional environment is that of a deltaic nature. Porosity is < 10% and permeability reaches a mere 2 m/d.

In the south east, Vryheid 4 is present. This domain was, too, deposited in a deltaic environment with thin coal seams. Porosity is < 2% and permeability <1m/d.

3.3.8 Tierberg Formation

This formation is fairly uniform, consisting mainly of bluish shale representing a basin-plain and prodelta environment (Veevers *et al.*, 1994). Only the upper 20 -50 m shows upward coarsening with siltstone, corresponding to the base of the Waterford (Viljoen, 2005), but this member is not mappable.

The formation thickness decreases from south to north (Viljoen, 2005).

Lateral variation is observed in the formation with the presence of interlayered thin soft yellowish illite horizons (Viljoen, 1994). These horizons are derived from volcanic tuff and vary in thickness from 2 cm in the south west close to the volcanic source, to 1.5 cm in the north east away from the source. These thin horizons can have a strong influence on the fissile nature of the rock as they are found to bind the fissile shale together. The relative percentage of these horizons displays a decrease from south west (20%) to north east (less than 5%).

The four illite horizon domains of relative proportion are defined:

The south west domain, also referred to as Tierberg 1, consists of 25% illite. Layers have an average thickness of 2.5 cm.

The north west domain, or Tierberg 2, contains 10% illite. Layers have an average thickness of 1.5 cm.

The north domain, or Tierberg 3, contains 0% illite.

The fourth, south domain known as the Tierberg 4, formed as a consequence of the metamorphic front of the Cape Fold Belt.

3.3.9 Volksrust Formation

This formation is not subdivided and consists of black silty shale with thin siltstone or sandstones deposited in a shallow water shelf environment. Thin phosphate and carbonate beds as well as concretion are relatively common.

The Volksrust merges with the Tierberg in the northern outcrop area and with the undifferentiated Ecca in the southern outcrops.

3.3.10 Skoorsteenberg Formation

This arenaceous unit is not subdivided and consists of sandstone (50%) and shale (50%). There are five sandstone units present up to 60 m thick and interbedded with shale. They represent submarine fan deposits separated by basin plain deposits.

3.3.11 Kookfontein

This formation comprises cycles of laminated dark-grey shales alternating with clastic rhythmites at the bottom and alternating siltstone and sandstone at the top. It represents prodelta sedimentation in a gradually shallowing water body.

This unit has been subdivided into two domains according to the degree of metamorphism:

The south domain, as Kookfontein 1, displays low grade tectonic metamorphism.

The north domain, as Kookfontein 2, displays no metamorphism.

3.3.12 Waterford Formation

This formation has been subdivided into two domains:

The south domain, referred to as Waterford 1, is characterised by arenaceous deposits comprising sandstone (75%), mudrock (25%) and clastic rythmites deposited in a delta front. Numerous sandstone bars are present averaging 6 m in thickness.

The northern domain, referred to as Waterford 2, consists of fine grain sandstone (50%), siltstone, shale, rythmites and calcareous concretions. It is likely that deposition occurred in a shallow sea.

3.3.13 Adelaide Subgroup

Palaeocurrent mapping has indicated that the sediments were derived from different sources (Johnson et al. 1997):

The west source deposited bluish, greenish, greyish-red mudstones (75%) and is known as Adelaide 1.

The south and south east source deposited alternating grey mudstone (75%) and fine to medium grain sandstone, known as Adelaide 2. Sandstone bars are present with an average thickness of 6 m, locally reaching a thickness of 60 m.

In the northern part of the basin (eastern source), coarse to very coarse grained sandstones are common, known as Adelaide 3. The porosity of the sandstone tends to increase in this area (Rowsell and de Swart, 1976).

Finally, the Cape Fold Belt generated a tectono-metamorphic front that affected the southern part of the Karoo basin with low grade metamorphism in the zeolite field, forming Adelaide 4 in the west and Adelaide 5 in the East.

3.3.14 Katberg Formation

This formation is rich in sandstone with the areneous material varying from 50 to 75%. In the south west a tectonic wedge of Katberg consists of 90% sandstone and conglomerate.

3.3.15 Burgersdorp Formation

This formation is not subdivided and consists of grey and red mudstone (65 to 85%) and sandstone (25 to 15%). Flood basins and lacustrine palaeo-environment may have dominated.

3.3.16 Molteno Formation

This formation comprises alternating medium to coarse grain sandstone (50%) and mudstone (50%). The depositional environment was dominated by braided rivers flowing from a tectonically active source.

3.3.17 Elliot Formation

This formation consists of alternating green-grey mudrock (90%) and subordinate fine grain sandstone (10%). The lower arenaceous unit corresponds to meandering river sedimentation and the upper mudrock dominated unit reflects a playa deposit. Palaeocurrents suggest northerly and north westerly transport.

3.3.18 Clarens

This formation consists of eolian sand and mud-volcanic deposits.

3.4 The Dolerite Sill Map

Dolerite sills from the 1 : 250 000 geological maps were extracted and merged into the 1 : 1 000 000 lithological map (Figure 4).

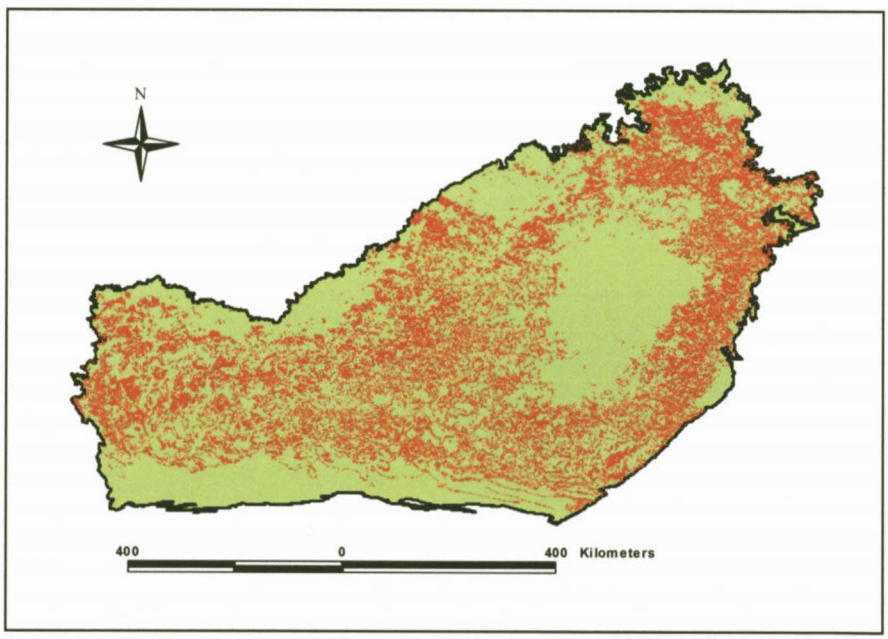

Figure 4. The seamless map of the dolerite sills.

3.5 The Quaternary Geology Map

This map was compiled using 1 : 250 000 geological maps and merging them to create Figure 5. The formations classified under the term 'Quaternary' include fluvial, Cenozoic, terasses, calcrete and ferricrete.

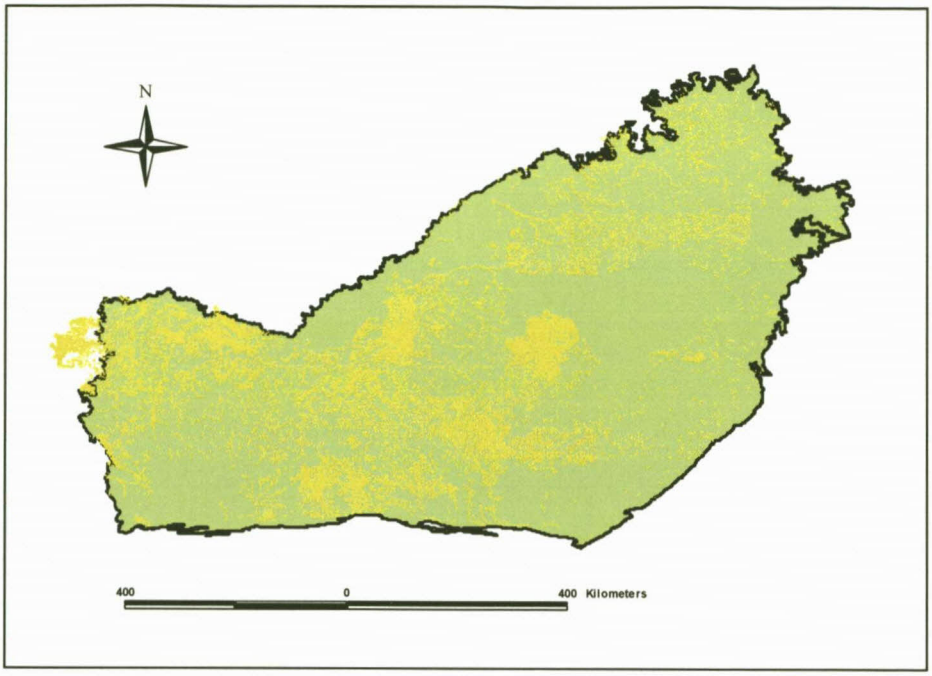

Figure 5. The alluvial deposits of the Karoo basin (in yellow), extracted from 1 : 250 000 geological maps.

3.6 The Dolerite Dykes Map

This map was created using 1 : 250 000 geological maps and merging them to create Figure 6.

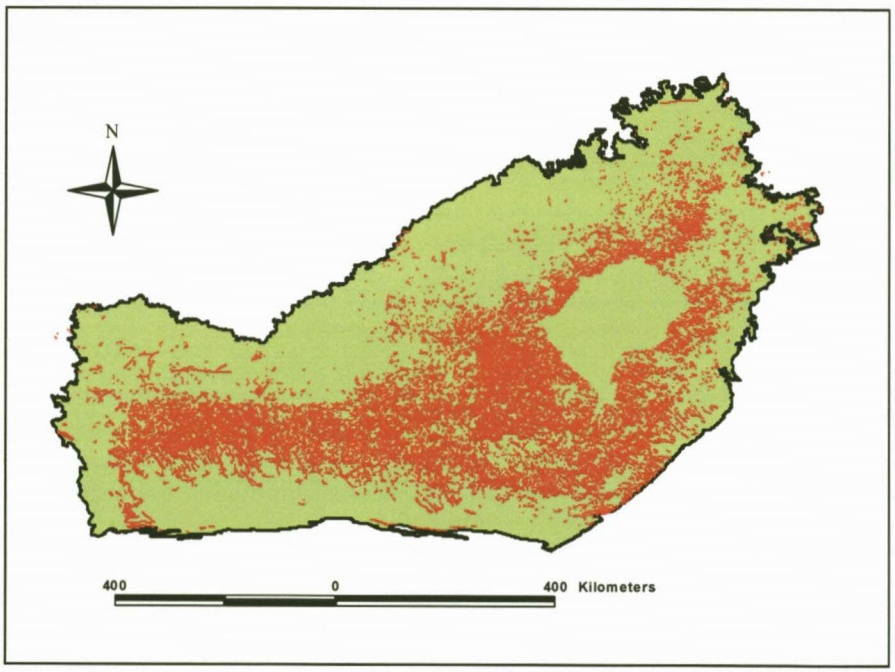

Figure 6. Dolerite dykes of the Karoo basin, extracted from 1 : 250 000 maps.

3.7 The Geological Faults Map

The faults were extracted from the 1 : 1 000 000 Geological map (Figure 7). Generally, the Karoo Basin did not experience extensive post-depositional faulting. The Tugela fault in the east and the Craton margin fault in the west are the major tectonic features that were reactivated post Karoo deposition. The map does not, however, show the neotectonic activity for which there is not complete information for the Main Karoo Basin.

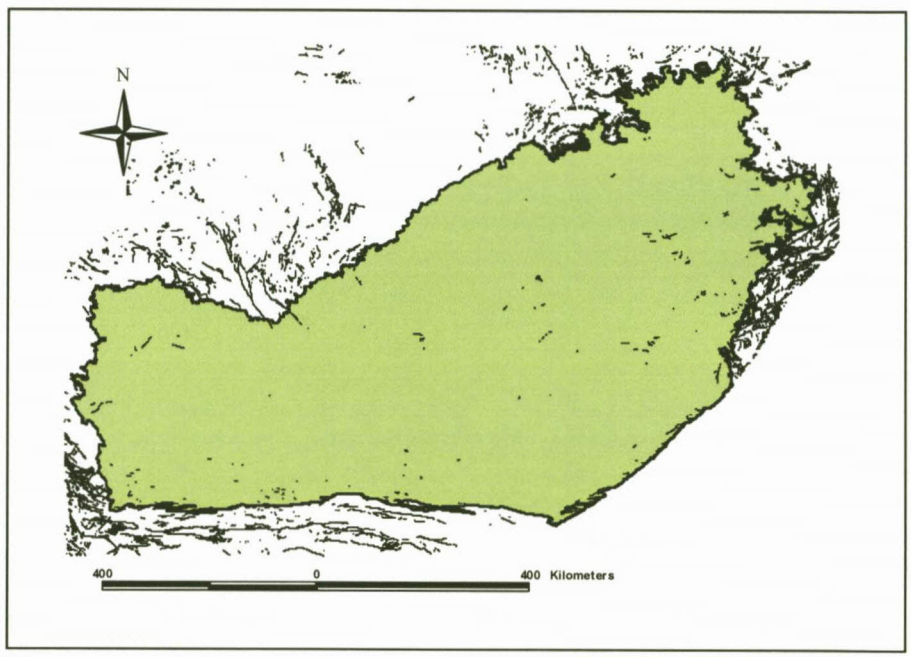

Figure 7. The Karoo in the South African tectonic framework. Very few faults are affecting the Karoo Basin.

3.8 Satellite Imagery and Aerial Photography

Together with the geological coverages described above, satellite and aerial imagery can be used to identify potential groundwater development zones. Different combinations of layers can be used to provide detailed images of the areas of concern which greatly aid in borehole siting. The detail available includes geological structures such as dolerite dykes and well as topographical information such as elevation and presence of steep cliffs.

Figure 8 shows how dolerite dykes can initially be identified from aerial photography, and further defined using additional layers such as satellite imagery or 1:250 000 geological maps (Arcview GIS).

Figure 8. An example of an aerial photography layer displaying a dyke running roughly NW-SE.

Figure 9 shows an example of satellite imagery over which dykes have been placed and the level of detail this provides. Once a structure has been identified on the satellite image, the additional layer of dykes can be added to determine the extent of the structure. In addition, this imagery illustrates changes in elevation, in other words, presence of steep cliffs and/or mountains.

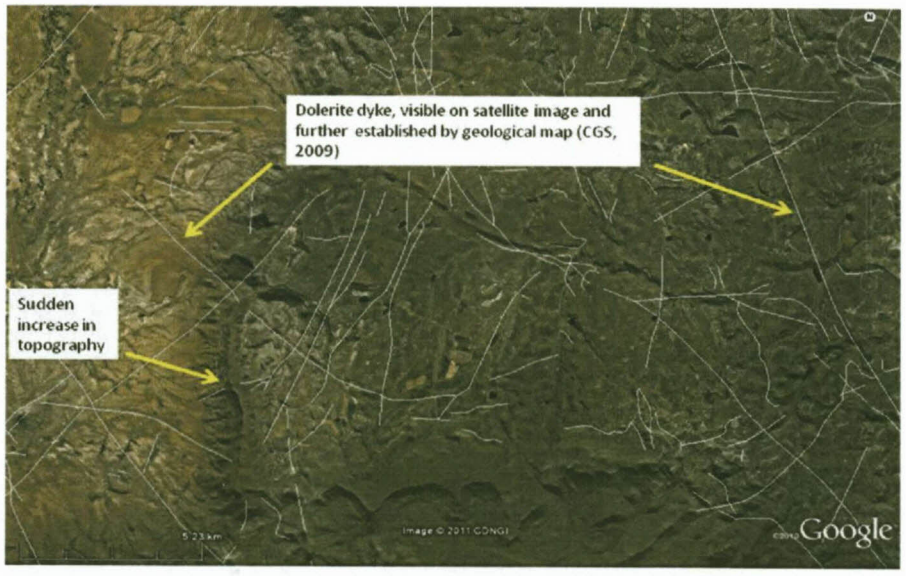

Figure 9. An example of satellite imagery showing topography and dykes extracted from 1 : 250 000 geological maps.

If aerial photography such as aeromagnetic data is available in an area of interest, the layer can be placed on top of satellite imagery to indicate the presence of dykes and thus aid in further geophysical exploration. If dykes can be identified, more detailed geophysics can be undertaken in those particular areas of interest as the information such as the strike of a dyke is provided (Figure 10).

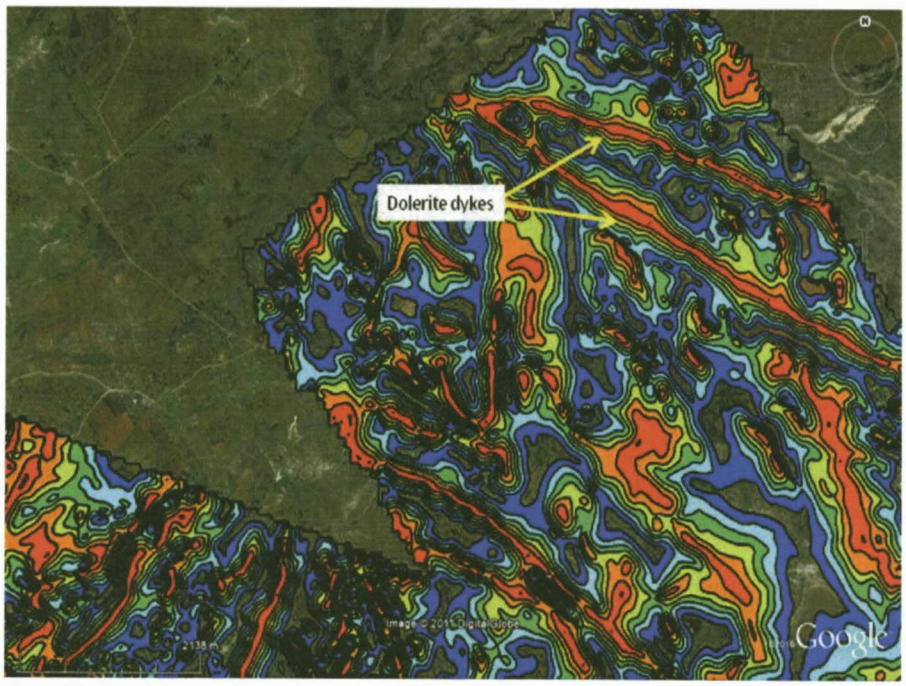

Figure 10. An example of aeromegnetic data from Matatiele in the Eastern Cape Province placed on top of a satellite image (Aeromagnetic data source: Alfred Nzo District Municipality: Regional Bulk Readiness Implementation Study).

Finally, topographic maps or contours can greatly aid in the delineation of a study area. Topographic boundaries may be used when there are no apparent geological structures (such as major dykes) to indicate the extent of an aquifer or recharge zone. Figure 11 below is an indication of how an area can be delineated using these boundaries.

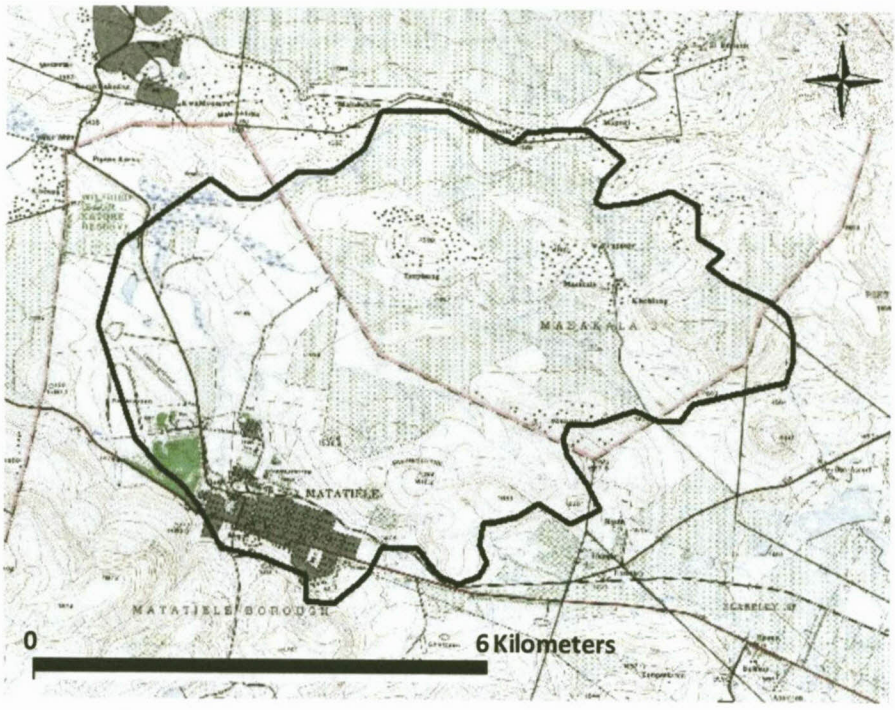

Figure 11. A delineated area using topographical boundaries.

3.9 Recommendations

Satellite imagery should be used to delineate study areas and identify provisional borehole sites.

Various combinations of layers should be used to develop a more complete "picture" of the study area and to incorporate as much information as possible regarding geological structures and boundaries.

During the wellfield design these layers can be imported to reproduce your area of interest

Chapter 4

4 Development of the Transmissivity Map

4.1 Literature Review

Previous transmissivity maps have been developed by Conrad (2005), Rosewarne (2008), and Woodford in 2010 (Dondo *et al.,* 2010). Conrad (2005) produced a transmissivity map as part of the WRC Project Number K5/1498 (Figure 12). This process applied the rough guide proposed by Kirchner and van Tonder, (1995), which assumed:

$T = 10\,Q$ Equation 1

Where:

T = transmissivity (m^2/d)

Q = borehole yield (L/s)

Borehole yields were obtained from the NGDB for the country and multiplied by ten to obtain single transmissivity values per km^2 cell. A downfall of this method, in addition to its simplistic approach, is the nature of the borehole data obtained. Values obtained represent drilling "blow yields", which usually are higher than borehole sustainable yields, and are likely to overestimate transmissivity values. Furthermore, the geology was not considered in the preparation of this map thus it only reflects information in areas where boreholes were drilled, and not the geology that is responsible for changes in permeability. For the purpose of estimating single borehole yields, the ranges adopted are not useful; for example, a transmissivity range of 100 – 1000 m^2/d is equivalent to yields of 1 – 10 L/s, which is a significant difference when considering Karoo borehole yields.

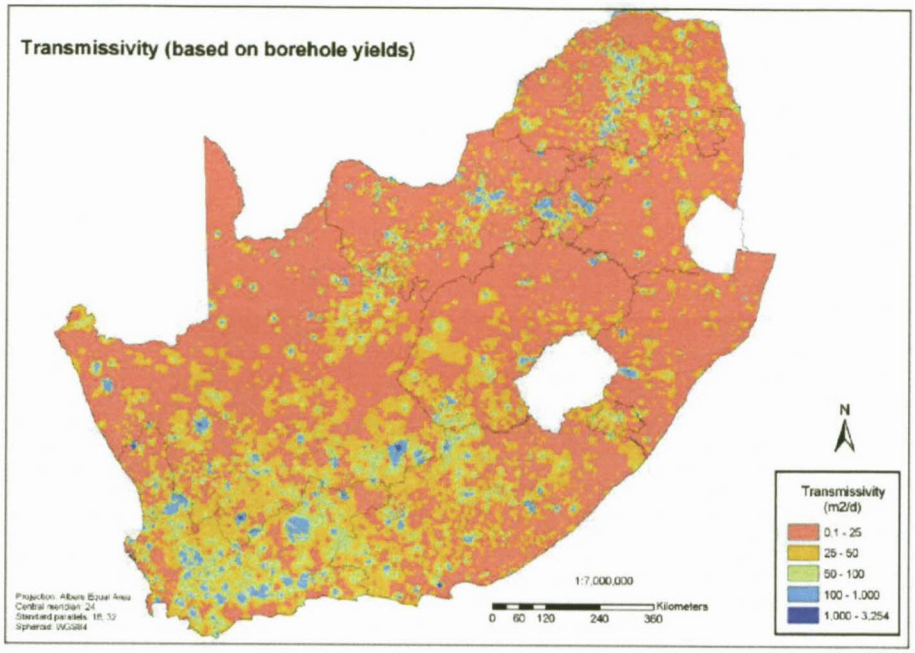

Figure 12. A transmissivity map based on data obtained from NGDB (Conrad, 2005).

Rosewarne (2008) produced a map of average transmissivity values across South Africa (**Figure 13**), extrapolating point values across the country thereby creating broad areas of various ranges of transmissivity. The map is useful in terms of its extensive coverage as one can observe general transmissivity trends across the country as well as identify smaller areas of high transmissivity (potentially high yielding boreholes). A limitation, however, arises in the applicability of the map when looking at a local scale (which it was clearly not intended for), as one requires point values for potential borehole sites when estimating their yields. Certain areas are densely populated with borehole data from which transmissivity values were calculated, but others have few, if any data, thus the reliability of the estimates provided is low. When a transmissivity value for a specific location is required, it may be difficult to use the value provided, firstly because there was potentially no data available (single value extrapolated to a large area), and secondly because the range provided for the area (lithology) is too broad (e.g. 25 – 100 m^2/d).

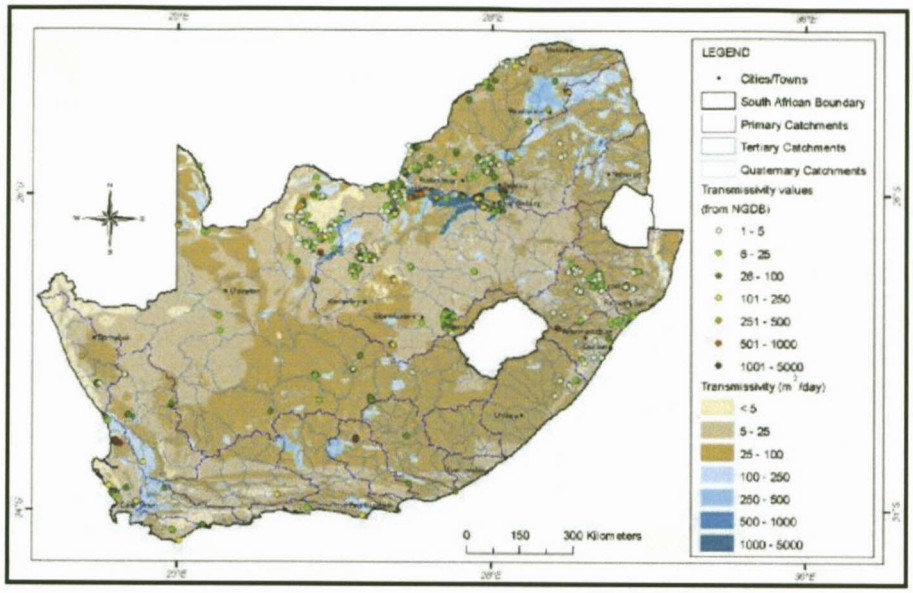

Figure 13. WR2005 average transmissivity map (Rosewarne, 2008)

Woodford (in Dondo *et al.,* 2010) produced a regional average transmissivity map for the eastern Karoo Basin, which lies in the Eastern Cape and KwaZulu-Natal Provinces (Figure 14). This map is significantly more detailed regarding transmissivity values in comparison to Conrad (2005) and Rosewarne (2008) as values were assigned to lithologies as well as groundwater structural targets such as dolerite dykes, sills, inclined dolerite sheets, dyke intersections, folded sediments and alluvium. The range of values assigned, however, is not useful if a single transmissivity value is needed to establish potential borehole yields because the upper range ceases as >30 m^2/d. The method for developing the transmissivity map was, however, far more advanced than the Conrad or Rosewarne methods, and involved analysing hundreds of pumping test data and then developing numerous relationships between borehole yields and transmissivity values. This is described in greater detail in this chapter, as it formed the basis of the methodology adapted to develop the Main Karoo Basin Transmissivity Map.

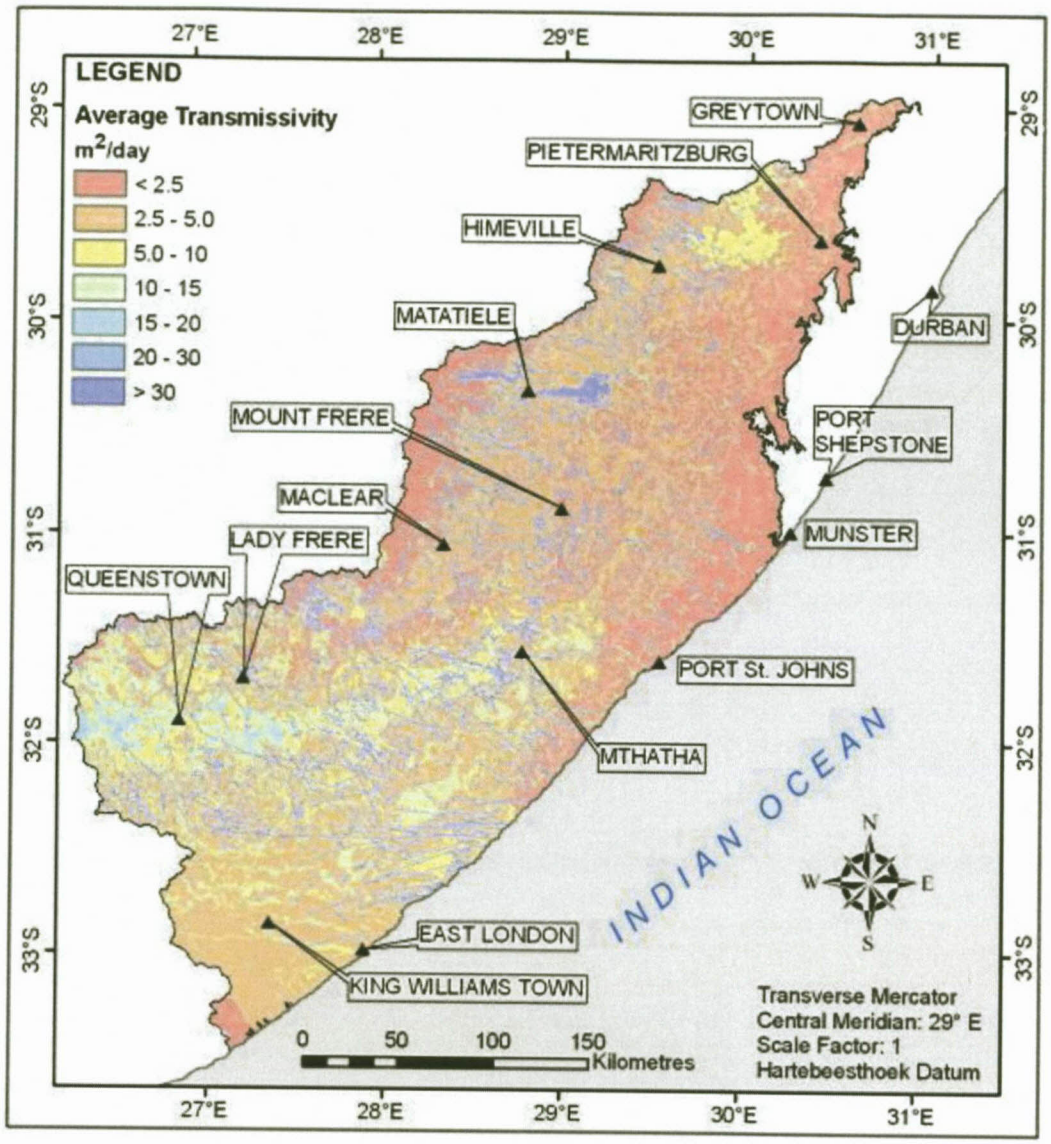

Figure 14. A regional average transmissivity map for the eastern Karoo Basin (Dondo *et al.*, 2010).

4.2 Introduction

This chapter aims to address the concerns raised in the literature review of the previous transmissivity maps produced, such as the quality of data used, the lack of geological targets and the applicability of the maps. This will be done by creating transmissivity maps using extensive borehole data and incorporating the geology and structural targets considered during borehole siting. The Transmissivity maps of the Karoo Basin were developed to provide guidance on potential borehole yields. Whilst this is seemingly an impossible task owing to the heterogeneous nature of fractured rocks, the approach took both existing

borehole yields and geology into account, and provides a range of possible values. The user will have to choose which values to use based on local borehole yields or experience of the area. Because the maps are based on geology, they can also be used as a starting point in locating high groundwater potential areas and even possible drilling targets. The map provides ranges of transmissivity values for each hydrogeological domain (based on lithologies and in some cases, sub-divided lithologies), dolerite dykes and sills, fractured margins of sills and areas of thick alluvium. The ranges, however, are a guideline as one can either use the values provided or alternatively, use values from existing data in the study area if it is available. The reason why a transmissivity map is of great value is because of the direct correlation between the yield of a borehole (Q) and the transmissivity of the aquifer (T), the yield increasing as the transmissivity increases and vice versa. The Cooper-Jacob approximation of the the Theis (1935) transient state radial flow equation (Cooper and Jacob, 1946) (Equation 2) illustrates this and in addition one can see the similar relationship between available drawdown (s) and the yield. It is thus vital for the user of this tool to be confident in assigning transmissivity values on a localised scale to potential borehole sites, considering the transmissivity of the formation in which it lies as well as any intrusive dolerites present, or any structures such as faults or folds that may increase local transmissivity. On a regional scale, however, an adequate estimation of groundwater availability can be made using the aquifer assured yield model.

$$Q = \frac{4\pi Ts}{2.3log\frac{2.25Tt}{r^2S}}$$ Equation 2

This becomes:

$$T = \frac{2.3Q}{4\pi s} log\frac{2.25Tt}{r^2S}$$ Equation 3

and:

$$s = \frac{2.3Q}{4\pi T} log\frac{2.25Tt}{r^2S}$$ Equation 4

Where:

Q = yield (m^3/day)

T = transmissivity (m^2/day)

s = available drawdown (m)

t = pumping time (days)

r = radius of the borehole (m)

S = storativity

4.3 Methodology used in assigning transmissivity values to lithologies and groundwater structural targets

Woodford's method is the most comprehensive approach to date in developing a regional transmissivity map, thus with the guidance of Dr R. Murray (Groundwater Africa) and the assistance in data processing by Dr C. Musekiwa (CGS), this method was used and further developed to produce the map for the Main Karoo Basin. Essentially, Woodford's approach has been extrapolated to the entire Karoo Basin by applying various equations to the lithological domains, dolerite dykes and sills, and areas of potentially thick alluvium (defined, using a GIS approach, as the intersection of primary rivers with geologically defined alluvium).

Woodford's approach, which is described in detail in Dondo *et al.*, 2010, involved analysing numerous pumping tests in order to produce equations that relate borehole yields to aquifer transmissivity. He dissected the drawdown versus time curves from hundreds of tests, taking into account the nature of fractured Karoo aquifers and their response to pumping:

1. Early-time period: transmissivity value obtained represents that of the shallow, weathered and jointed formation directly surrounding the aquifer.

2. Mid-time period: transmissivity value represents a period where the hydraulics in the aquifer changes from a semi-confined to unconfined as the weathered, jointed section is dewatered and/or major water-bearing fractures are being dewatered.

3. Late-time period: transmissivity value represents the bulk aquifer, the rock mass surrounding the borehole. The typical semi-confined nature of Karoo aquifers suggests that this period represents the surrounding rock, the volume of which is dependent on the duration of the pump test and the hydraulic parameters of the aquifer.

Figure 15 shows the typical stages of pumping test curves that were used to differentiate the flow characteristics listed above.

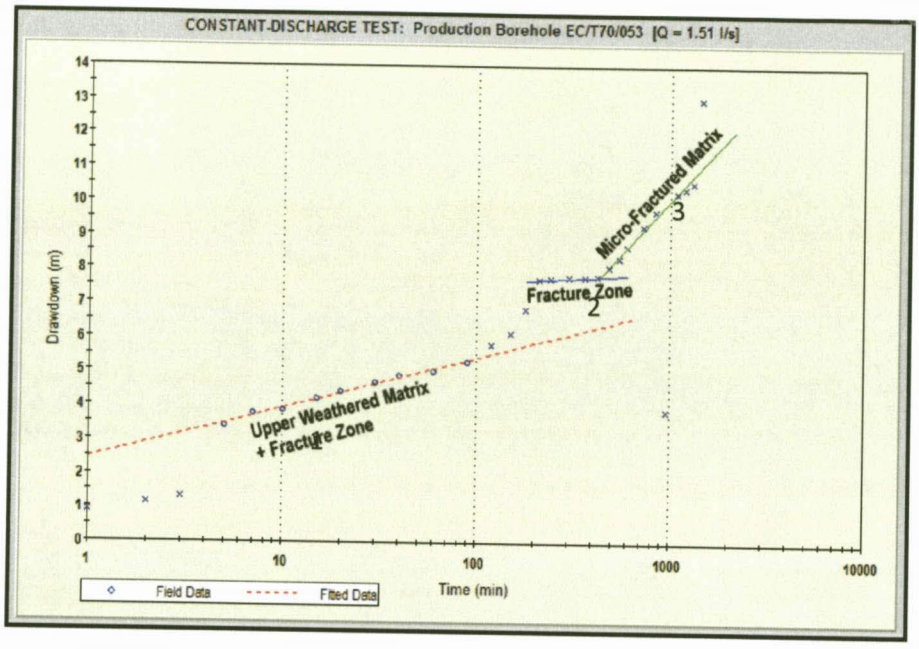

Figure 15. A time-drawdown curve displaying the response during pumping, the three phases of flow can be clearly distinguished (Dondo *et al.*, 2010).

Once transmissivity values were determined for each portion of the drawdown curves for each lithology and groundwater target structure (e.g. dyke, sill, sheet, etc), graphs were produced by plotting the constant discharge pumping test rate versus transmissivity and fitting a power function (Equation 5) to the data. These graphs were then used to develop generalised equations that relate transmissivity to borehole yield (actually constant discharge test rates) for each lithology and structure.

$$T = A \times Q_p^{\,b} \qquad \text{Equation 5}$$

Where:

T = transmissivity

A and b = constants

Q_p = yield of the lithological domain

With the use of the Cooper-Jacob equation, transmissivity values were derived from the different segments of the time-drawdown curve, namely early, middle and late time. The early time curve is represented by T_E (Pt 1, Figure 15), the middle by T_M (Pt 2, Figure 15) and the late by T_L (Pt 3, Figure 15). These equations were derived for the matrix and all groundwater target structures, and can be found in Dondo *et al.,* 2010, along with a detailed explanation of the methodology.

Woodford's method was adapted to obtain ranges of transmissivity values to cover the entire Main Karoo Basin as part of this thesis. The process carried out entailed further assessment of the early-, mid- and late-time period equations in order to select which equations yielded the most realistic transmissivity values. Previous drilling reports from towns and villages across the Karoo were researched for their transmissivity values to be compared with the transmissivity values obtained from the equations. The transmissivity-yield equations used are listed in Table 1. The high yielding nature of the Cedarville flats in the Matatiele area required them to have a separate column in yield calculations.

Table 1: The transmissivity-yield equations used in developing the Transmissivity Map.

	Parameter	Equation	Dataset	Reasons for use/Assumptions
Matrix	Lower T	$T_L = 1.36Qp^{1.14}$	Median of boreholes on relevant lithology	Late time curve represents flow through entire matrix
	Upper T	$T_M = 18.8Qp^{1.14}$	Median of boreholes on relevant lithology	Mid time slope represents the fractured and weathered part of matrix thus giving the highest yield
	Middle T	Harmonic mean of above	Median of boreholes on relevant lithology	Required a conservative value
Sills	Lower T	$T_M = 24.84Qp^{1.13}$	Harmonic mean of lower 33% of *whole* dataset	Required as conservative a value as possible
	Upper T	$T_M = 24.84Qp^{1.13}$	Median of upper 33% of *whole* dataset	Average was used instead of arithmetic mean as boreholes sited in the centre of sills generally have lower yields than boreholes on dykes
	Middle T	$T_M = 24.84Qp^{1.13}$	Median of middle 33% of *whole* dataset	Applying the harmonic mean of the upper and lower provided values that were too conservative

Dykes	Lower T	$T_M = 30.18Qp^{1.02}$	Harmonic mean of lower 33% of *whole* dataset	Required as conservative a value as possible
	Upper T	$T_M = 30.18Qp^{1.02}$	Arithmetic mean of upper 33% of *whole* dataset	Wanted to obtain the highest possible value from the data available
	Middle T	$T_M = 30.18Qp^{1.02}$	Median of middle 33% of *whole* dataset	Applying the harmonic mean of the upper and lower provided values that were too conservative
Sill margins	Lower T	$T_M = 24.84Qp^{1.13}$	Harmonic mean of lower 33% of boreholes positioned on sill margins	Required as conservative a value as possible
	Upper T	$T_M = 24.84Qp^{1.13}$	Arithmetic mean of upper 33% of boreholes positioned on sill margins	Wanted to obtain the highest possible value from the data available
	Middle T	$T_M = 24.84Qp^{1.13}$	Median of middle 33% of boreholes positioned on sill margins	Applying the harmonic mean of the upper and lower provided values that were too conservative
Alluvium	Lower T	$T_E = 5.1Qp^{1.15}$	Harmonic mean of lower 33% of boreholes positioned on alluvium	Required as conservative a value as possible
	Upper T	$T_E = 5.1Qp^{1.15}$	Arithmetic mean of upper 33% of boreholes positioned on alluvium	Wanted to obtain the highest possible value from the data available
	Middle T	$T_E = 5.1Qp^{1.15}$	Median of lower 33% of boreholes positioned on alluvium	Applying the harmonic mean of the upper and lower provided values that were too conservative
Cedarville Flats	Lower T	$T_E = 5.1Qp^{1.15}$	Harmonic mean of lower 33% of boreholes positioned on Cedarville flats	Required as conservative a value as possible
	Upper T	$T_E = 5.1Qp^{1.15}$	Arithmetic mean of upper 33% of boreholes positioned on Cedarville flats	Wanted to obtain the highest possible value from the data available

	Middle T	$T_E = 5.1Qp^{1.15}$	Median of lower 33% of boreholes positioned on Cedarville flats	Applying the harmonic mean of the upper and lower provided values that were too conservative

The following points should be noted in relation to the equations that were used:

- The transmissivity equation for the dykes and sills was applied to the whole data set and not just to the boreholes positioned on the dykes and sills as this data has an uneven spread; the amount of data is too small thus the results appeared incorrect. Furthermore, it must be noted that the location of boreholes in relation to dykes in the GIS scale that was used is not accurate. The position of the dykes on the 1:250 000 Geological maps are not always accurate, many dykes are not mapped, and some borehole co-ordinates may not have been obtained using a GPS. As a result of these factors, not all boreholes that were sited on dykes, are classed as "dyke-boreholes" in the database used.

- Only boreholes with yields >10 L/s were available for the Cedarville Flats and these values were used in the calculations of the Upper T values. The Middle and Lower T values were estimated based on experience in the field, using yields of 5 L/s and 2 L/s respectively.

- The dykes' equation was applied to the arithmetic mean of the upper 33% because the higher yielding boreholes ultimately represent the fractured part of the aquifer as flow through Karoo aquifers is primarily governed by the aperture and connectivity of the fractures. Dykes intruding the Karoo lithologies caused fracturing, which suggests that it may be appropriate to utilise the higher yielding boreholes in the calculation of the dykes. Additionally, the use of the arithmetic mean simply gives more weight to the larger values thus further increasing the transmissivity.

- Even though there is generally an uneven distribution and density of data amongst lithologies, the transmissivity values obtained, although in some cases significantly variable (e.g. Adelaide 4), were left as calculated because they are based on real data.

The final transmissivity values can be seen in Tables 2 - 4. The table was separated into lower, middle and upper values, and furthermore into lithologies and structures. The lower values, including matrix and all structures, range from 0.2 to 11 m^2/d with an average of 2.8

m^2/d; the middle values range from 0.6 to 81 m^2/d with an average of 16.3 m^2/d; and the upper values range from 4.4 to 483 m^2/d with an average of 116.1 m^2/d. The location of each formation (hydrogeological domain) used in Tables 2 - 4, and a brief description of how they were delineated is shown in Figure 16 and captured in the next section.

Table 2: Lower transmissivity range for all formations and groundwater structural targets

Formation	Lower T (m^2/d) Range					
	Matrix	Dyke	Sill	Sill margin	Alluvium & intergranular	Alluvial basin
Adelaide-1	2.0	2.0	1.8	1.3	0.2	11
Adelaide-2	1.2	1.7	1.0	1.0	0.2	11
Adelaide-3	0.5	1.3	0.8	0.8	0.2	11
Adelaide-4	3.9	4.0	2.6	1.3	0.2	11
Adelaide-5	0.8	2.0	1.2	1.3	0.2	11
Burgersdorp	1.1	1.6	1.0	4.0	0.2	11
Clarens	0.9	2.2	1.4	2.5	0.2	11
Drakensburg	0.7	1.3	0.7	0.7	0.2	11
Dwyka-1	0.8	1.1	0.6	0.4	0.2	11
Dwyka-2	0.8	2.0	1.2	0.7	0.2	11
Dwyka-3	0.5	1.0	0.6	0.4	0.2	11
Ecca	1.0	2.5	1.5	2.6	0.2	11
Elliot	0.7	1.5	0.9	2.5	0.2	11
Katberg	1.3	2.1	1.3	1.1	0.2	11
Molteno	0.8	1.8	1.1	0.8	0.2	11
Msikaba	0.3	2.2	1.4	1.4	0.2	11
Pietermaritzburg	1.3	2.7	1.7	1.7	0.2	11
Prince Albert-1	0.7	1.2	0.7	1.8	0.2	11
Prince Albert-2	0.5	1.3	0.7	1.8	0.2	11
Tierberg 1+4, Fort Brown	1.0	6.7	4.7	0.8	0.2	11
Tierberg-2	1.0	1.6	0.9	0.8	0.2	11
Tierberg-3	1.0	1.4	0.9	0.6	0.2	11
Volksrust	0.7	1.7	1.0	1.2	0.2	11
Vryheid-1	0.4	0.8	0.5	0.6	0.2	11
Vryheid-2	0.5	1.3	0.7	0.6	0.2	11
Vryheid-3 and -4	0.9	1.9	1.2	2.2	0.2	11
Waterford-1 & -2	1.4	2.0	1.3	1.9	0.2	11
Whitehill	0.9	1.8	1.1	1.2	0.2	11

Table 3: Middle transmissivity range for all formations and groundwater structural targets

Formation	Middle T (m^2/d) Range					
	Matrix	Dyke	Sill	Sill margin	Alluvium & intergranular	Alluvial basin
Adelaide-1	3.7	42	36	35	5.3	33
Adelaide-2	2.2	27	22	21	5.3	33
Adelaide-3	0.9	15	11	15	5.3	33
Adelaide-4	7.3	81	70	35	5.3	33
Adelaide-5	1.5	19	15	35	5.3	33
Burgersdorp	2.1	26	21	40	5.3	33
Clarens	1.7	20	16	7.3	5.3	33
Drakensburg	1.3	17	13	13	5.3	33
Dwyka-1	1.5	18	14	15	5.3	33
Dwyka-2	1.5	19	15	5.1	5.3	33
Dwyka-3	0.9	12	8.6	15	5.3	33
Ecca	1.9	23	18	18	5.3	33
Elliot	1.3	16	13	7.3	5.3	33
Katberg	2.4	27	22	15	5.3	33
Molteno	1.5	19	15	13	5.3	33
Msikaba	0.6	3.2	2.1	2.1	5.3	33
Pietermaritzburg	2.4	27	22	25	5.3	33
Prince Albert-1	1.3	16	12	15	5.3	33
Prince Albert-2	0.9	12	8.8	15	5.3	33
Tierberg 1+4, Fort Brown	1.9	22	18	16	5.3	33
Tierberg-2	1.9	23	18	16	5.3	33
Tierberg-3	1.9	23	18	15	5.3	33
Volksrust	1.3	16	12	10	5.3	33
Vryheid-1	0.7	9.4	6.9	8.4	5.3	33
Vryheid-2	0.9	13	10	8.4	5.3	33
Vryheid-3 and -4	1.7	20	16	14	5.3	33
Waterford-1 & -2	2.6	30	25	23	5.3	33
Whitehill	1.7	18	14	48	5.3	33

Table 4: Upper transmissivity range for all formations and groundwater structural targets

Formation	Upper T (m^2/d) Range					
	Matrix	Dyke	Sill	Sill margin	Alluvium & intergranular	Alluvial basin
Adelaide-1	27	282	210	420	44	255
Adelaide-2	17	176	112	167	44	255
Adelaide-3	8.5	84	51	84	44	255
Adelaide-4	54	483	389	420	44	255
Adelaide-5	11	128	87	420	44	255
Burgersdorp	16	179	93	222	44	255
Clarens	12	110	70	55	44	255
Drakensburg	10	91	72	72	44	255
Dwyka-1	11	144	100	112	44	255
Dwyka-2	11	133	70	79	44	255
Dwyka-3	14	88	54	112	44	255
Ecca	14	121	70	95	44	255
Elliot	10	123	71	55	44	255
Katberg	18	170	99	158	44	255
Molteno	11	128	86	86	44	255
Msikaba	4.4	70	27	27	44	255
Pietermaritzburg	18	144	79	139	44	255
Prince Albert-1	9.1	137	84	159	44	255
Prince Albert-2	7.2	57	48	159	44	255
Tierberg 1+4, Fort Brown	14	204	153	177	44	255
Tierberg-2	14	176	99	177	44	255
Tierberg-3	14	117	86	111	44	255
Volksrust	10	75	44	53	44	255
Vryheid-1	5.4	62	40	62	44	255
Vryheid-2	7.2	78	41	62	44	255
Vryheid-3 and -4	12	95	61	105	44	255
Waterford-1 & -2	19	242	134	199	44	255
Whitehill	13	122	87	122	44	255

In developing the final Transmissivity Maps (lower-T, middle-T and upper-T), judgement was used in which combinations of transmissivity values to use. For example, it was felt that the lower T-values for the matrix are reasonable estimates for the entire Karoo Basin, so only the lower T-matrix values were used (the T-middle and T-upper maps both use T-lower matrix values rather that middle and upper matrix values). The final combinations of ranges that were used to produce the lower, middle and upper T-value maps, are as follows:

- T-lower map: All lower values used
- T-middle map: The matrix and sills lower values are used, with the rest of the values from the middle (dykes; sill margins; alluvium & intergranular; alluvial basin)
- T-upper map: The matrix and sills lower values are used, with the rest of the values from the upper (dykes; sill margins; alluvium & intergranular; alluvial basin)

4.4 GIS methodology in creating the Transmissivity Maps

The GIS processing was done using ArcGIS Spatial Analyst by Dr C. Musekiwa of the CGS, Bellville as part of the WRC project K5/1763. Expert geological knowledge from the Council for Geoscience on the lithology of the 1: 250 000 geological maps of the study area was used to subdivide the area into lithological domains (Figure 16). The subdivision was based on the following criteria:

i) Distance from the source (distal or proximal) and direction of transport: The further from the source the less coarse the material (the ratio of sandstone/mudstone generally decreases).

ii) Deposition environment (continental, delta, shore): Environmental deposition of a unit can change from fluvial, deltaic, to prodeltaic to shoreline with consequences for lithology and grain size (coarse sandstone, siltstone, mudstone, shale).

iii) Lateral variation: interfingering with another unit, diachronous formations are numerous in the Karoo with specific consequence for the mudstone/sandstone/shale ratio and the thickness.

iv) Degree of metamorphism: The Karoo can be subdivided into separate metamorphic and diagenetic zones. Firstly the Cape Fold Belt has generated a tectono-metamorphic front that affected the southern part of the Karoo Basin with low grade metamorphism in the zeolite field. Secondly sediment burial under the Drakensberg pile has created a low calcite metamorphism condition. Thirdly dolerite intrusions have created regional thermal metamorphism.

v) Porosity: the Karoo sandstone and siltstone porosities were done by Rowsell and de Swardt (1976) from tests on drill cores from SOEKOR. North of latitude 29° higher porosity and permeabilities are encountered. These figures should however be taken with caution since they are average tests done on samples taken at different depths along the boreholes and do not reflect sub-surface conditions.

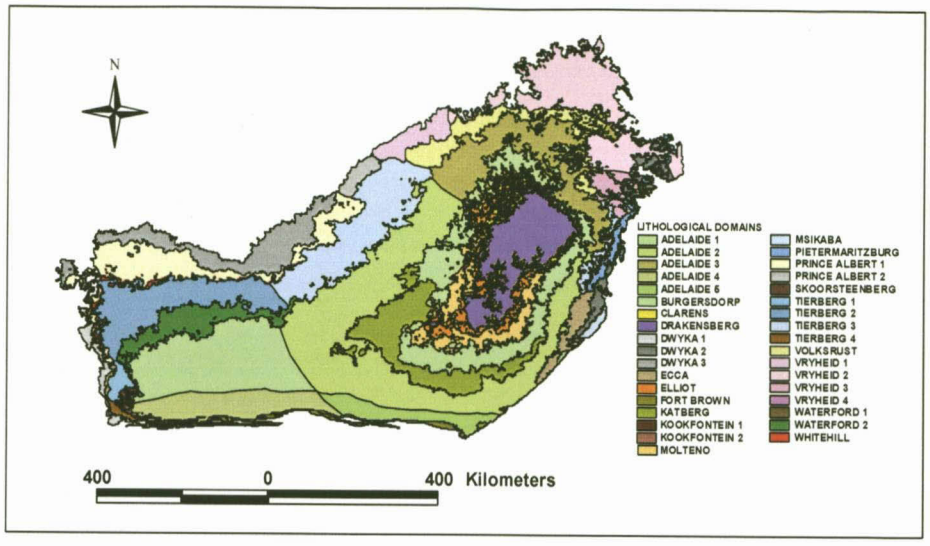

Figure 16. The lithological domains in the study area.

The following geological features were then clipped to the lithological domains:

i) dolerite sills

ii) dolerite dykes

iii) sills margins

The other geological features, namely alluvial basins and alluvium/intergranular areas were not subdivided into domains.

The dolerite sills and dykes were extracted from the 1: 250 000 Geological maps. The sill margin was created by buffering the outside of the sills by 150 m and this buffered area was then called the "sills margin" (Figure 17).

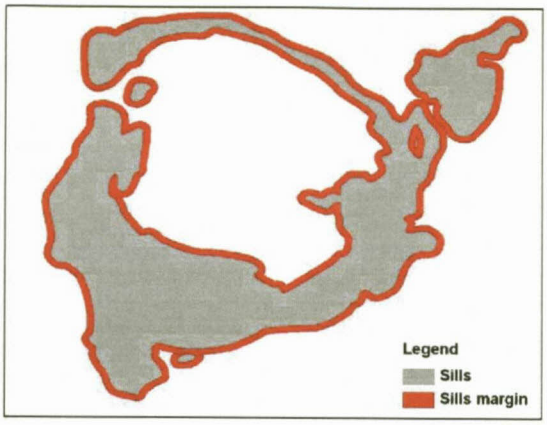

Figure 17. Illustrating the sills and the sills' margin layers

The alluvial basin dataset consists of the Cedarville flats alluvium (around Matatiele). The alluvium intergranular was created by combining the following datasets (Figure 18):

i) Areas classified as "integranular with borehole yields from 2 – 5 L/s and yields >5 L/s" from DWA's 1: 500 000 scale geohydrological maps.

ii) The result of intersecting major rivers (buffered by 300 m) with the alluvium from 1:250 000 geological maps.

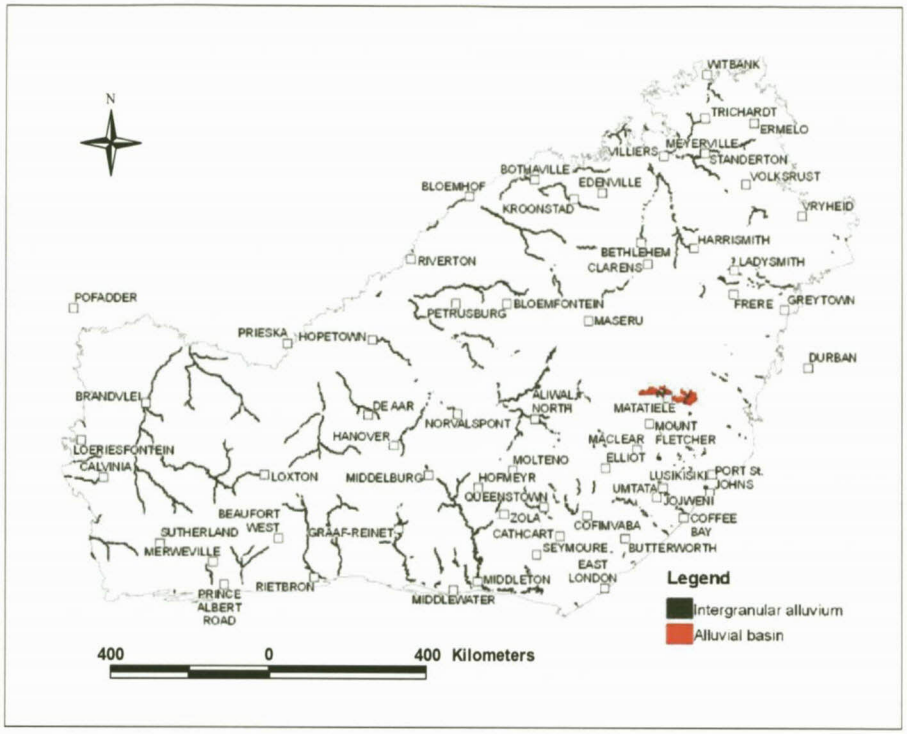

Figure 18. The alluvial basin data and the intergranular alluvium

For creating the final Transmissivity Maps, the following procedure was followed:

i) Raster files of lower, middle and upper T-values were created for each lithology, the alluvial basin, the intergranular alluvium and each structural target (dykes, sills and sill margins);

ii) These were then combined using the values shown in Tables 2-4 to create the final Transmissivity Maps.

The process is illustrated in Figure 19.

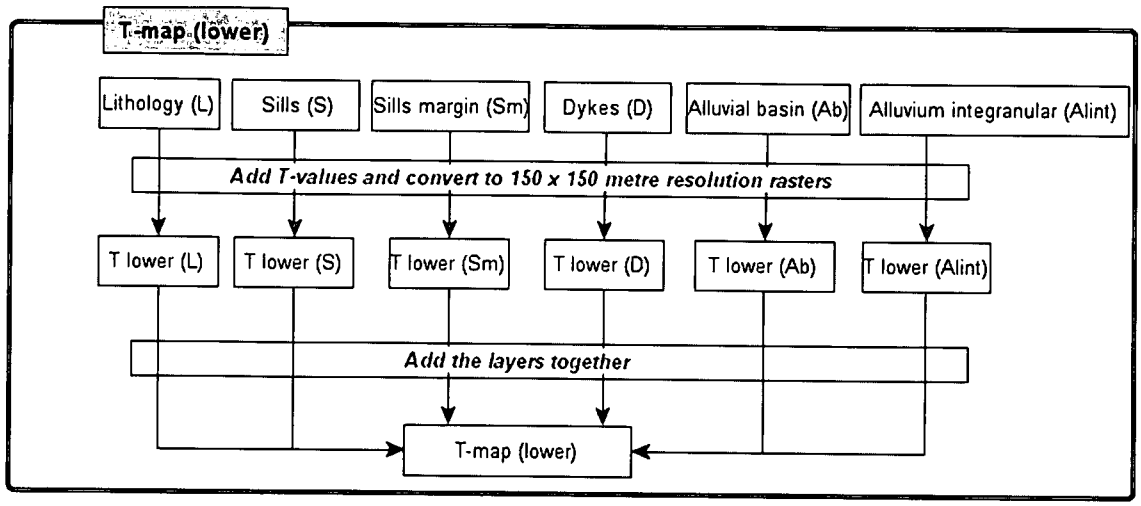

Figure 19. A flow chart showing the process of creating the T-maps; the T_lower map is used as an example.

4.5 The final Transmissivity Maps

The final Transmissivity Maps are shown in Figures 20 – 25. It must be noted that these maps were produced as "working" maps, and can only be used as such in electronic format. At small scales, they appear rather "uneventful", however, as the scale increases, so the high transmissive areas start to stand out and linear zones, e.g. dykes, can be seen.

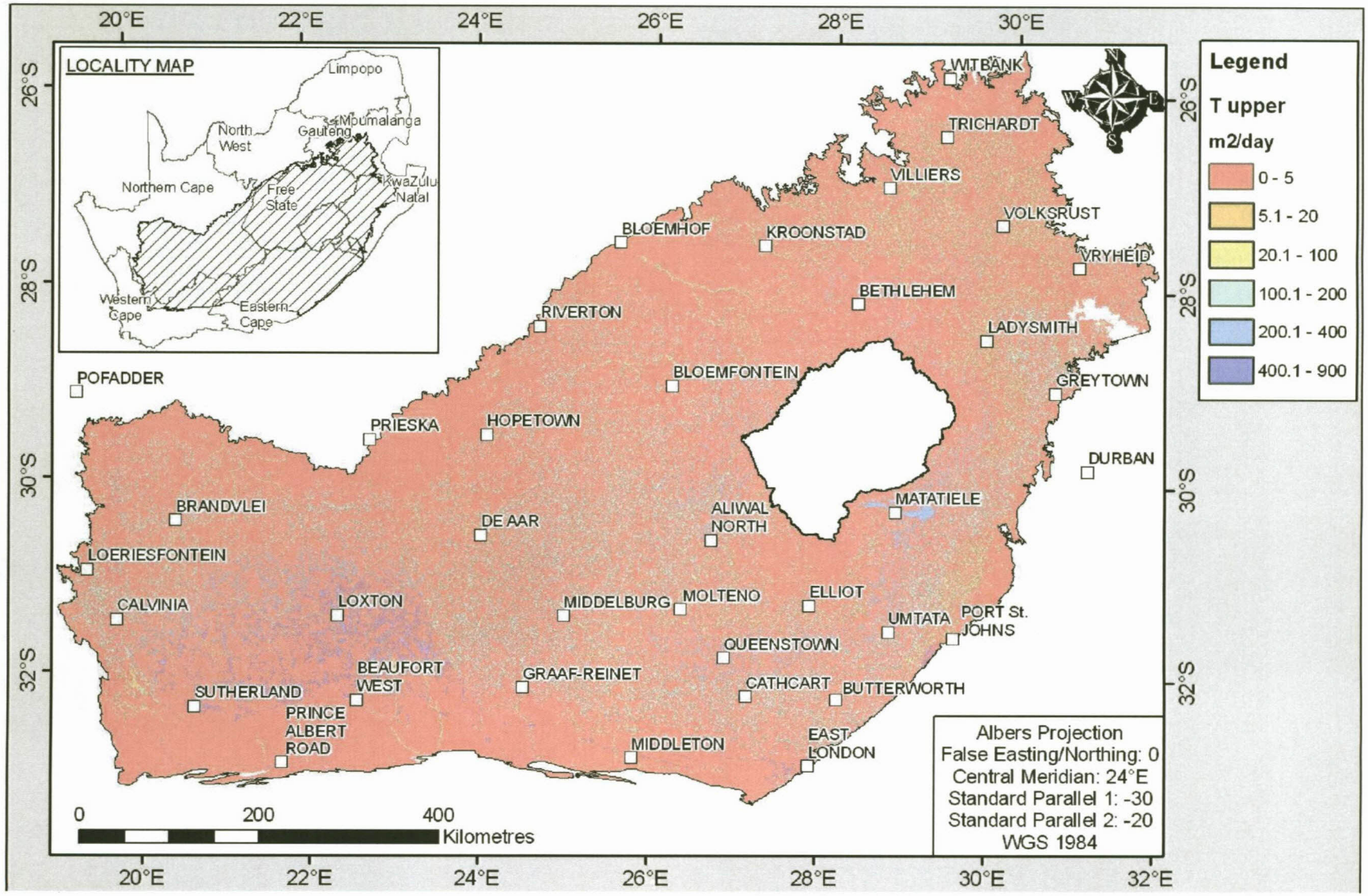

Figure 20. T-upper map of the Main Karoo Basin.

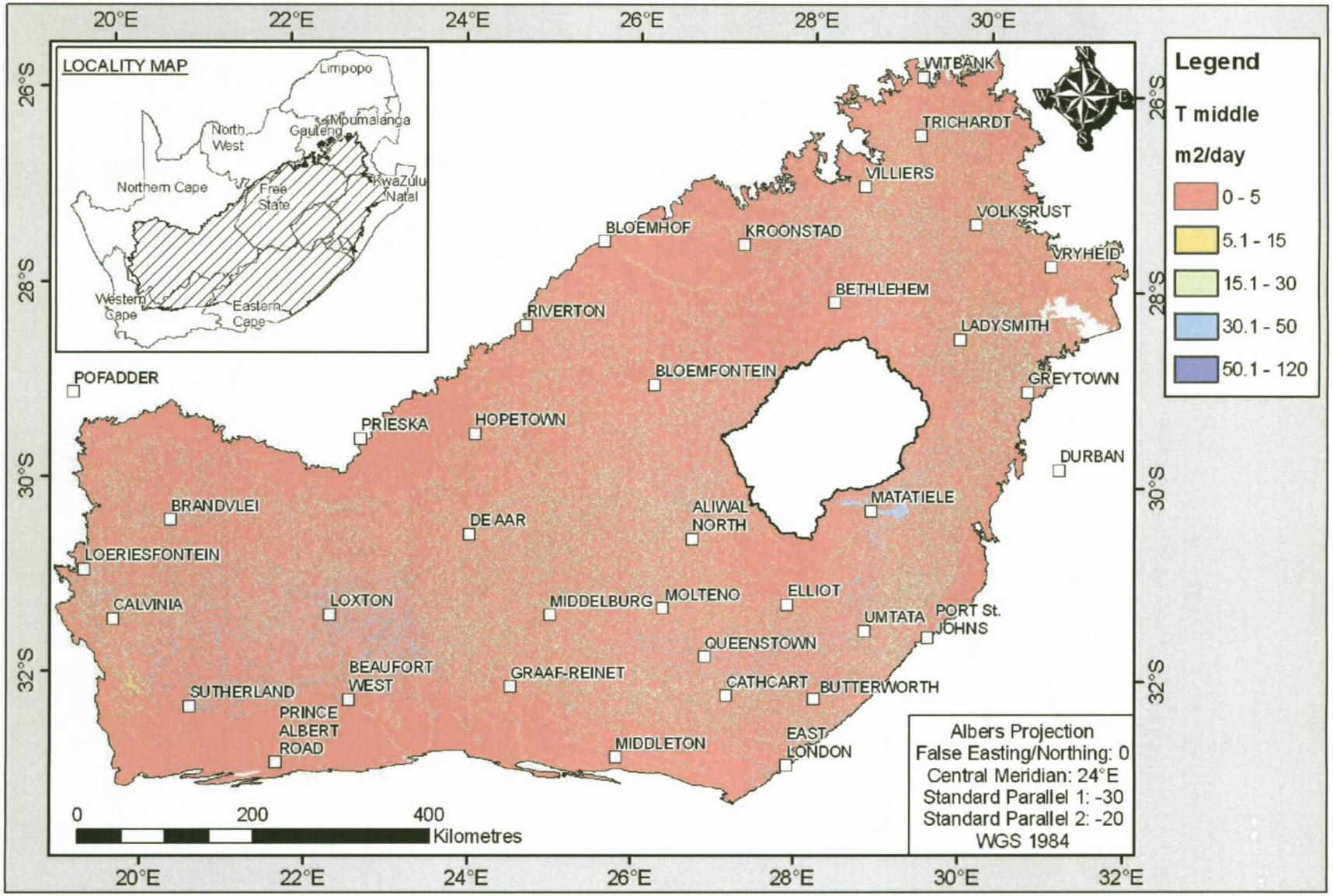

Figure 21. T-middle map of the Main Karoo Basin.

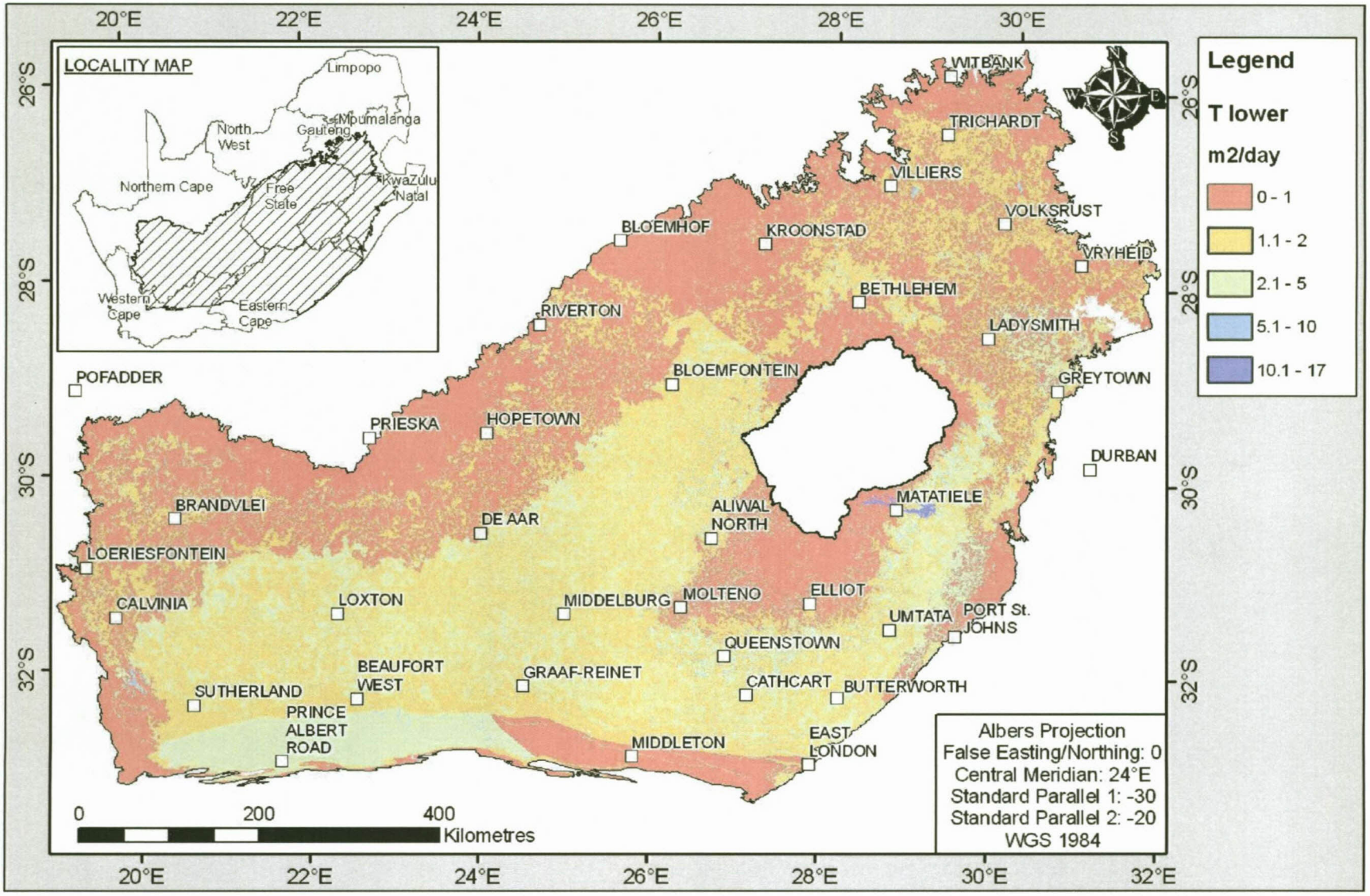

Figure 22. T-lower map of the Main Karoo Basin.

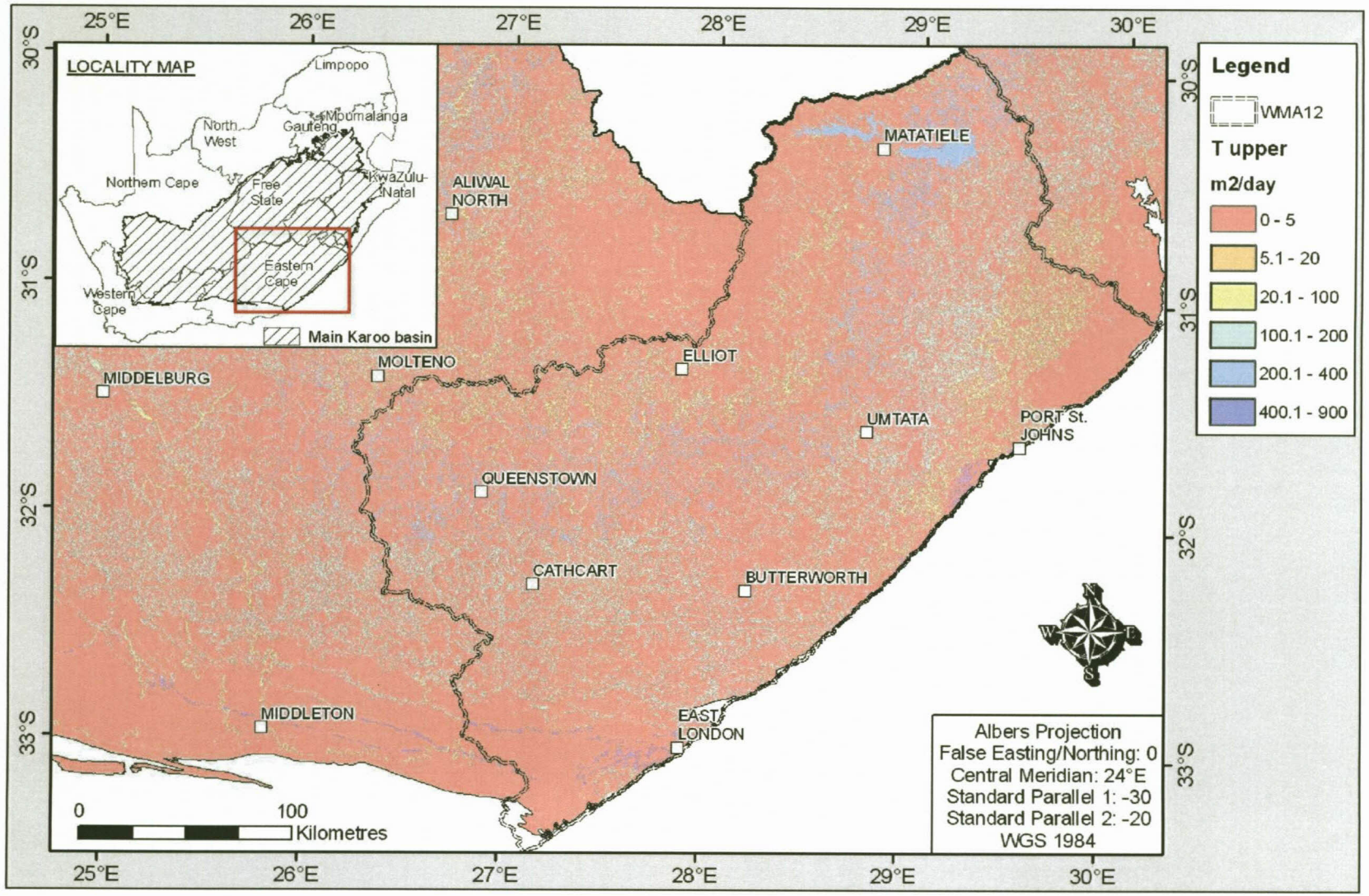

Figure 23. T-upper map for WMA12.

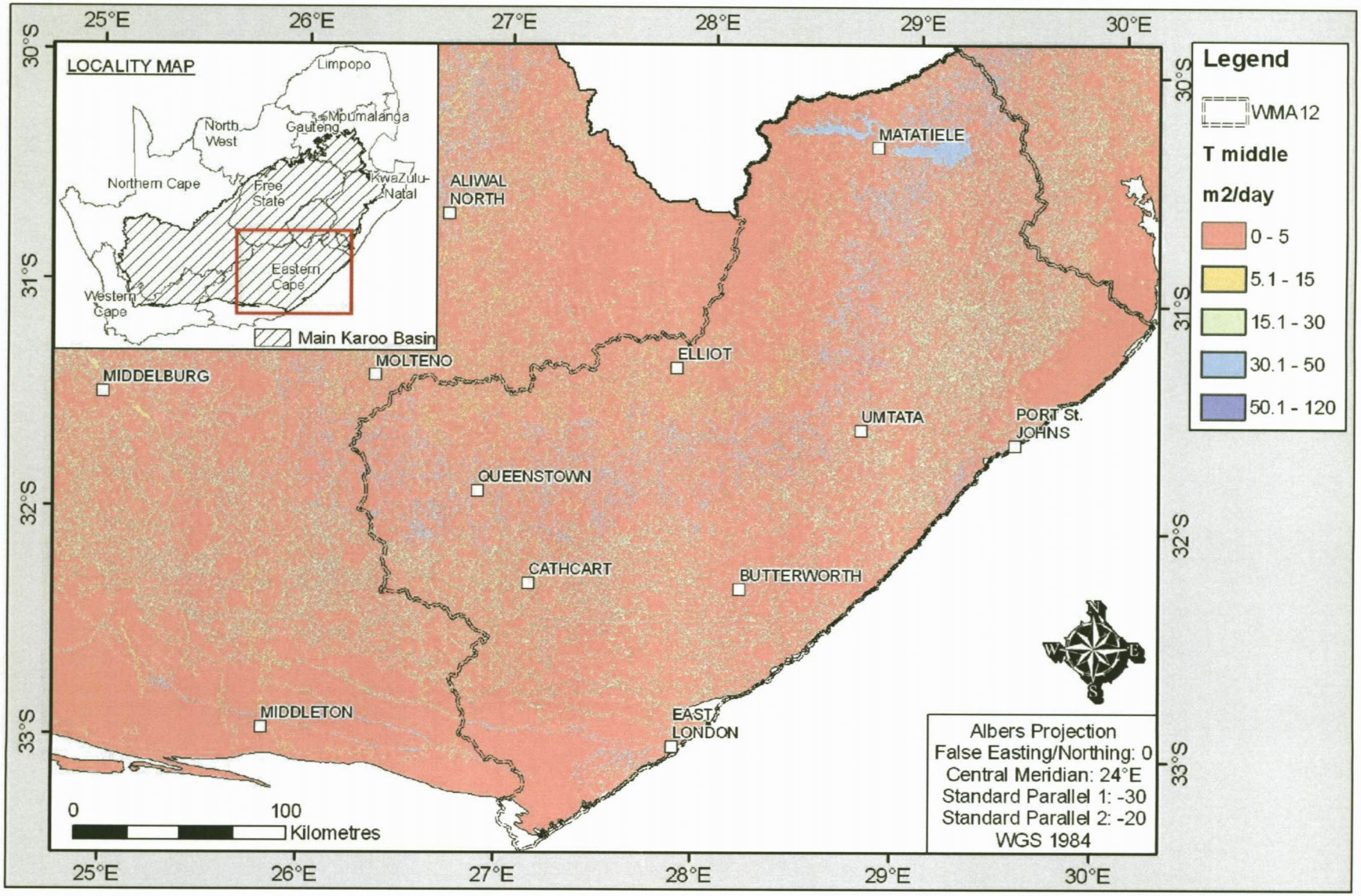

Figure 24. T-middle map for WMA12.

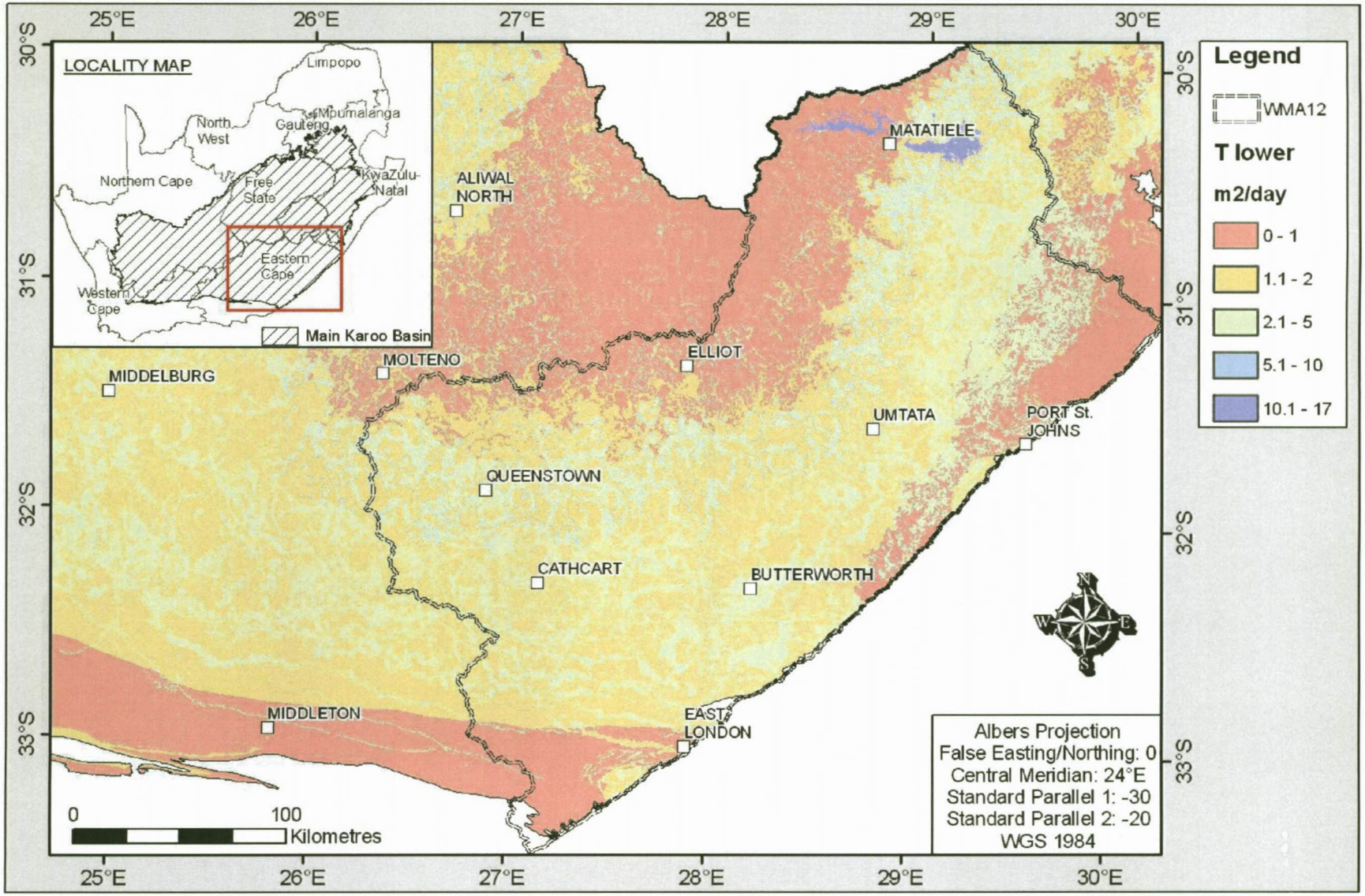

Figure 25. T-lower map for WMA12.

Figure 26 below shows how the maps can be used in electronic format to provide guidance in selecting transmissivity values.

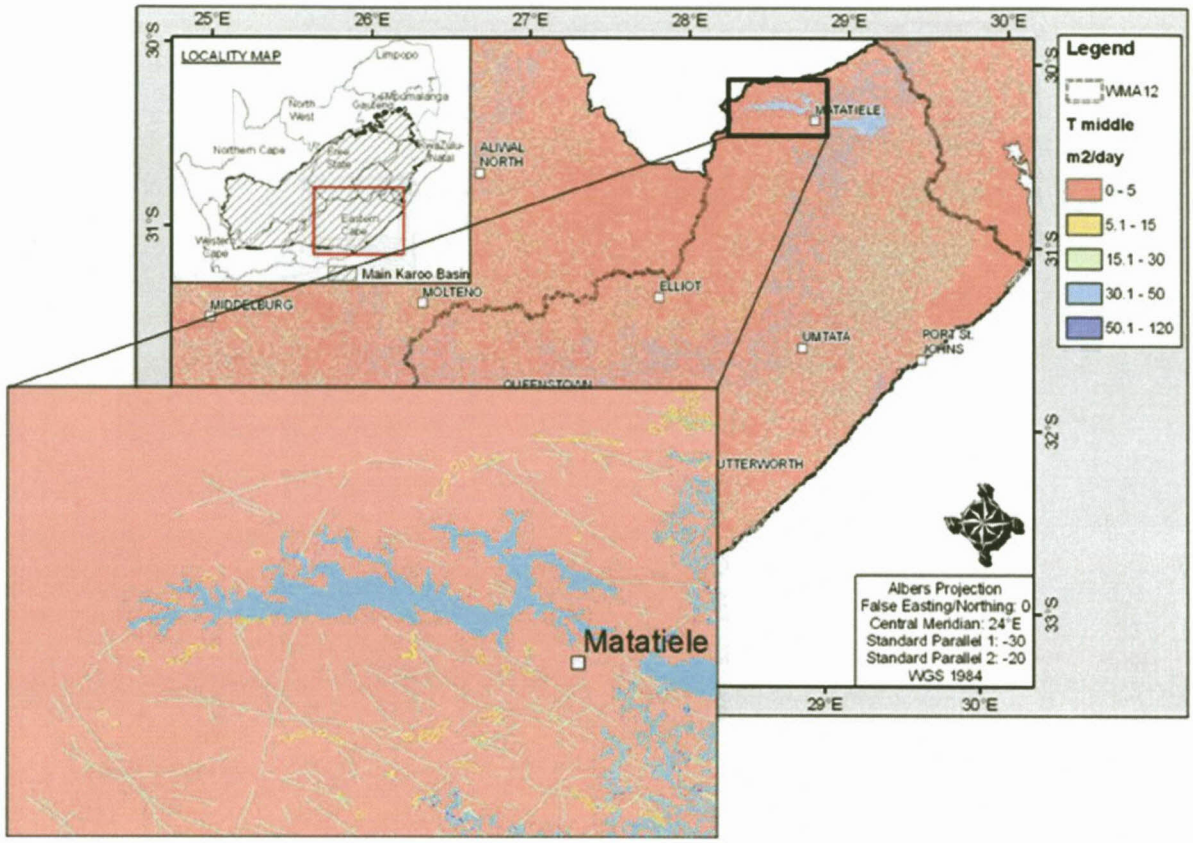

Figure 26. A detailed image of the area surrounding Matatiele, clearly displaying zones of high transmissivity.

4.6 Conclusion

The aim of this chapter was to address the concerns raised in the literature review regarding the previous transmissivity maps produced. This was be done by expanding on Woodford's method (in Dondo *et al.* 2010) whereby transmissivity maps were created using extensive borehole data and incorporating the geology and structural targets considered during borehole siting. While these Transmissivity Maps are the most detailed maps ever produced for the Main Karoo Basin, they can clearly be improved upon. Key to this would be developing new transmissivity-yield relationships for the entire Karoo Basin – a task that would require interpreting hundreds, if not thousands of pumping test data; and accurately relating groundwater structural targets, like dykes, sills, ring-

structures, etc to borehole yields. In the chapter on Case Studies, it will be shown how accurate the Transmissivity Map is in relation to transmissivity values that have been obtained from pumping test data.

Chapter 5

5 Aquifer Assured Yield Model

5.1 Literature Review

5.1.1 Background

The first negative effects of large scale groundwater abstraction resulted in early debate of the concept of a safe yield. In 1920, Meinzer described this concept after large-scale abstraction began in the USA, and since then many individuals have further discussed and expanded on this concept and on approaches to quantifying groundwater. The development of *datasets* with estimates of groundwater availability for the country, however, has only in recent times been established. Prior to the production of the datasets, various individuals attempted to quantify the groundwater resources of South Africa, such as Enslin (1970), but these attempts have not been considered sufficiently accurate (Baron *et al.,* 1998). In 1995 Vegter produced a map titled "The Groundwater Resources of South Africa" (Vegter, 1995), which was a useful indication of groundwater availability on a regional scale. His work was further developed in 1998 by Baron, Seward and Seymour (Baron *et al.,* 1998), who produced the *'Groundwater Harvest Potential'* Map of South Africa. Recharge, aquifer storage and time periods between recharge events were used to determine the sustainable yield which represented the volume of groundwater that can be abstracted per year without depleting the aquifer. It provided the first national estimate of the sustainable groundwater resource, and could be applied at a regional scale with moderate accuracy. This method, however, does not consider the abstractable portion of groundwater and also includes baseflow, thus values obtained are high in comparison to more recent estimates (Baron *et al.,* 1998).

In 2003, the Department of Water Affairs produced Phase 2 Groundwater Resources Assessment (GRAII) (DWAF, 2006), which aids in allocating groundwater use. A GIS model was produced on a 1 km by 1 km grid which was later summarised per quaternary catchment. It is applicable to both large and small scale quantification (the former occasionally having low confidence), and can be updated with further research and expansion. The yields provided were intended to be reliable during droughts, allow for increased availability when recharge is above average and must consider environmental and social issues (DWAF, 2006). The database is designed using a number of components which have been incorporated in the Aquifer Assured Yield Model (AAYM). These

components are aquifer storage, aquifer recharge, average regional groundwater level and maximum allowable water level drawdown (MAWD).

Assigning groundwater yields with levels of assurance seems to have never been done before, even though it is the most common method used by surface water engineers and hydrologists. This may be a consequence of the concept of groundwater storage, which is considered "open" or "infinite" in comparison to the dams or reservoirs with fixed volumes that the surface water professionals deal with, and thus the concept should not apply to groundwater as it does to the science of reservoir yield quantification. The concept of providing an assured groundwater yield estimate, however, seems reasonable and worthy of pursuit. The work presented in this chapter is pioneering and thus should be considered as an initial assessment because a first attempt to produce a "perfect" methodology and model is simply not possible. It requires an iterative process of development, testing, modifying and continuous re-testing. This model is currently being upgraded as part of the WRC's K1763 project, and the revised model, programmed by Dr R Dennis of the IGS, is expected to be complete in June 2011.

5.1.2 Concept of the assured yield

Although more recent models have shifted away from the original concept of a safe yield, many still neglect to specify the degree of risk of a supply shortage, which relates to the variability of rainfall and thus recharge. By overlooking this element, it is assumed that the supply is guaranteed, which is unlikely unless the volume to be abstracted is negligible in comparison to the rate of recharge and volume of groundwater in storage (Woodford, WRC Project K1763, Deliverable 4f, 2010).

Natural groundwater systems are in equilibrium when in their steady, or unstressed, state. Thus to assume that the recharge to a system is directly equivalent to the abstractable volume of groundwater, originally referred to as the *safe yield*, is incorrect. Natural recharge is, essentially, not necessarily available for abstraction as it may be needed down-gradient by rivers and baseflow. It is therefore a complex investigation to determine the safe yield as it is difficult to establish the origin of the groundwater abstracted by pumping boreholes (Balleau, 1988 & Sophocleous, 1998).

An alternative to the safe yield has thus been incorporated, named the assured yield, which has been primarily implemented by civil engineers and hydrologists to determine the reliability of the yield as a specified rate. The assured yield is a risk based estimation determined by statistical

analysis of long-term time-series data such as inflow and storage and is dependent on the demand as well as the design parameters of the system. The suggested reliability or risk of failure can be characterised in terms of a time period during which supply cannot meet the demand, in other words, when the assured yield may not be supplied in full. For example a 90% assurance of supply defines a risk of shortages on average in 10 out of every 100 years. The volume of storage in an aquifer is vital in this assessment as the storage acts as a buffer during times of drought. When considering this volume, the use of groundwater and surface water must be evaluated as they are closely interlinked with regards to their recharge, discharge and storage fluctuations (Woodford, WRC Project K1763, Deliverable 4f, 2010). Surplus groundwater removed from a system can be taken when:

1) more water has entered the system (i.e. increased recharge)

2) less water has left the system (i.e. decreased discharge)

3) water can be removed from storage

(Woodford, *et al.,* WRC Project K1763, Deliverable 4a, 2008)

5.2 Introduction: The Aquifer Assured Yield Model (AAYM)

The aim of this chapter is to evaluate and critically review the AAYM Version 1.0.77 in terms of the parameters incorporated in the model, the sensitivity of the model to the parameters used in the determination of an assured yield and the results in comparison to previous established databases such as the GRAII AGEP and HP. It must be noted that the AAYM is only designed for initial planning and assessment of groundwater resource development where alternative options for water supply are being considered, and there is a lack of spatial and temporal hydrological information.

The AAYM is a single-cell, lumped parameter model which makes use of existing geohydrological data such as GRAII Average Groundwater Exploitation Potential (AGEP) Drought and Normal conditions (DWAF, 2006), WR2005 (Midgley *et al.,* 1994) and various other data sources for individual parameters. It is a simple groundwater balance model that reproduces storage dynamics based on variable volumes of inflow and outflow. The model assumes the following:

- Karoo fractured-rock aquifers can be adequately represented as single-layer conceptual hydrogeological system.
- The aquifer is unconfined to semi-unconfined and characterised by a specific yield.

- The aquifer system is 'water-tight' in that no groundwater inflow from or outflow to adjoining aquifers occurs (i.e. net inflow = outflow)
- Groundwater abstraction takes place evenly across the entire surface area of the aquifer system.

The water balance equation describing the lumped box model is given as follows:

$$\Delta S = R + Q_I - E_T - Q_O \qquad \text{Equation 6}$$

Where:

R = potential recharge to groundwater system

Q_I = groundwater inflow to the system

Q_O = groundwater outflow from the system

E_T = evapotranspiration

ΔS = change in groundwater storage in the system

Equation 6 is balanced and represents the aquifer system when it is in steady state. Estimates for Q_I, E_T and Q_O are obtained through the various data sets which can be seen below in Table 5.

Table 5: Flow parameters used in the AAYM and their sources.

	Parameter	**Units**	**Source**
Inflow	Inflow/Recharge	% MAP	GRAII
Outflow	Evapotranspiration	mm/a	Schulze (1997)
	Outflow/Baseflow	mm/a	GRAII, Pitman, Schulze, Hughes

The development of the Assured Yield Model was carried out by the following team: Mr A. Wooford, Dr R. Murray, Mr P. Ravenscroft, Miss K. Baker and Dr R Dennis. Initially, the model was programmed by Mr Woodford, with input from Dr Murray and Mr Ravenscroft, and later by Miss Baker. Mr Woodford, however, left the country which resulted in the ceasing of further development of the model by the end of 2009, referred to as AAYM version 1.0.77.

5.2.1 Model parameters

Quaternary catchment

The models are based on a Quaternary catchment scale, the areas of which relate to surface water boundaries i.e. topographical boundaries as shown in Figure 27. The assumption is made that a water balance approach, that includes a groundwater component, can be applied to such an area.

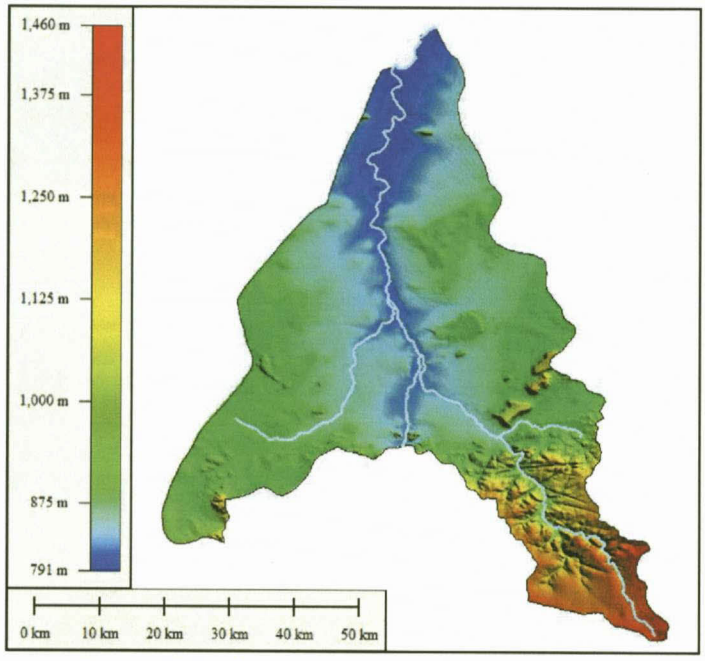

Figure 27. Surface water catchment area

The implication of this assumption is that the boundaries of the catchment area are treated as natural groundwater divides and that all groundwater will also report to the draining system at one point or another as shown in Figure 28.

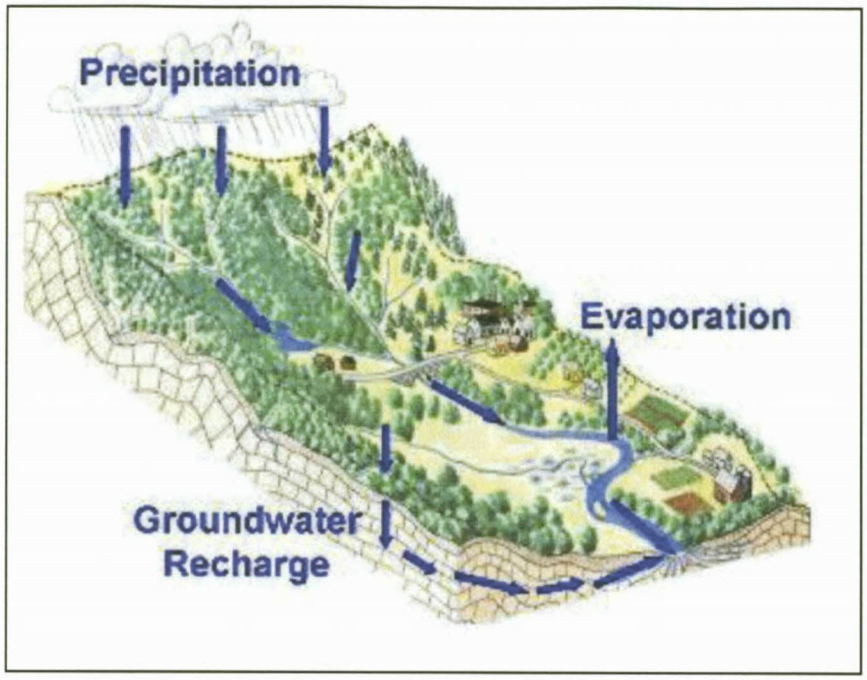

Figure 28. Conceptual model of quaternary catchment

Recharge from rainfall

The model simulates aquifer storage changes based on recharge from rainfall and abstraction from the system. A monthly time series of rainfall recharge is calculated by the model, using GRAII's average recharge factor (as % MAP) (DWAF, 2006) and the WR2005 (Midgley *et al.*, 1994) monthly time series of rainfall, which is on average 1020 months, from October 1919 to September 2004 (Woodford, 2010). These rainfall records are developed through combining data from individual rainfall stations from all zones across South Africa. Within the rainfall zones, are quaternary catchments, thus more than one quaternary catchment will be found in a zone (Dennis, WRC Project K1763, Deliverable 16, 2011).

Threshold

The threshold is defined as the minimum amount of rainfall required in order for recharge of an aquifer to take place; no recharge will occur if rainfall is below this value. Bean (2003) describes a relationship between recharge and GRAII's Static Water Levels (SWL) of fractured aquifers in terms of a time lag between rainfall and water level response. Recharge within these aquifers can occur either via preferred pathways, for example fracture flow and animal burrows, characterised by a short time lag, or through the rock matrix during periods of low rainfall, typically producing lengthy

time lags. Time lags, however, can be site specific varying spatially from borehole to borehole in an aquifer, as well as varying temporally over months or years in a single borehole. Variations depend on a number of factors including land use, moisture content of the unsaturated zone and pumping rates. In field conditions, a single threshold applied throughout the seasonal variations will not hold true as arid and semi-arid environments are characterized by extended periods of very low rainfall with intermittent episodic recharge events (Bean, 2003). Extended periods of below average rainfall will naturally require a different (lower) threshold compared to the average threshold. It is therefore apparent that an aquifer in an arid to semi-arid climate will require multiple thresholds when considering field conditions. Although recharge is a complex process that depends on a number of factors which can differ in time and over a catchment, the AAYM only allows for a single value to be applied, which is obtained as regional data sets based on parameters applied at a quaternary catchment scale.

Threshold = MAP/12 Equation 7

(Bean, 2003)

The option of the implementation of a threshold is provided in the AAYM and is user specified. If the user does not wish to apply a threshold, the default value can remain, which is zero.

Baseflow

The debate on baseflow and its role in surface and groundwater interaction has been ongoing for many years. The determination of this value is either obtained through baseflow separation or recession curve estimations. Various models exist that estimate this component on quaternary catchment scale (Dennis, WRC Project K1763, Deliverable 16, 2011). A monthly baseflow was produced by conversion of the mean annual baseflow (MAB/12) thereby providing a constant baseflow value for each month of the year to be used in AAYM (Woodford, WRC Project K1763, Deliverable 4f, 2010). The variation of baseflow is non-linear and depends on changes in aquifer storage and volume of runoff (Woodford *et al.,* WRC Project K1763, Deliverable 4a, 2008). Different options within the mean annual baseflow tab include GRAII (DWAF, 2006), Pitman (default) (Midgley *et al.,* 1994), Schultze (Schultze, 1997), and Hughes (which incorporates interflow, thus providing relatively high values in comparison to other estimates) (Hughes *et al.,* 2007). Generally, the GRAII values are the lowest and the Hughes' the highest, with the two remaining baseflow values lying in

between. An additional, *user specified* baseflow option is available whereby the user can enter a different annual baseflow value. The selected baseflow value will be used in the AAYM as a constant value to ensure that a specific volume of water is reserved for baseflow. In steady and transient conditions the model will make use of the allocated baseflow as stress conditions are reached.

Evapotranspiration (EVTP)

Evapotranspiration refers to the volume of water removed from the storage of an aquifer by evaporation, and transpiration from plants. Its application in AAYM is limited both horizontally and vertically. Spatially, evapotranspiration is restricted to the area (a default, but adjustable value) represented by the percentage of a catchment area exposed to evapotranspiration, referred to as the riparian zone. Vertically, the area extends from the regional water level lying below surface, to a user specified depth below the water level referred to as the Evapotranspiration Extinction Depth (ED) (Woodford, WRC Project K1763, Deliverable 4f, 2010 & Dennis, WRC Project K1763, Deliverable 16, 2011). It is a simulated annual output of AAYM and requires the selection of the rate at which it will occur, the maximum rate occurring at surface either running at a *constant* rate, ceasing at the ED, or decreasing towards the ED at a *linear* (default) or *exponential* rate.

Equation 8 is used to estimate monthly groundwater evapotranspiration from the riparian zone:

$$EP_{AAYM}(t) = [EP(i) - R_R(t)] \times \left[\frac{D_E - WL_R(t-1)}{D_E}\right]^{Pf} \qquad \text{Equation 8}$$

Where:

EP_{AAYM} = monthly time series of evapotranspiration (mm)

EP = mean Penman-Monteith potential evapotranspiration for a given month (i = 1... 12) of the year

R_R = rainfall (mm) for a given month in the time series (t = 1 to 1020; i.e. from October 1919 to September 2004)

WL_R = previous months (t - 1) regional water level (metres below surface)

D_E = extinction depth (m)

P_f = 0 (constant EVTP rate), 1 (linear EVTP rate, default), 2.5 (exponential EVTP rate)

(Dennis, WRC Project K1763, Deliverable 16, 2011)

AAYM operates on potential and actual evapotranspiration. Potential evapotranspiration refers to the greatest amount of vapour that is able to enter the atmosphere from an area with certain meteorological conditions. Actual evapotranspiration is the actual amount of vapour that enters the atmosphere, and depends on the meteorological conditions as well as the ability of the vegetation and hence water to meet the atmospheric demands (Kirchner *et al.*, 1991).

It is recommended that firstly, evapotranspiration be applied at a linear rate, and secondly that the extinction depth be set according to MAP. The values used in testing the model are listed in Table 6. These values are rough estimates and were applied as a first attempt to gain a better understanding of the role evapotranspiration plays in the AAYM.

Table 6: ED values used in testing the AAYM

MAP (mm/a)	ED (m)
0-200	1
200-400	2
>400	4

Maximum Allowable Water Level Drawdown (MAWD)

The MAWD is only used when the model is run in the assured yield mode. It is a user specified level (usually based on management restrictions) representing the lowest level the regional groundwater level may reach (Woodford, WRC Project K1763, Deliverable 4f, 2010).

5.2.2 Application of AAYM Model Version 1.0.77

The AAYM operates in two consecutive modes, ambient and assured yield:

Ambient mode

The first, *'ambient'*, mode is run following the selection of parameters and their relative operation to determine the initial water balance of the quaternary catchment. The parameters must be realistically set to obtain a satisfactory water level balance. This mode operates with no abstraction and is run by selecting the 'Run Ambient Model' tab (Figure 29).

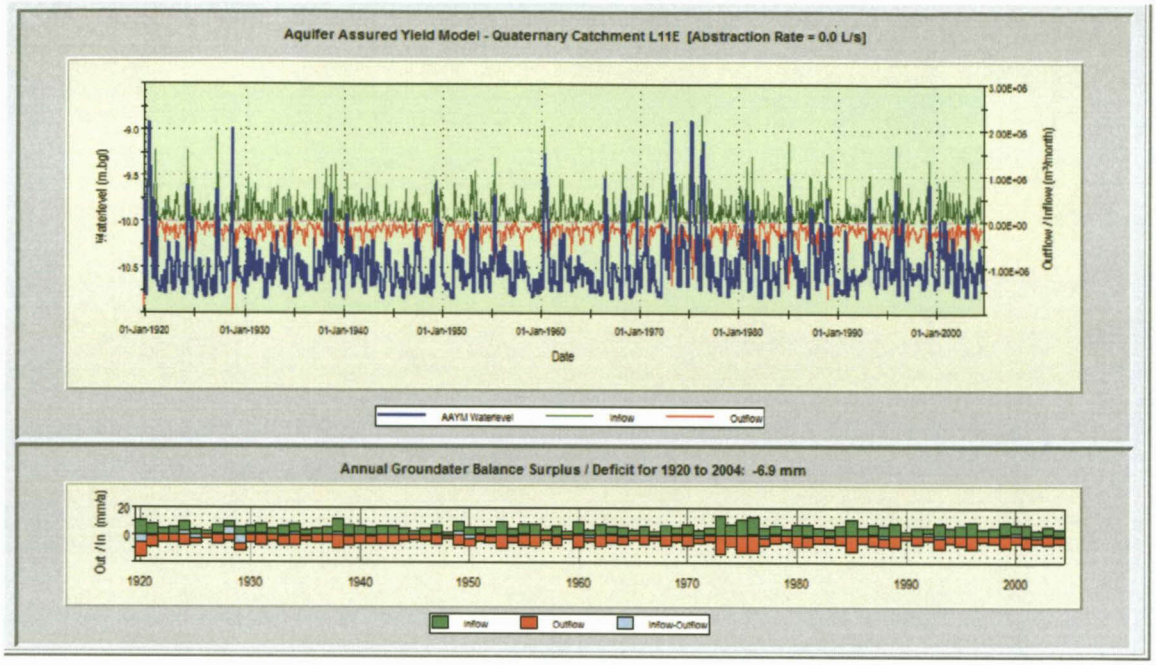

Figure 29. AAYM output – Ambient mode

Assured Yield Mode

Once an appropriate water balance is obtained, the model can be run in the assured yield mode whereby various assured yields will be determined as the AAYM applies an increasing abstraction on the catchment and the water level is monitored relative to the MAWD. The catchment will experience a drop in regional water level as abstraction from the system is gradually increased and whenever the water level crosses the MAWD, at any time between 1919 and 2004, this will count as one failure (see Figure 30 below, the circles indicate failures). Abstraction will continue to be increased until the regional water level remains below the MAWD for the entire period of time. The yields determined increase in level of assurance of supply, from 90% to 100%. This operation can be run by selecting the 'Run Assured Yield Model' tab.

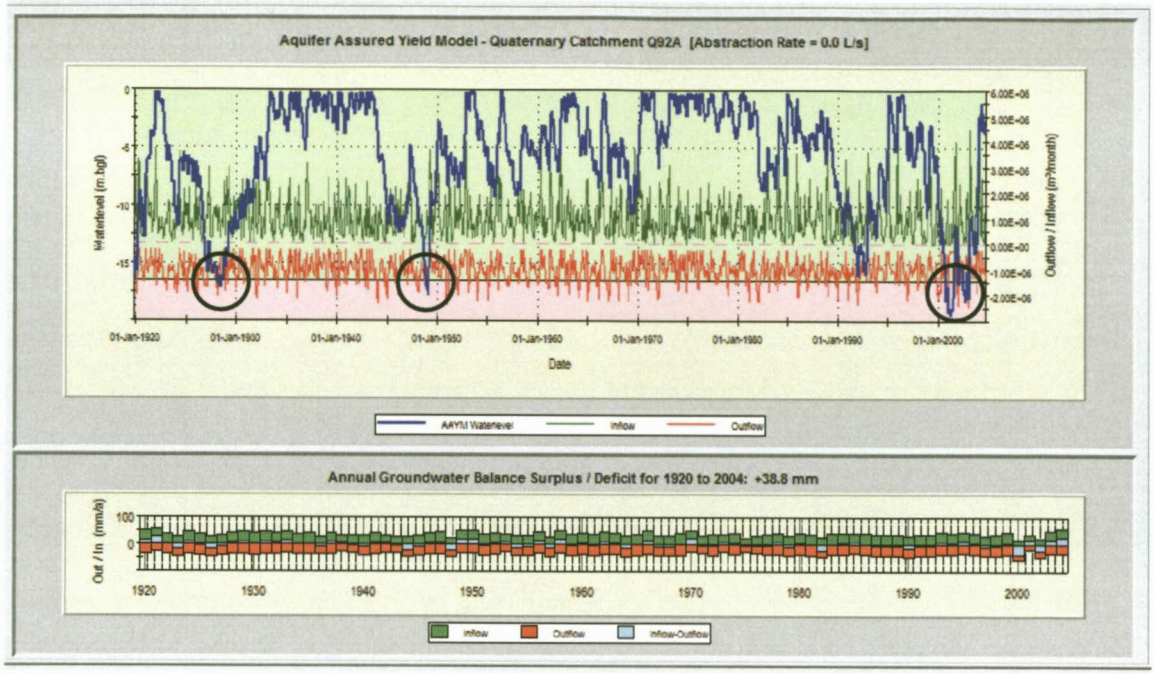

Figure 30. AAYM output – Assured Yield mode

The model displays the following outputs during these modes of operation:

- Output spreadsheet.
    - In Ambient mode: This contains relevant information such as potential and actual recharge to the system, potential and actual evapotranspiration, potential and actually baseflow and the average regional water level. This spreadsheet can also be exported and saved as an excel file.
    - In assured yield mode: This contains the 90%, 95%, 98% and 100% aquifer yields in $m^3/km^2/a$ and L/s, as well as the associated exceedance probabilities.
- The Graph aquifer storage simulation displays a graphical output of the ambient mode. This displays the regional water level with total aquifer inflow and outflow (See Figure 29 above).
- The Graph aquifer yield simulation displays a graphical output of assured yield mode (see Figure 30 above). This shows the probability of the regional water table exceeding the MAWD once in any 12 month period and the probability of exceedance in all 12 monthly time periods; a vertical line indicates the position of the aquifer yields at various levels of

assurance; and two vertical lines showing the position of GRAII's AGEP drought and normal aquifer yield estimates.

- Summary water balance graph.
    - 'Average' annual catchment water balance. Showing effective groundwater recharge, surface water runoff and 'other' water components of the water balance such as evapotranspiration, seen in Figure 31. All values are in mm/a and % MAP.

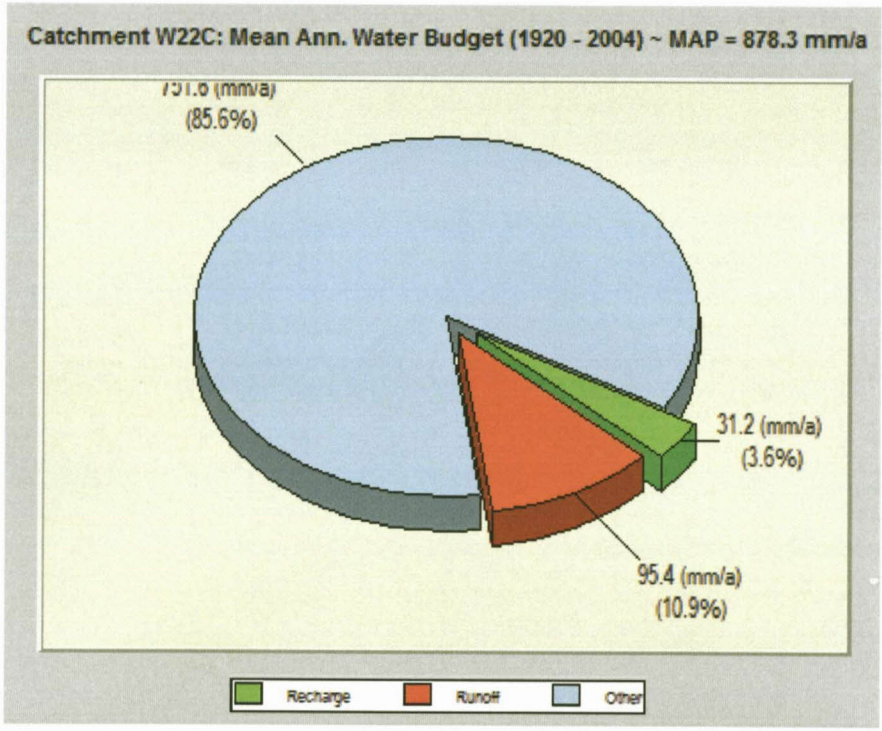

Figure 31. Average annual catchment water balance.

    - 'Average' annual catchment groundwater balance. This shows the total abstraction, baseflow loss to rivers, changes in aquifer storage, evapotranspiration losses from the riparian zone and effective recharge (Figure 32). All values are in mm/a and % of the input to and losses from the aquifer system.

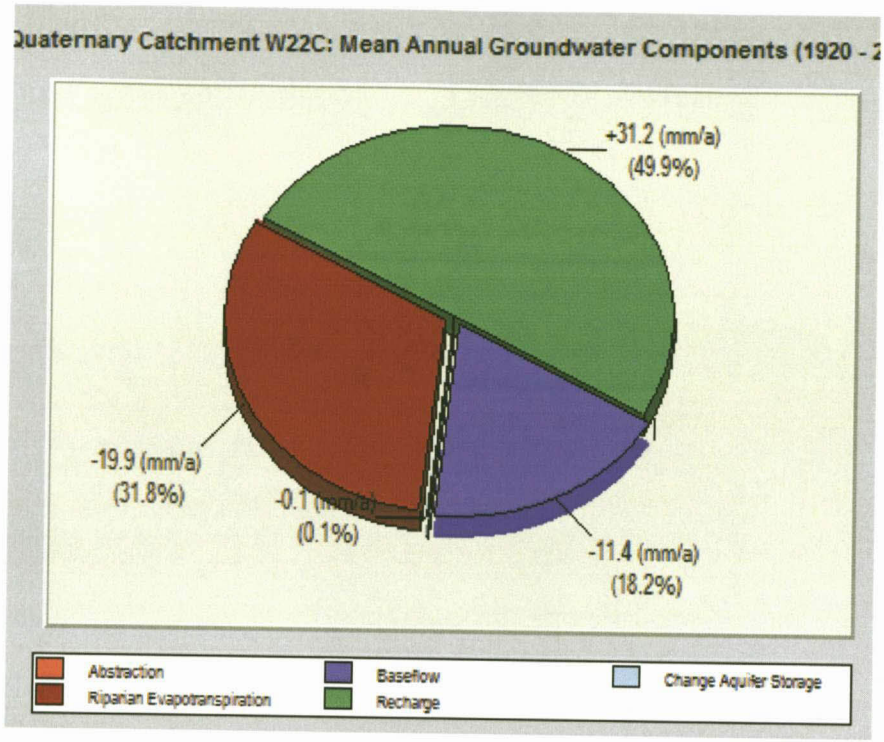

Figure 32. Average annual catchment groundwater balance.

(Woodford, WRC Project K1763, Deliverable 4f, 2010)

5.3 Methodology and results

As part of critically reviewing the AAYM, four main processes were carried out in this chapter:

1. Assessing whether AAYM water levels mimic reality
2. Conducting a sensitivity analyses
3. Establishing guiding principles on applying the AAYM
4. Comparing the AAYM yields with GRAII and Harvest Potential yields

5.3.1 A Comparison between AAYM Groundwater Levels and Measured Groundwater Levels

(Taken from WRC Project K1763, Deliverable 14, Progress Report no. 2, Appendix 4, Baker & Murray, 2009).

In order to assess whether the AAYM's groundwater level trends resemble reality, modeled water levels were compared to actual borehole water levels. Borehole water level data was obtained from DWA and only those boreholes that have been monitored for several years were used in this assessment. General information has been given regarding the area in which the boreholes are found (Tables 7 - 9). In many cases it is evident that the actual water levels are affected by nearby abstraction, and therefore are not suitable for use.

Trends in simulated AAYM water levels were compared to actual groundwater level trends from DWA monitoring boreholes (Figures 33 - 35). In this exercise, actual water levels (i.e. depth) are not relevant as the aim here was to establish whether the AAYM reasonably represented reality in relation to water level trends – i.e. do AAYM water levels show a corresponding rise when actual groundwater levels rose? Actual water levels can be significantly different to AAYM water levels as actual water levels may be deep if the borehole is located in a high-lying area, and shallow if located in a valley.

Results

Table 7: Borehole information – N14D

Quaternary catchment	**N14D**
Town	Aberdeen
MAP (mm)	289.7
Boreholes	N1N0042: Production borehole or close to production borehole N1N0046: Nearest monitoring borehole N1N0047: Furthest monitoring borehole that represents ambient or unaffected conditions the best.
Topography/geology	All boreholes lie near a primary river. Geology consists of Adelaide Formation mudstone of the Beaufort Group.
General comments	The most similarities in water level variations are observed between AAYM and N1N0047. Peaks and dips can be traced in borehole N1N0046 although it displays a higher degree of irregularity due to the closer proximity to the pumping borehole.
WL fluctuations	AAYM and N1N0047 water levels fluctuate less than 2 m.
Lag time between AAYM and borehole water level	Approximately 1 year.

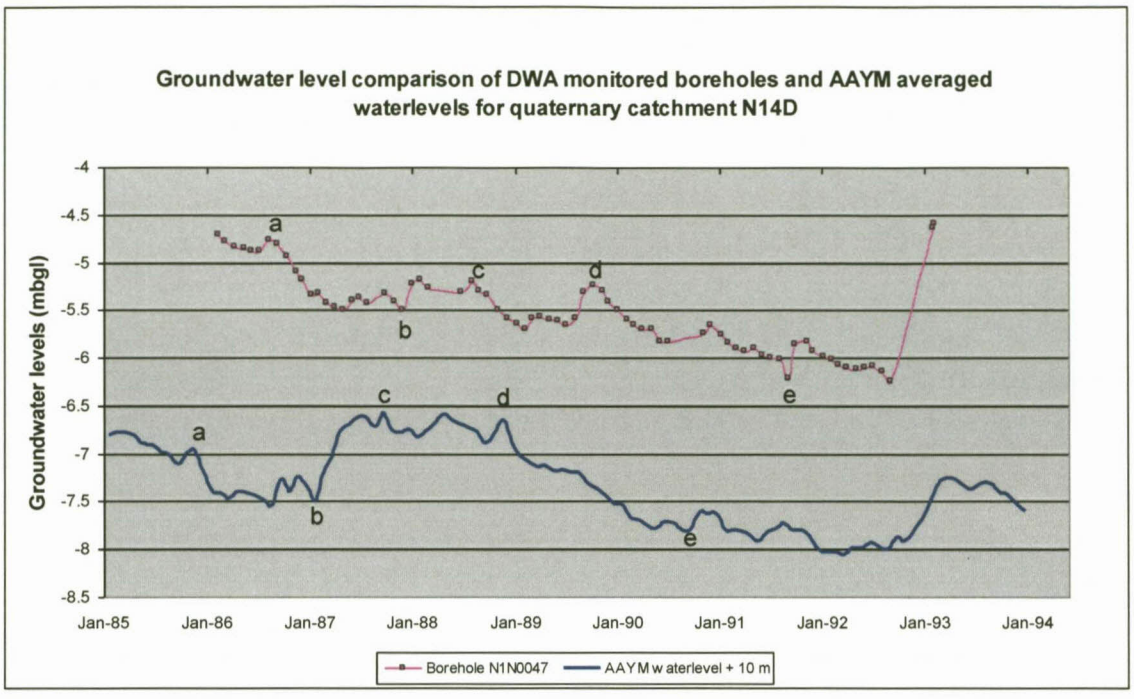

Figure 33. Water level trends – N14D.

Note: AAYM water levels were raised by 10 m in the above graph to cater for easy comparison.

Table 8: Borehole information – N13A

Quaternary catchment	**N13A**
Town	Graaff-Reinet
MAP (mm)	381.3
Boreholes	N1N0025, N1N0091, N1N0092, N1N0503, N1N0505, N1N0506, N1N0507 N1N0506 appears to be least affected by pumping
Topography/geology	N1N0025 lies on a hill slope on a drainage area. The remaining boreholes lie near a secondary river on alluvial material. Geology consists of the Adelaide Formation mudstone of the Beaufort Group.
General comments	N1N0506's water levels virtually match the AAYM water levels.
WL fluctuations	The long-term fluctuations are very similar with the AAYM being slightly more exaggerated than the borehole.
Time lag between AAYM and borehole water level	~1 year

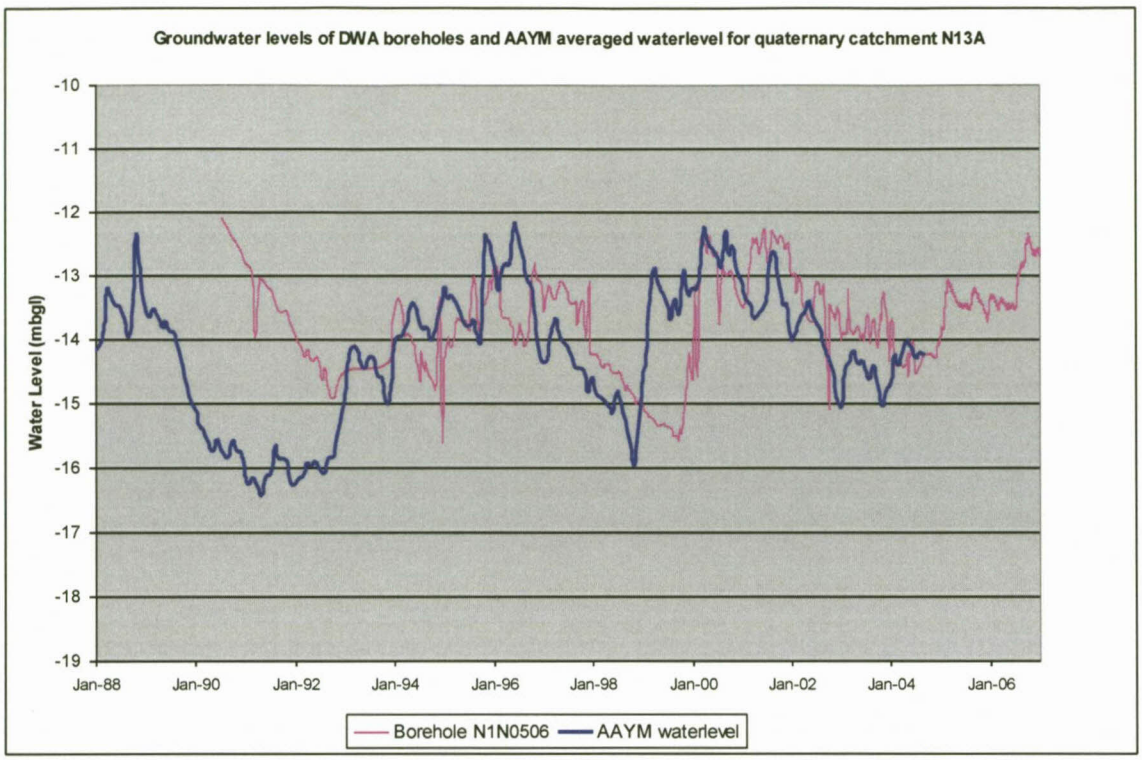

Figure 34. Water level trends – N13A.

Table 9: Borehole information – L11F

Quaternary catchment	**L11F**
Town	Beaufort West
MAP (mm)	219.8
Boreholes	J2N0062, J2N0109
Topography/geology	J2N0062 and J2N0109 lie in a flat (alluvial?) plain. The geology consists of the Adelaide Formation of the Beaufort Group: sandstone, mudstone and shale.
General comments	The AAYM water levels are relatively static whereas the boreholes' water levels tend to drop between 2 – 4 m over the monitoring period.
WL fluctuations	The fluctuations to events (recharge) appears to be similar (eg the mid-1984 response in J2N0062).
Time Lag of AAYM to borehole water level	~1 year

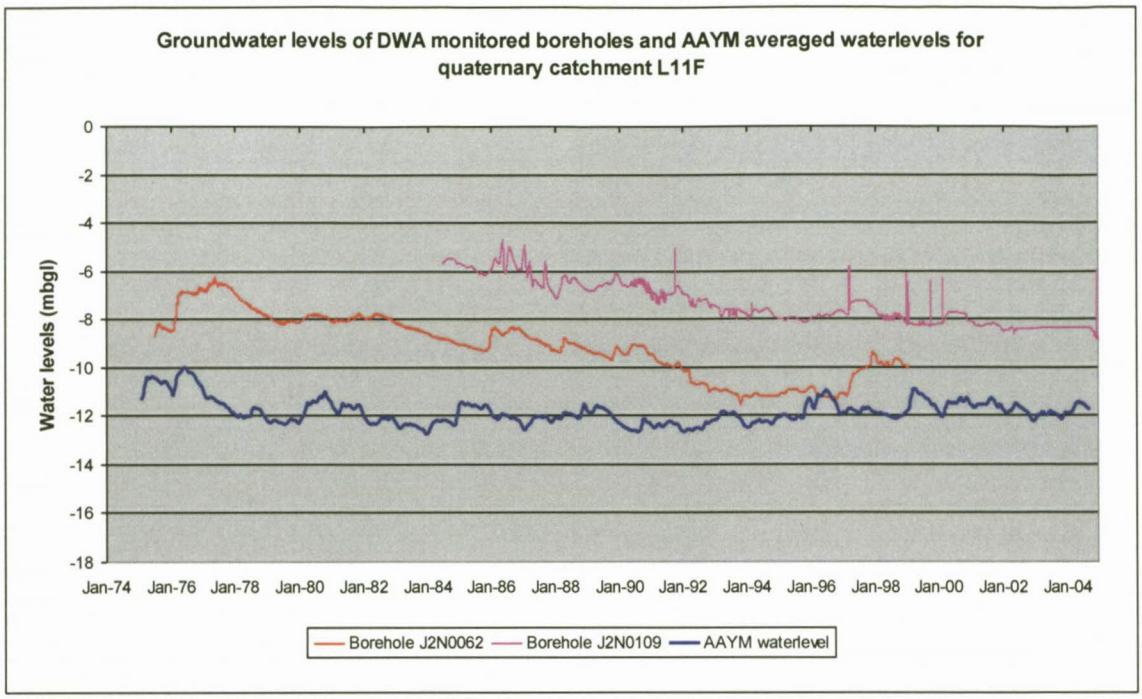

Figure 35. Water level trends – L11F.

Observations

The comparisons shown indicate that the AAYM does reflect natural water level trends. The main difference is that in reality the water level response is delayed after rainfall events (or lack thereof), whereas the AAYM water levels show immediate responses (as the model does not include a delay function). Most of the DWA boreholes water levels are near wellfields, and therefore the effect of abstraction influence many of the DWA monitoring boreholes. Those DWA boreholes that appear to either not be affected by pumping or affected in a minor way were selected for review.

5.3.2 Sensitivity analysis

Due to the incorporation of various unknown variables into the model such as evapotranspiration, threshold and MAWD, a number of sensitivity analyses were carried out as part of this chapter in order to understand the effect each parameter has on the model's results (the results being water level graphs and assured yields). The sensitivity of the model was established by observing the change in model results when increasing the values assigned to each parameter. Results from the sensitivity analyses are presented in Figures 36 -43.

i) Evapotranspiration area

The project team as part of the WRC Project No. K5/1763 derived default values of the area on which evapotranspiration occurs for each quaternary catchment using the 1:500 000 scale rivers coverage that was sourced from the WR2005 database, as follows:

- The river sections were buffered by 100 m for each of the 7 stream orders.
- The buffered river coverage was then intersected with the quaternary catchment coverage.
- The total buffered river area was then summed per quaternary catchment and converted to a percentage 'riparian' area per quaternary catchment.

(Woodford, WRC Project K1763, Deliverable 4f, 2010)

It was unsure whether this percentage of area was correct, thus a sensitivity analysis of these values was carried out in this thesis and the results assessed.

Results

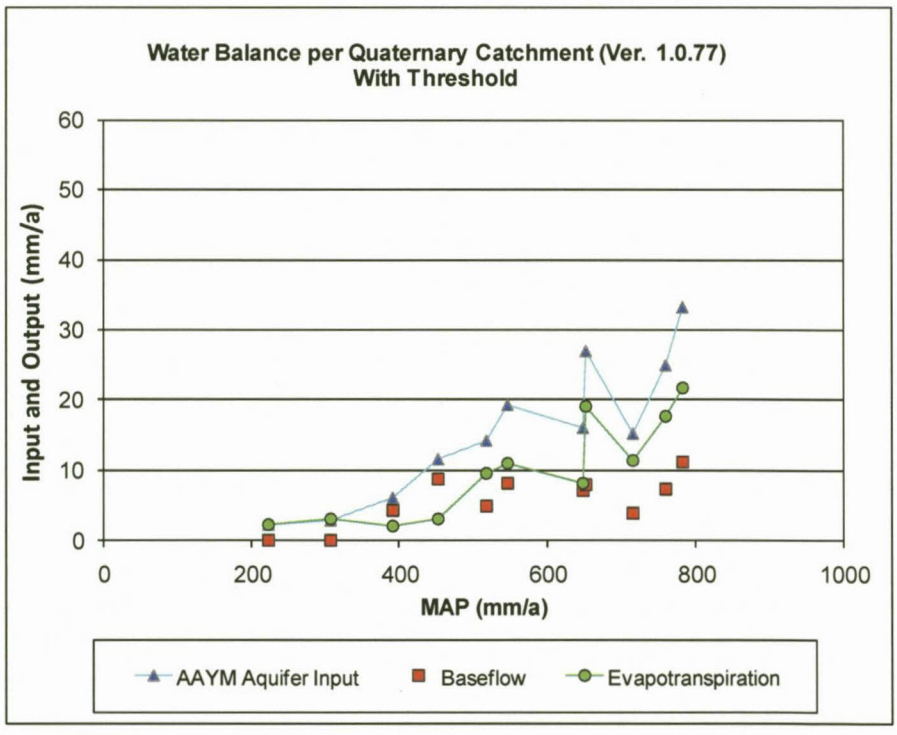

Figure 36. Aquifer input (recharge), baseflow and evapotranspiration for selected quaternary catchments with a recharge threshold applied.

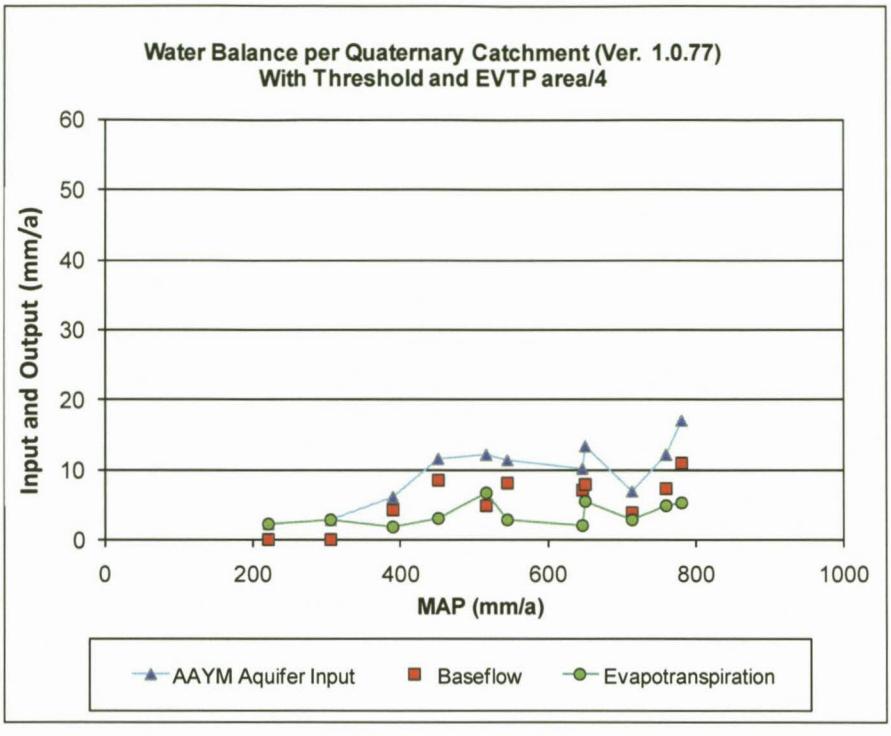

Figure 37. Aquifer input, baseflow and evapotranspiration for certain quaternary catchments with a recharge threshold applied and divide the area over which evapotranspiration occurs by 4.

Figures 36 and 37 show the effect of evapotranspiration on the volume of inflow (recharge) into the aquifer. The division of the area over which evapotranspiration occurs causes a noticeable decrease on the rate of evapotranspiration taking place, as is to be expected. From MAP 200 – 450 mm/a, there is no effect on the aquifer input, but from 450 mm/a onwards, there is a decrease in aquifer input into the system. Since evapotranspiration is a major process by which water is removed from the aquifer system, it would be expected that dividing the area in which this process occurs would result in an increased aquifer input (effective recharge). The opposite has occurred, where with less evapotranspiration the aquifer loses less water and thus accepts less water (i.e. is full more often). It can therefore be assumed that evapotranspiration plays a major role in allowing for storage within the aquifer to become available and allow for allowing recharge to occur.

ii) Recharge Threshold

A threshold value applicable for all catchments in the Karoo Basin is unknown, thus an initial value of MAP/12 (Bean, 2003) has been applied and the results assessed below in order to attempt to develop some guideline of acceptable values to be implemented (Figure 38 - 39).

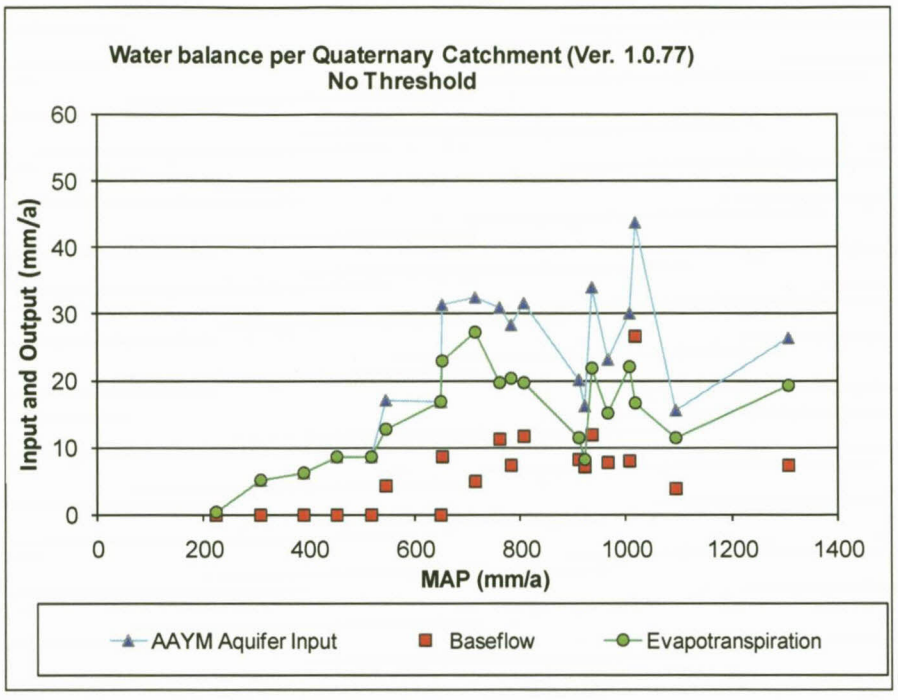

Figure 38. Aquifer input, baseflow and evapotranspiration for certain quaternary catchments without applying a recharge threshold.

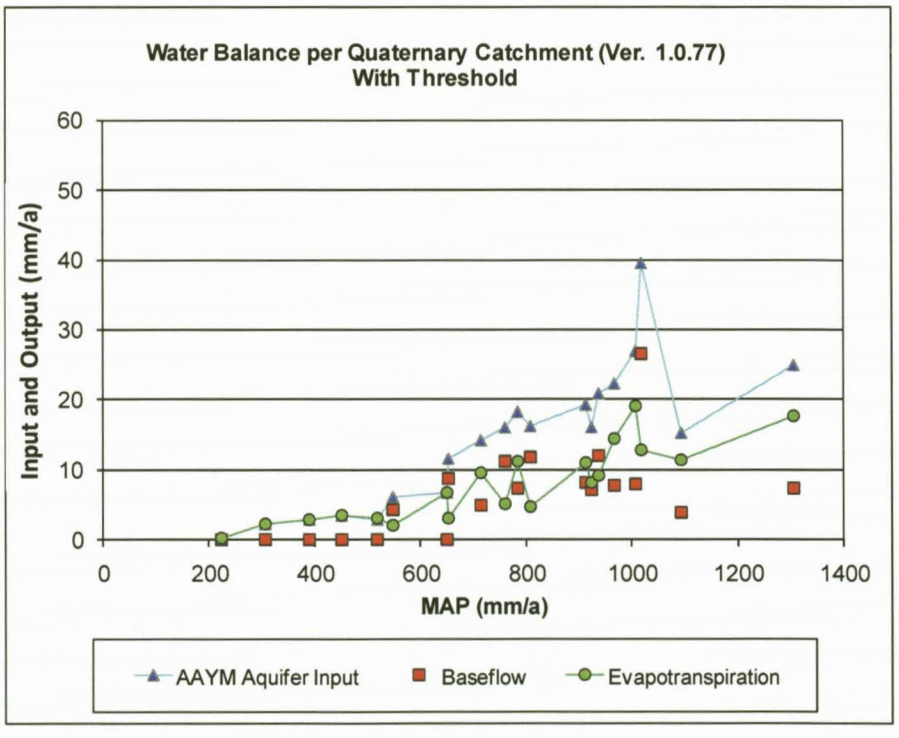

Figure 39. Aquifer input, baseflow and evapotranspiration for certain quaternary catchments once a recharge threshold has been applied.

Figures 38 and 39 illustrate how the threshold halves the AAYM aquifer input and more than halves the EVTP for catchments with MAP <900 mm/a. Areas with MAP above 900 mm/a, however, are not affected by a threshold (Figure 39). Depending on the water balance of the system, the threshold may have to be increased for areas with a higher MAP, from around 900 mm/a. This rule, however, cannot be applied to every catchment with a high MAP and must be assessed on an individual basis.

iii) MAWD

The MAWD was tested on a number of catchments in the Karoo Basin across a range of MAP values, noting the assured yields as the MAWD was increased. Below illustrates this process in catchments L11F (Figure 40), C83D (Figure 41) and V11G (Figure 42),

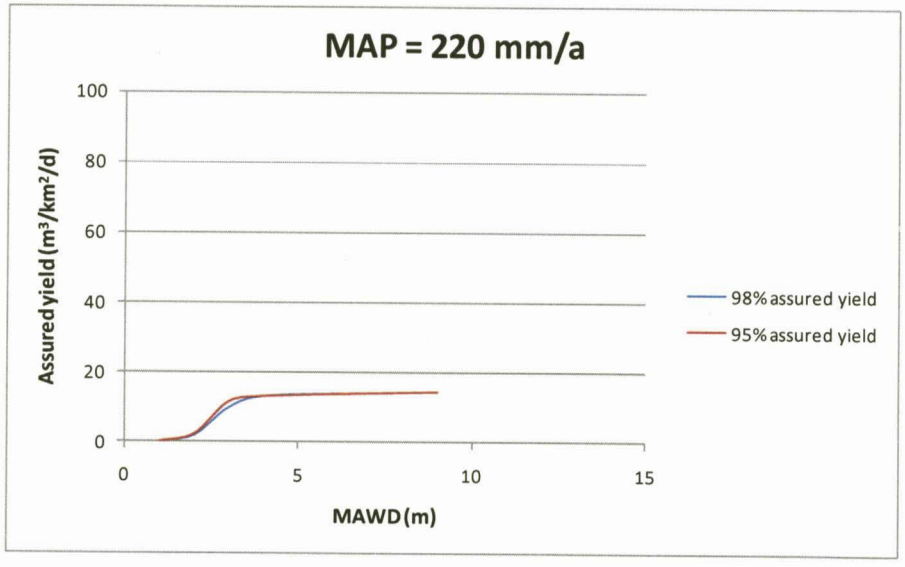

Figure 40. The 95 % and 98% assured yields with MAWD for quaternary catchment L11F.

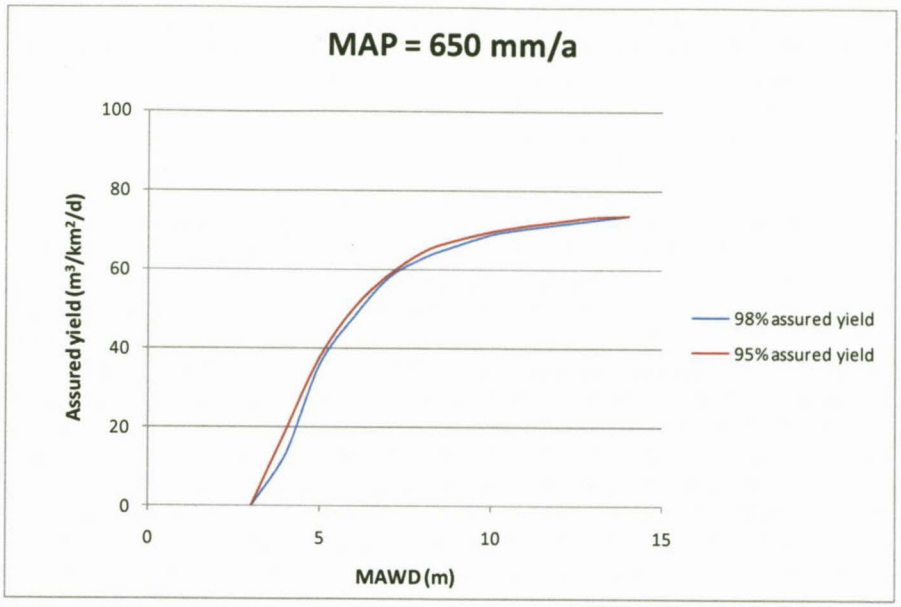

Figure 41. The 95 % and 98% assured yields with MAWD for quaternary catchment C83D.

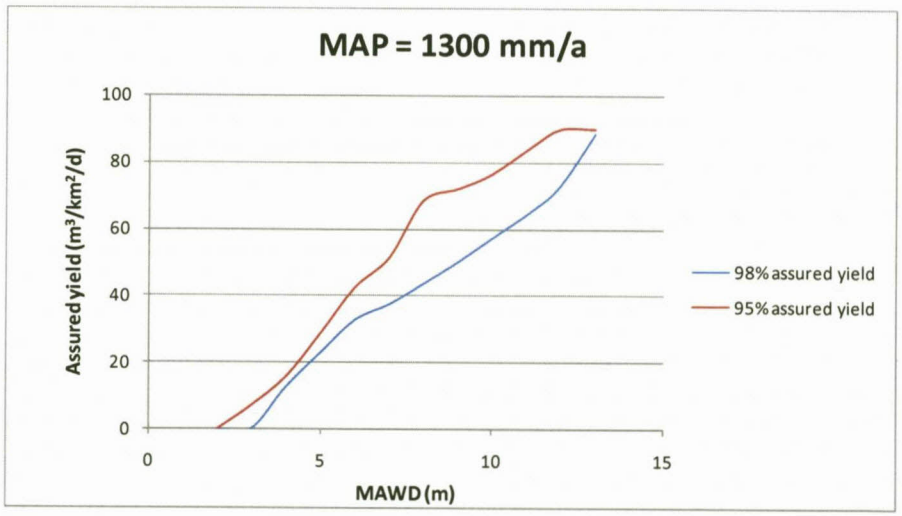

Figure 42. The 95 % and 98% assured yields with MAWD for quaternary catchment V11G.

Figures 40, 41 and 42 show how the sensitivity of the AAYM assured yields to the MAWD values differs for areas with different MAP. A steep slope indicates a rapid increase in assured yield and thus a high sensitivity of AAYM to the range of MAWD values in which the increase occurs. The range of MAWD values in which these steep slope segments lie shifts with increasing MAP. When MAP is around 0 – 200 mm/a, the model is most sensitive to MAWD values of 2 – 5 m (Figure 40). With increasing MAP, around 600 mm/a, the model is most sensitive to MAWD values of 3 – 7 m (Figure 41). Finally, with high MAP (MAP of >1000 mm/a) it appears that there is a constant increase of

assured yield with increasing MAWD, suggesting a constant sensitivity of AAYM to MAWD values implemented (~2.5 – 14 m, Figure 42). These results also show that the model appears not to work well for areas with very high rainfall. The curves in Figure 42 are "uneven" and the assured yield values are mostly less than those of the lower rainfall area. This does not mean that the model is necessarily "wrong", it may mean that more work is required to provide guidance on how to assign input parameters in the high rainfall areas.

In areas with lower MAP (~200 mm/a), the assured yield curve flattens out when MAWD is increased due to the limited rate of recharge available to the aquifer system. Increasing the MAWD will not make a difference if the recharge isn't increased. Thus for high MAP areas, there is potentially a substantial rate of recharge available ('potential recharge'), but there may not be sufficient space in the aquifer to accept the water. By allowing further water level drawdown, more water will be removed from storage in the aquifer system thus providing more space for recharge, which may result in greater assured yields. This potential recharge can be observed in Figure 43 below. The GRAII recharge increases (almost exponentially) with increasing MAP which has an effect on the potential recharge of catchments. The greatest difference between potential recharge and aquifer input (effective recharge) exists at the highest MAP with a recharge difference of roughly 50 mm/a.

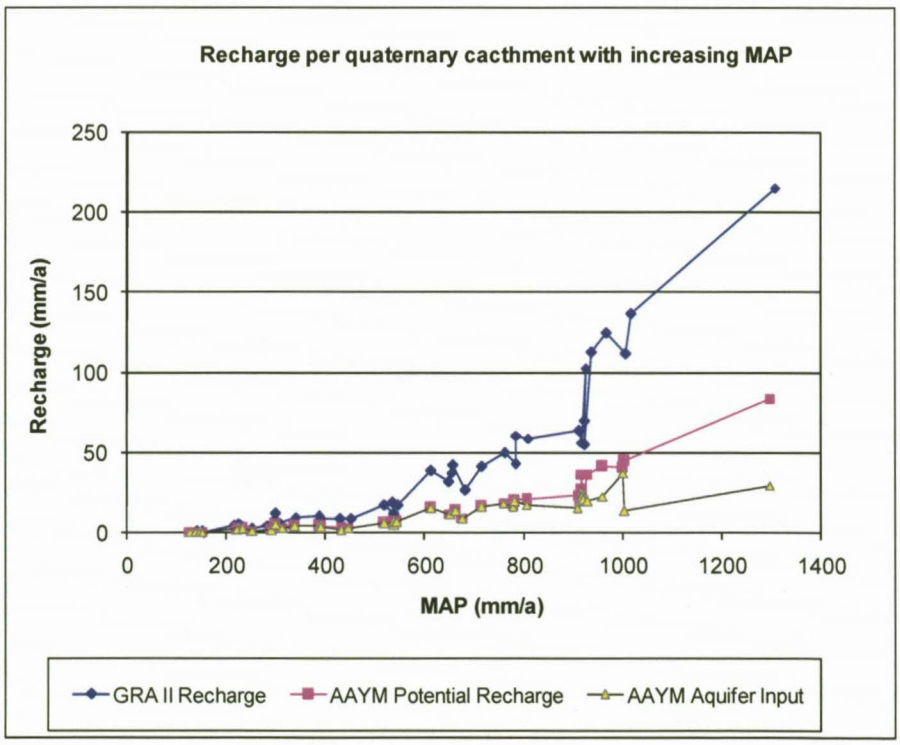

Figure 43. GRAII, AAYM potential and AAYM effective recharge with increasing MAP.

5.3.3 Establishing guiding principles on applying the AAYM

In addition to the sensitivity analyses, the model was run for a large number of quaternary catchments spread across the Karoo Basin and characteristics of the catchments were noted such as MAP, MAR and baseflow. This process was done to establish a rough guide of values to be assigned to each parameter for each drainage region (Table 10). The procedure followed for each quaternary catchment involved 3 steps:

1) Setting an Extinction Depth (ED)

   This is based on the MAP of the quaternary catchment (see Table 6).

2) Applying a Recharge Threshold

The implementation of a threshold was based on personal judgement for each catchment, with MAP and the shape of the steady state water level curve as the determining factors. If the MAP was high (>400 mm/a) and the water level was near surface (which was often the case), it was understood that the model was allowing too much water to enter the system. An initial threshold of MAP/12 was therefore applied (Equation 7). Once the threshold and MAWD was set, the model was run in transient state. The final yields and water levels were then noted while reassessing the threshold value that had been applied. If the assured yields appeared to be unrealistically small (e.g. 0.06 L/s for a quaternary catchment) and/or water levels were excessively low (sometimes reaching 200 m.bgl), the threshold was decreased to MAP/24, and if results were still unrealistic, the threshold was removed altogether.

After each of these steps the following results were recorded:

- Potential aquifer recharge (mm/a)
- Aquifer input/accepted recharge (mm/a)
- Actual evapotranspiration from the riparian zone (mm/a)
- Baseflow (mm/a)
- Average water level (m.bgl)

3) Setting a Maximum Allowable Water level Drawdown (MAWD)

AAYM is programmed to read the MAWD from the GRAII average regional water level. The GRAII water level is measured in m.bgl and the MAWD is the level below the regional (or static) water level, in m.bswl. In other words, if the GRA II water level is 20 m (i.e. the average water level for the quaternary catchment obtained from the GRAII database) and the MAWD is 5 m, AAYM reads the MAWD at 25 m. A simple calculation is therefore required to relate the user defined MAWD to the AAYM MAWD. A MAWD of 5 m is used in this model as GRA II uses an MAWD value of 5 m when determining AGEP values.

The method of setting 5 m MAWD can be described using the example below for quaternary catchment C60G (Figure 44): Firstly, determine the lowest point of the AAYM water level (25.4 m) and add 5 m to this value (i), thus giving the water level 5 m leeway when abstraction commences. This point (30.4 m) must then be modified to the by subtracting the GRA II water level from 30.4 m (ii), giving the MAWD:

(i) 25.4 (lowest water level) + 5 = 30.4

(ii) 30.4 – 21.4 (GRA II average water level) = 9

MAWD = 9 m

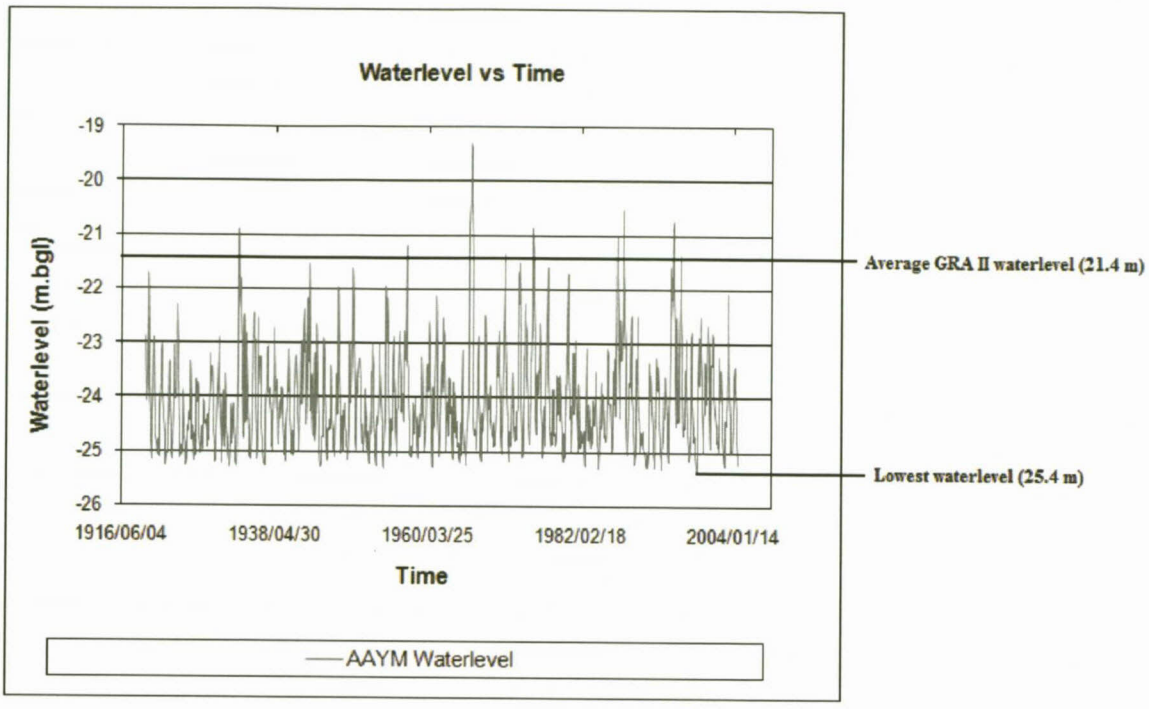

Figure 44. Graph showing the AAYM water level of quaternary catchment C60G to determine MAWD from the lowest water level.

Table 10: Guidelines for assigning input parameters for the AAYM per drainage region

Region	Number of Quaternary Catchments	MAP range (mm/a)	Guideline
B	22	657 – 715 (mean = 685)	Threshold = MAP/12
C	157	320 – 892 (mean = 589)	Threshold = MAP/12
D	234	80 – 1056 (mean = 470)	Threshold = MAP/12
E	41	84 – 285 (mean = 196)	Threshold = MAP/24
J	34	98 – 295 (mean = 178)	Threshold = MAP/24
L	27	152 – 367 (mean = 226)	MAP<300, threshold = MAP/24 MAP>300, threshold = MAP/12
N	28	214 – 411 (mean = 312)	MAP<300, threshold = MAP/24 MAP>300, threshold = MAP/12
Q	69	289 – 804 (mean = 423)	For MAP<400, no threshold MAP>400 threshold = MAP/24
R	30	452 – 1036 (mean = 702)	Threshold = MAP/24
S	58	453 – 818 (mean = 613)	Threshold = MAP/24
T	133	683 – 1277 (mean = 864)	Halve the baseflow Threshold = MAP/24
U	34	758 – 1170 (mean = 923)	Threshold = MAP/24
V	82	665 – 1353 (mean = 845)	Halve the baseflow Threshold = MAP/24
W	56	685 – 1061 (mean = 834)	Threshold = MAP/24
X	9	682 – 889 (mean = 766)	Halve the baseflow Threshold = MAP/24

It is difficult to determine any general relationship between the requirements of input parameters and the MAP of a particular region. Certain areas appear to be significantly more sensitive to parameters such as baseflow or threshold than other areas. In addition, certain catchments failed completely during testing, that is, they are incapable of initially sustaining a balanced, steady-state system, and subsequently the water levels fall rapidly over time. An example of both parameter sensitivity and failing system occurs when catchments have low recharge (~0.01 %MAP) and produce a graph that appears unrealistic, starting at the top left corner and ending at the bottom right corner (i.e. indicating insufficient inflow). The results, however, correlate well to the GRAII results. These particular catchments (an example is E31C) are very sensitive to baseflow. If a small value for baseflow is used (e.g. 0.0115 mm/a) this will stabilise a graph displaying water level such as that

mentioned above. Once a threshold is implemented, the baseflow in this example must be reduced to 0.0075 mm/a in order to re-stabilise the graph. When the model is run, the difference between implementing a baseflow to obtain a realistic graph and leaving the system as is, is negligible. This is one example of many illustrating the unique balance of each quaternary catchment and the need to investigate each individually.

5.3.4 Comparing the AAYM yields with GRAII and Harvest Potential yields

The third process entailed comparing the assured yield results from the AAYM, with readily accessible databases that had provided previous regional estimates of groundwater yields, namely GRAII AGEP Drought and Normal, and Harvest Potential (HP) (Figure 45). The definitions of both databases are:

Average Groundwater Exploitation Potential (AGEP) is the volume of water that can be sustainably abstracted on an annual basis if sufficient production boreholes can be sited on the aquifer system or catchment. This value is determined under normal rainfall and drought conditions (DWAF, 2006).

Harvest Potential (HP) is the maximum volume of water sustainably abstractable from a unit area without depleting the aquifer. This value accounts for yield inconsistencies of and between different aquifer systems (DWAF, 2006)

A downfall of the AGEP and HP values is that they are static, providing only a single value on a quaternary catchment scale. The parameters used in the calculation of their yields are known, but cannot be modified. This becomes problematic when a user is investigating a particular area which has parameters values that differs quite significantly to the generalised settings applied to the quaternary catchment, such as baseflow or recharge values. The new AAYM has addressed these issues by displaying all parameters used in the determination of the final assured yields and allowing the user to adjust the default parameter values provided. In addition, the source of each value or dataset implemented is given which will allow the user to make an informed decision regarding whether or not to adjust the default value. The user may also adjust the values based on knowledge of the study area from previous work carried out. Furthermore, the AAYM uses a database that can be regularly updated. Thus when more recent databases are developed, such as improved values for baseflow or evapotranspiration, these values can replace the older parameter values and will be accepted by the AAYM.

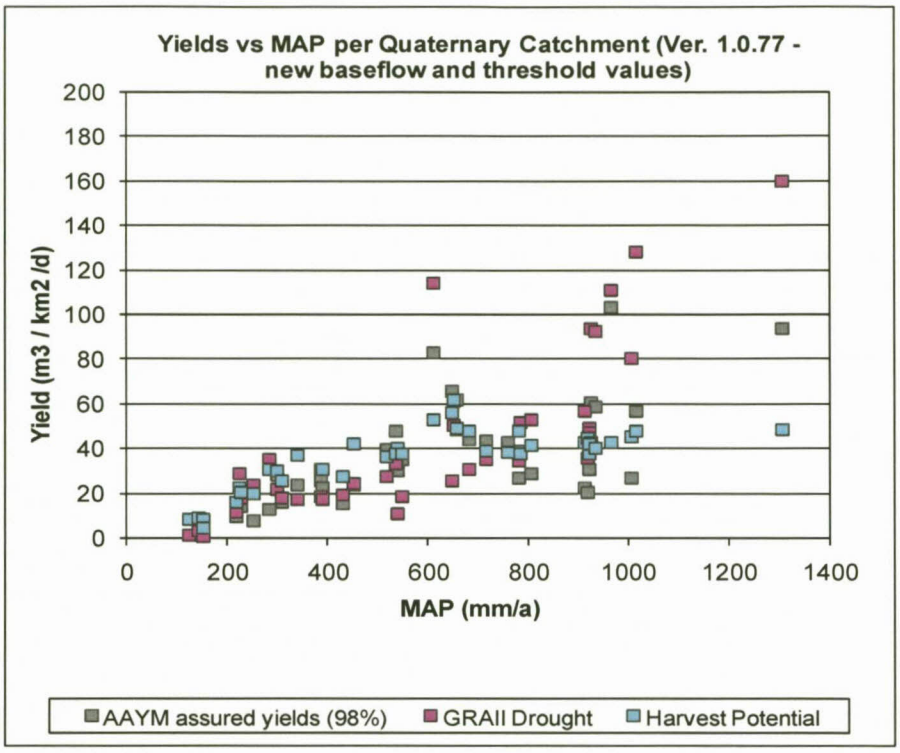

Figure 45. AAYM yields versus GRA II and Harvest Potential yields

Figure 45 shows that AAYM yields appear acceptable when compared to GRA II and HP yields. The yield increases moderately with increasing MAP and at times lies in between the AGEP drought and HP yields. Yields appear relatively low at MAP 800-1000 mm/a, which could be due to the one of the following reasons: firstly, evapotranspiration may remove a significant volume of water before it can infiltrate beyond the extinction depth. Water levels are generally near surface in areas of high rainfall and thus evapotranspiration constantly removes water that would otherwise enter the aquifer. This is the case in rainfall areas with a MAP above 600 mm/a - water levels are always above the extinction depth and so evapotranspiration occurs throughout the period of investigation. Secondly there may not be sufficient space for the water to enter the aquifer. The aquifer may already be full and unable to accept any more water. In order for more of the available recharge to reach the aquifer, space would have to be created, which is only possible through pumping or increasing the baseflow.

An third option as to why assured yields are lower than GRAII and HP yields where MAP is 800 – 1000 mm/a is that this may reflect a flaw in the model or the parameters have been incorrectly assigned. Yields should increase with increasing MAP and the reason for this not occurring in the model must still be established.

5.4 Flaws

1) The AAYM waterlevel begins at or near to the GRA II average regional waterlevel. This is of concern in some quaternary catchments where AAYM waterlevels are higher than the GRA II waterlevel as the waterlevel displays a quick rise (Figure 46) lasting from a few months up to as long as 10 years. The rise becomes problematic when the MAWD must be set, as it seems more correct to set the point of MAWD in relation to the waterlevel once it has corrected itself, but this may result in the MAWD being set above the initial (lower) waterlevel thus causing the system to 'fail' within the first few years.
2) In Figure 46, it can be seen how the water level (blue line) rises unrealistically rapidly in the first few years. This is because the AAYM water level averages 2.89 m and a GRA II average regional waterlevel is 20.91 m, and the model is designed to start at the GRAII level and move to the AAYM average water level.

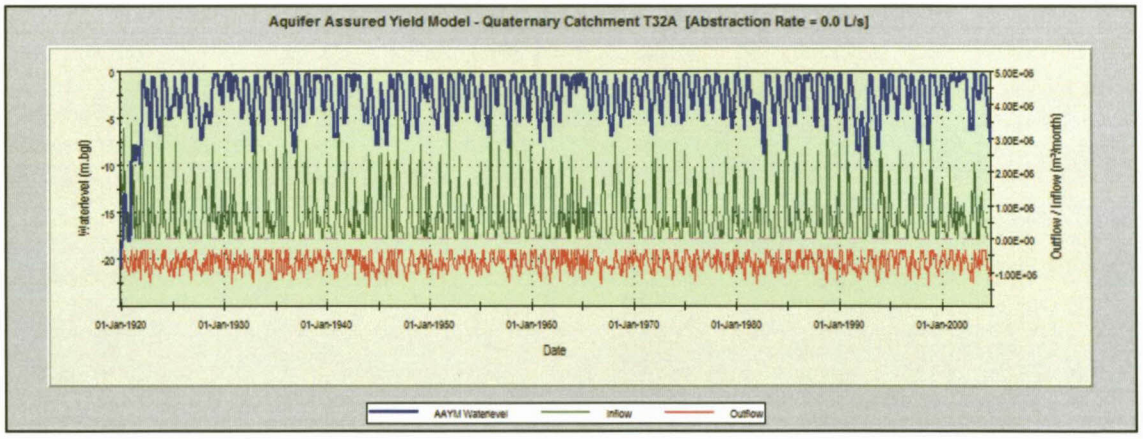

Figure 46. AAYM waterlevel of quaternary catchment T32A (MAP of ~800 mm/a) prior ro incorporating abstraction.

3) AAYM produces aquifer yield graphs which may, for some quaternary catchments, display an irregularity with increasing level of assurance (Figure 47). It may not necessarily be the yield that is fluctuating, but the probability of exceedance. It suggests that the regional groundwater level is rapidly fluctuating as abstraction lowers the waterlevel, but abstraction provides more space for recharge. Perhaps these rapid waterlevel fluctuations occur due to a high sensitivity of the groundwater system to increased abstraction. Recharge may occur more rapidly when abstraction takes place as there is no shortage in the availability of water for recharge (which is evident in potential recharge significantly exceeding actual recharge, Figure 43), which causes a sudden and short lived period of lower exceedance probability.

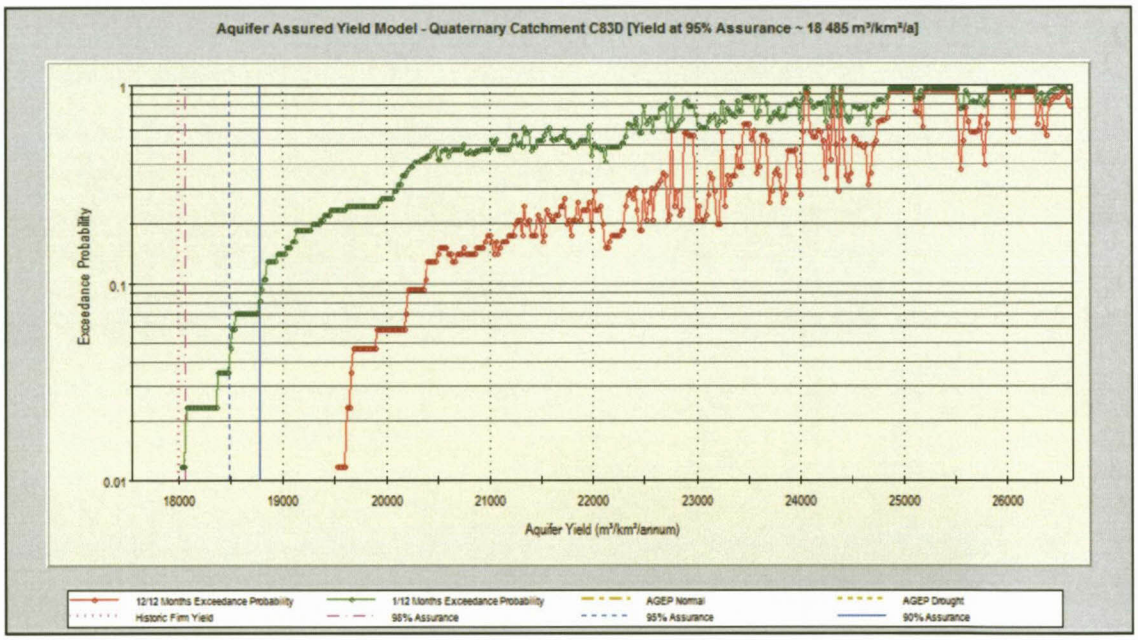

Figure 47. Increasing assured yields with increasing probability of exceedance for quaternary catchment C83D.

3) Some quaternary catchments from the group selected produce incorrect yields whereby the 98% yield is higher (occasionally significantly higher) than the 95% yield. This may be due to a mathematical error in the programming of AAYM. Quaternary catchments with this error include E23J, E31H, N24C, N14D, Q93A and C23L, and all have an MAP of <650 mm/a.

5.5 Conclusions and recommendations on the way forward

Minimal work has been done before regarding the assigning of groundwater yields with levels of assurance, even though it the most common method used by surface water engineers and hydrologists. The reason for this may be due to the differing concepts between surface water and groundwater systems.

This chapter aimed to evaluate and critically review the AAYM Version 1.0.77 in terms of the parameters used, the sensitivity of the model to the parameters used in the determination of an assured yield and the results in comparison to previous established databases such as the GRAII AGEP and HP. The work presented is pioneering and thus should be considered "work-in-progress" as a first attempt to produce a "perfect" methodology and model is simply not possible. It requires an iterative process of development, testing, modifying and re-testing. Furthermore, additional testing is still needed in order to expand on the concepts presented above. Some of the key conclusions from the model are:

- The model generally provides similar yield estimates to that of the GRAII AGEP Drought and Harvest Potential, with AAM yields generally falling between the two (with GRAII being slightly higher side and HP slightly lower).
- The model's yields in high MAP areas (greater than about 1000 mm/a) are somewhat conservative and thus should be reassessed regarding their parameter estimations such as baseflow and threshold values.
- The yield results from the model are mostly sensitive to the recharge threshold, baseflow and MAWD, thus more work is required to obtain better input data in these fields and further guidance on how to apply these input parameters in the model.
- There appear to be a few problems with the model. These are elaborated on in the recommendations below.

Recommendations

The challenge of obtaining realistic baseflow estimates is a concern, as current estimates by Hughes, Schultze, van Tonder and Pitman vary significantly. The key challenges regarding data remain realistic baseflow and evapotranspiration data sets. With respect to evapotranspiration, it is the area

over which this occurs that is the greatest challenge, and not so much as in evapotranspiration rates (which are fairly well documented in scientific literature).

From the flaws listed above it appears that a change of input data by the user is required as well as further modifications of AAYM programming.

1) Problem (1) regarding the rapid rise of certain quaternary catchment waterlevels could be managed by setting a reliable recharge threshold thereby changing the volume of water entering the system which changes the waterlevel. Increasing a recharge threshold will lower a waterlevel and decreasing a recharge threshold will raise a waterlevel. Other options include either modifying the programming so the AAYM waterlevel does not start from the GRA II average regional waterlevel, or programming the model to disregard waterlevels of the first 10 years.

2) Inputs per quaternary catchment may be generalised for areas with MAP <300 mm/a and > 700 mm/a, but quaternary catchments within this MAP range (300-700 mm/a) may have very variable inputs. It appears that catchments in this range of MAP may be sensitive to input parameters, the recharge threshold in particular, thus each of these quaternary catchments should be run individually with input values set according to their particular waterlevels.

3) Additional outputs of the AAYM are the summary graph pie charts displaying the mean annual water budgets and the mean annual groundwater components (Figure 48). One concern is the components of 'Other' in the mean annual water budget, which essentially represents evapotranspiration. Perhaps this label should be changed to 'Evapotranspiration' to avoid any confusion.

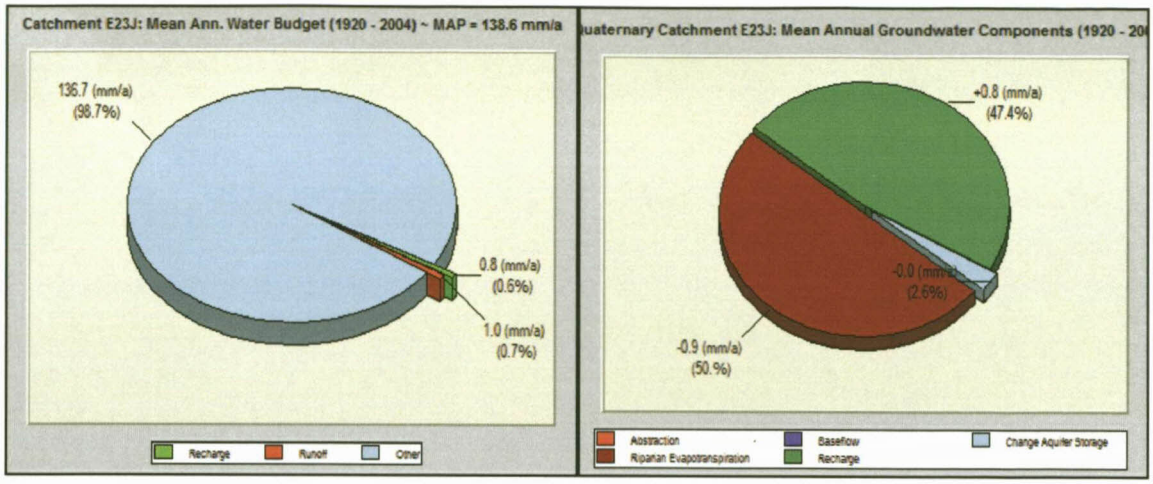

Figure 48. Output pie charts of Mean Annual Water Budget and Mean Annual Groundwater Components for quaternary catchment E23J with an MAP of 138.6 mm/a.

Finally, further testing of the AAYM Ver. 1.0.77 should be done on each individual quaternary catchment. The model needs to be run for each catchment, probably a number of times, in order to obtain appropriate realistic looking graph, therefore enabling a balanced aquifer system upon which abstraction can commence. No two catchments are the same as each has their unique combination of input and output parameters. A number of catchments will be able to run with the same settings, but these setting are generalized and include parameters such as threshold values and extinction depths.

Chapter 6

6 Wellfield Model

6.1 Literature Review

When designing a wellfield, a number of parameters and factors must be considered such as the number of production and monitoring boreholes needed, the pumping rates and daily pumping duration of each borehole, the aquifer parameters (to establish borehole interference and spacing) and environmental considerations such as potential impacts on surface water bodies and groundwater dependant ecosystems. Limited amount of information on design was found during this literature review therefore this chapter addresses the factors felt important and essential to be taken into account when designing a wellfield. The following section provides a brief review on these factors.

Wellfield design focuses on borehole interference, and thus looks at the effect of abstraction from one borehole on another in order to optimise spacing. Although recharge to the aquifer and the wellfield area affects borehole water levels, for optimising borehole spacing it is aquifer permeability (or transmissivity) that is of paramount importance. Localised effects on borehole water levels such as impermeable boundaries and sources of likely recharge such as nearby rivers or lakes, should however, be taken into account in wellfield design. If needs be, a sophisticated numerical model that takes recharge, boundaries and spatial differences in aquifer parameters into account can be run to estimate aquifer water levels over a given time period.

Cone of depression

During pumping, horizontal flow occurs in the direction of the well resulting in the decrease of hydraulic heads with increasing proximity to the well. The maximum drawdown occurs at the abstraction well and decreases radially, from the well outwards. This resultant shape is referred to as the cone of depression; its shape is dependent on aquifer characteristics and the slope of the water table. The cone of depression will increase with depth and extent over the duration of pumping. The *rate* of expansion, however, decreases over time as every extension of the cone releases double the

volume of water than previously released (Freeze & Cherry, 1979; Johnson, 1975). The cone enlarges until one of three conditions occur, either the system reaches a point where the natural discharge of the aquifer is equal to the pump rate; or where natural recharge, from a surface water body or from precipitation within the radius, enters the aquifer to equal the pump rate; or finally where leakage from overlying or underlying aquifers enters the aquifer to equal pump rate. Expansion of the cone will terminate when one or more of the above scenarios occur, which may take from a few hours up to several years (Johnson, 1975).

Transmissivity is thus an important aquifer parameter determining drawdown shape and extent, and refers to the *rate* at which groundwater moves through a medium in a unit time per unit gradient. If an aquifer's transmissivity is high, groundwater is able to move through the aquifer rapidly during pumping resulting in a gentle drawdown slope but an extended radius of influence as a medium allowing for a greater rate of groundwater flow can affect a larger area during a certain time period. Conversely, an aquifer with a low transmissivity will produce a steep drawdown curve during pumping and limited areal extent of drawdown (Johnson, 1975). Additionally, storativity plays a part in drawdown regarding the nature of the aquifer. Unconfined aquifers have larger storativity values (known as specific yield) than confined aquifers (known as specific storage). The storage coefficient in an unconfined aquifer is equal to the specific yield, which in turn results in a slow expansion of the cone of depression. As the aquifer is dewatered, however, the transmissivity decreases which results in an increase in drawdown in the abstraction borehole and aquifer. Usually, drawdown in a confined aquifer does not result in dewatering of the aquifer, but a rapid expansion of the cone of depression due to the small storage coefficient (Heath, 2004).

Well Interference

Multiple wells placed in close proximity to one another may result in well interference (i.e. additional drawdown due to abstraction from adjacent boreholes), the degree to which is dependent on aquifer transmissivity, abstraction rate, duration of pumping and storativity, of which transmissivity and pump rate are most important (See the Cooper - Jacob equation below, Equation 9). When a number of wells are in close proximity to one another the extent of drawdown of each well may overlap causing well interference. At the point of overlap, the total drawdown is equal to the sum of each drawdown. Well interference therefore results in an increase in drawdown in the aquifer. For wellfield design, this in turn implies a reduction in the amount of **available drawdown** in

the aquifer, thus reducing the yield of the wells. If a number of wells in a wellfield are pumped at the same rate and on the same pumping schedule, the interference each well will have on another well's drawdown is inversely proportional to the squared distance between the two wells (r^2) (Heath, 2004). Where a well field is developed to supply large volumes of water, as little well interference as possible is desired, thus it is necessary to calculate the size and shape of the drawdown cones (Johnson, 1975). Ultimately, the aim of wellfield design is to obtain an acceptable balance of abstraction and drawdown within the wellfield. If there are no environmental factors that affect the drawdown in the wellfield, the aim would be to maximise abstraction from numerous boreholes within the limits of the aquifer's sustainable yield.

6.2 Introduction to the Wellfield Model

6.2.1 The Cooper-Jacob equation

The Wellfield Model developed as part of the WRC project is based on the Cooper-Jacob approximation of the Theis (1935) transient state radial flow equation (Cooper & Jacob, 1946) (Equation 9). The strongest determining factors of drawdown are pump rate and transmissivity. The remaining components have been logged and therefore have a lesser effect on the drawdown value calculated. The implementation of this equation in the model is discussed below in the Methodology.

$$s = \frac{2.3Q}{4\pi T} log \frac{2.25Tt}{r^2 S}$$

Equation 9

Where:

s = available drawdown (m)

Q = pump rate (m^3/d)

T = transmissivity (m^2/d)

t = pump duration (days)

r = radius of the borehole (m)

S = storativity

Since it appears that a simple wellfield model that provides an indication of borehole interference is rare (after an extensive internet search), it was decided to develop a new model. After numerous discussions between Dr R. Murray (Groundwater Africa), Dr R Dennis (IGS) and Miss K. Baker, it was decided to base it on the Cooper-Jacob approximation of the Theis equation (Cooper-Jacob Equation 9). This equation is commonly used when recommending borehole abstraction rates (Murray, 1996; Van Tonder *et al.,* 2001) and is applicable to isotropic conditions. An alternative approach, which was considered, would have been to use a linear flow equation to simulate drawdown along dykes, for example. In the end, the Cooper-Jacob was chosen because of its common use. Later in the chapter a comparison is made between the two types of flow equations. The programme that was developed, called the Wellfield Model, was written by Dr R Dennis and the approach taken in its development is described below in the Methodology.

This chapter aims to test the Wellfield Model developed by Dr R Dennis as part of the WRC Project No. K5/1763 in terms of its credibility and practicality for the desired use, the design of a wellfield. This will be done by firstly testing it against the Cooper-Jacob equation, upon which is was based, in order to determine whether the model is correct. Secondly, numerous scenarios will be tested to determine the optimum design for each scenario and thirdly a wellfield design guideline will be produced regarding borehole spacing according to transmissivity for future users of the model.

6.2.2 Model design

Several methods were implemented in the development and assessment of the Wellfield Model. The methods built into the model include those of image wells and the Stang and Hunt equation. Both are described below.

Image Wells

Although numerous flow equations are based on the assumption that aquifers are of infinite aerial extent, in reality environments are not as simple and consist of numerous boundaries which often restrict groundwater flow in aquifers both laterally and vertically. Of importance when designing the wellfield model is the representation of no-flow boundaries and their behaviour in conceptual models, which is accomplished through the use of image wells. A no-flow boundary is understood as

a structure through which no flow can occur. In order to reproduce this concept an abstraction borehole can be placed on the other side of the no-flow boundary, the opposite side to the existing abstraction borehole. This "imaginary" borehole will abstract groundwater at the same rate and duration as the existing borehole. Equipotential lines intersect the boundary at right angles and flow lines are parallel. Thus to minimise your drawdown as a result of this no-flow boundary as well as to reduce any well interference, boreholes should be placed perpendicular to and as far away as possible from the boundary (Heath, 2004).

Stang and Hunt

Stang and Hunt presented an analytical solution for a conceptual model i.e. a homogeneous, isotropic aquifer of infinite aerial extent, with dominant lateral flow and constant T (Dupuit flow), overlain by an infinitely thin stream with a semi-pervious layer (Equation 10).

$$\frac{\Delta Q}{Q} = erfc\left(\sqrt{\frac{Sd^2}{4Tt}}\right) - \exp\left(\frac{\lambda^2 t}{4ST} + \frac{\lambda d}{2T}\right) erfc\left(\sqrt{\frac{\lambda^2 t}{4ST}} + \sqrt{\frac{Sd^2}{4Tt}}\right)$$

Equation 10

where λ is a constant of proportionality between the seepage rate per unit distance (y) through the streambed and the difference between river and groundwater levels (Figure 49). If the constant of proportionality λ is defined as

$$\lambda = \frac{k' w d}{b' T}$$

Equation 11

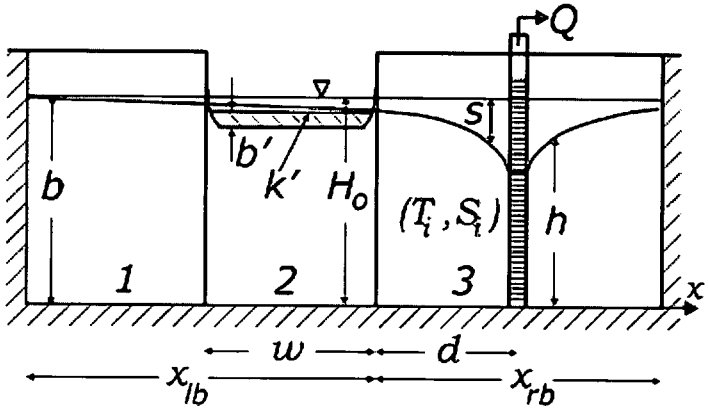

Figure 49. An image displaying the concept behind the Stang and Hunt equation.

Although this equation has been developed for a single borehole, it can be applied to a wellfield situation by using the total abstraction rate and the shortest distance from a borehole to the river (Witthueser, 2006).

6.3 Methodology

The Wellfield Model is a simple numerical model that was developed to assist in designing a wellfield by testing a number of borehole abstraction and spacing scenarios. Different scenarios can be run to evaluate the effect of groundwater abstraction on drawdown, and from this the most optimum theoretical wellfield design can be established. The user can place any number of boreholes in various positions depending on the surroundings, for example one can place boreholes along a dyke, or place boreholes perpendicular to impermeable boundaries. Shape files (geological maps and the Transmissivity Map) can be imported as base maps, which provide the location of targets when siting boreholes such as dolerite dykes or alluvium. One can assign the following parameters to each individual borehole: position (latitude; longitude), transmissivity (m^2/d), abstraction rate (L/s) and pump duration (days). Once the drawdown has been calculated for each borehole, the user can rearrange the boreholes and modify the assigned parameters in order to design a wellfield with optimum pumping rates and borehole spacing for each borehole.

The Wellfield Model was designed to follow a number of steps which are described below. The basic equation upon which drawdown was calculated is the Cooper-Jacob approximation of the Theis (1935) transient state radial flow equation (Cooper and Jacob, 1946).

1. Influence of abstraction: Abstraction boreholes in the wellfield will display a drawdown based on the Cooper-Jacob approximation, using r = 0.08 m (Equation 12). Thus all abstraction boreholes will display a drawdown.

$$s = \frac{2.3Q}{4\pi T} log \frac{2.25Tt}{r^2 S}$$

Equation 12

2. Influence of neighbouring boreholes: Drawdown at each borehole will be recalculated by taking into account all surrounding abstraction boreholes. Monitoring boreholes will exhibit a drawdown as a result of neighbouring pumping boreholes by using the Cooper-Jacob equation, where r is the distance between the abstraction borehole and the monitoring borehole. In addition, abstraction boreholes will be affected by neighbouring abstraction boreholes, whereby their drawdown is equal to the individual borehole drawdown plus the drawdown caused but the neighbouring borehole (using r equals the distance between the two).

3. Influence of a no-flow boundary: No-flow boundaries have been implemented using the effect of image wells. Once more making use of the Cooper-Jacob equation, the abstraction rate becomes the subject of the formula (Equation 13) using the known drawdowns of each borehole from the previous step.

$$Q = \frac{s4\pi T/2.3}{log\frac{2.25Tt}{r^2S}}$$

Equation 13

The distance between each borehole and the no-flow boundary must be calculated and this distance multiplied by two (distance to the imaging borehole). Using this value as r, and the calculated Q, the drawdown can be determined using the Cooper-Jacob equation, and this process is repeated for all no-flow boundaries. This value will then be added to the original drawdown of the borehole. The result is each borehole with its original drawdown from step 2, plus the newly calculated drawdown as a consequence of the no-flow boundary.

4. Influence of surface water (river): Following the first part of step 3, calculate the abstraction rates for each borehole (Equation 14). By using the calculated Q in the Stang and Hunt equation (Equation 10), the ΔQ can be calculated which is equivalent to the volume of water sourced from the river.

$$\frac{\Delta Q}{Q} = erfc\left(\sqrt{\frac{Sd^2}{4Tt}}\right) - \exp\left(\frac{\lambda^2 t}{4ST} + \frac{\lambda d}{2T}\right) erfc\left(\sqrt{\frac{\lambda^2 t}{4ST}} + \sqrt{\frac{Sd^2}{4Tt}}\right)$$

Equation 14

Carry out this calculation for all rivers, but use the shortest distance to the river each time. Subtract the sum of all the ΔQ's from Q and recalculate the drawdown to simulate the buffer effect of the river, thus modifying the initial drawdown of each borehole from step 3.

6.4 Testing the Wellfield Model with the Cooper-Jacob equation

Once the wellfield model was developed, it was tested against the Cooper-Jacob equation to ensure that there were no mistakes in the model. Two boreholes were placed close to one another within the model and their drawdowns assessed whilst increasing transmissivity or abstraction. Once this was completed, the Cooper-Jacob equation was setup in an excel spreadsheet in order to compare each of the results. Four scenarios were setup, two with a constant Q and T increasing, and two with a constant T and Q increasing. In all cases, the model was run for 360 days. Two examples of which can be seen below in Figures 50 & 51.

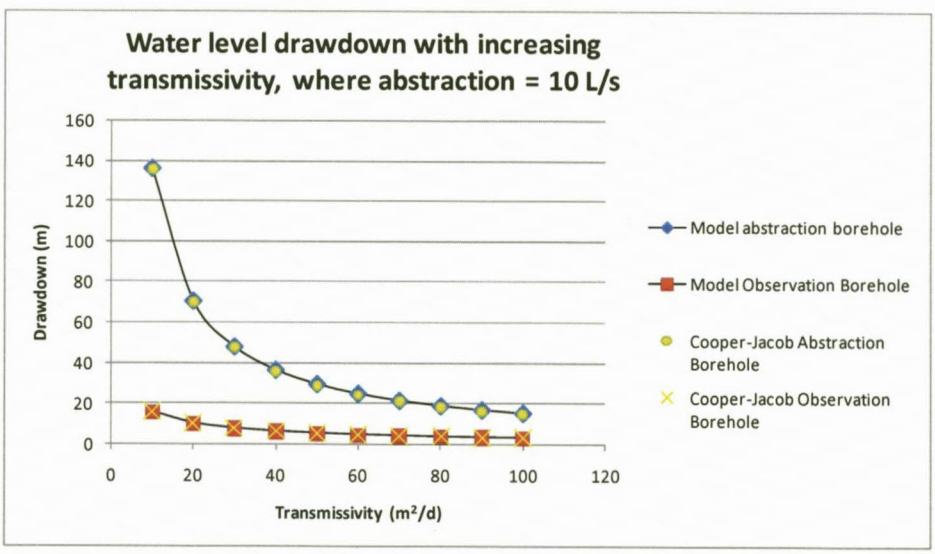

Figure 50. Comparison of the Wellfield Model with the Cooper-Jacob equation, with increasing transmissivity and abstracting 10 L/s.

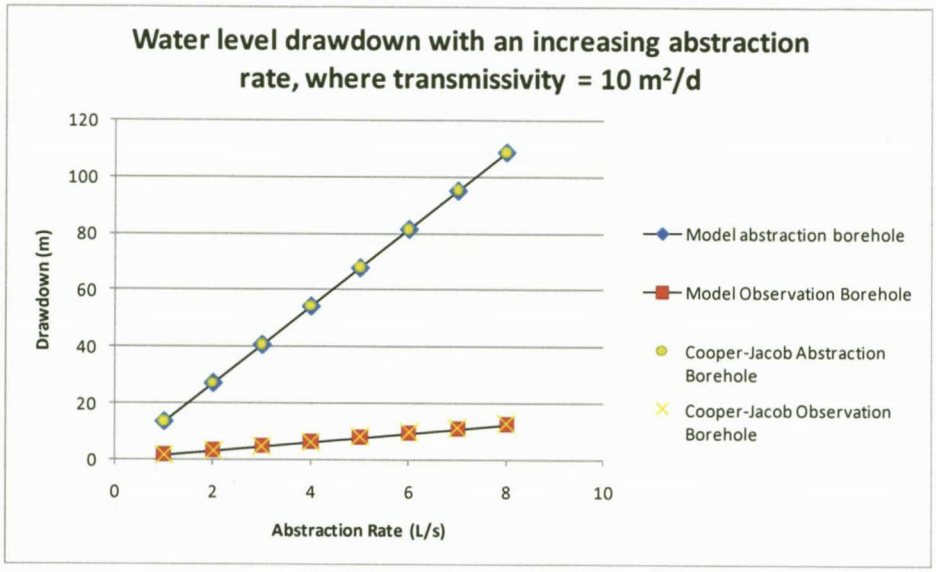

Figure 51. Comparison of the Wellfield Model with the Cooper-Jacob equation, with increasing abstraction and a transmissivity of 10 m^2/d.

The results show that the Wellfield Model works correctly according to the equations upon which it is based. As one can see, the Wellfield abstraction borehole and Cooper-Jacob abstraction boreholes lie on the same slope and the same can be said for the observation boreholes.

6.5 Testing various scenarios

Once it was determined that the Wellfield Model was running correctly according to the Cooper-Jacob equation, various wellfield scenarios were tested to provide guidance on wellfield design. The following process was carried out:

1. Establishing the relationship between transmissivity, abstraction and drawdown

2. Establishing spacing between two boreholes with different allowable interference/ drawdown between boreholes

3. Establishing and comparing borehole spacing between two and three boreholes

4. Comparing the Cooper - Jacob equation to a linear flow equation (the Boonstra-Boehmer equation).

6.5.1 Establishing the relationship between transmissivity, abstraction and drawdown

Two wellfield scenarios were run, one without a no-flow boundary, and the other with a no-flow boundary. In both cases, the model was run for 360 days.

Scenario 1: No boundary

Five boreholes were placed along a straight line (simulating a dyke-scenario) each 500 m apart, each with the same transmissivity and abstraction rate (Figure 52). The drawdowns were monitored when firstly transmissivity was increased, maintaining the same abstraction rate throughout, and then the abstraction rate increased and the transmissivity kept constant. The boreholes are numbered consecutively, from 1 to 5. It is expected that boreholes 1 and 5 will display the least amount of drawdown and borehole 3 the most.

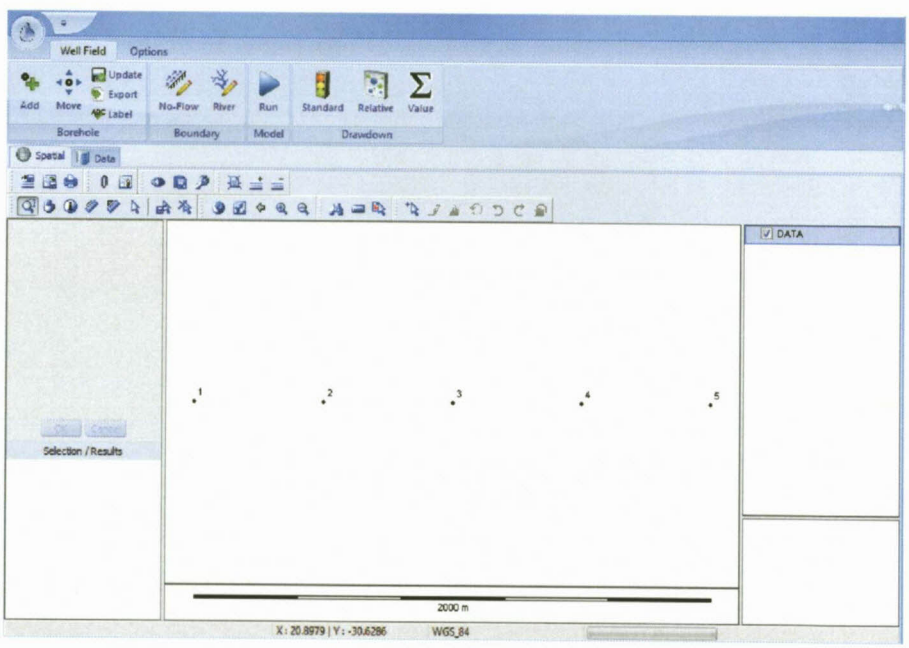

Figure 52. An image taken from the Wellfield Model indicating positions of the boreholes placed in a row.

Results:

- When abstracting 1 L/s from each borehole from an area with a transmissivity of 1 m^2/d, no borehole interference is apparent. Borehole interference occurs when T is increased from T = 2 m^2/d.
- From T = 1 – 5 m^2/d, boreholes 2, 3 and 4 all display the same drawdown. Only at T = 6 m^2/d does borehole 3 display the most drawdown.

The results indicate that the lower transmissivity range (1 – 5 m^2/d) limits the extent to which a borehole can gain water, which is why boreholes 2, 3 and 4 all have the same drawdown. Boreholes 2 and 4 cannot access water from the borehole 3 area unless the transmissivity is equal to or above 6 m^2/d. Thus in areas with very low transmissivity (from 1 – 5 m^2/d) boreholes can be spaced 500 m apart and each pumped at 1 L/s for 360 days and no excessive borehole interference will occur. Borehole interference will occur between adjacent boreholes but no overlapping of borehole interference will occur.

As expected, drawdown increases with decreasing transmissivity, and when transmissivity values are low, drawdown becomes excessive (Figure 53).

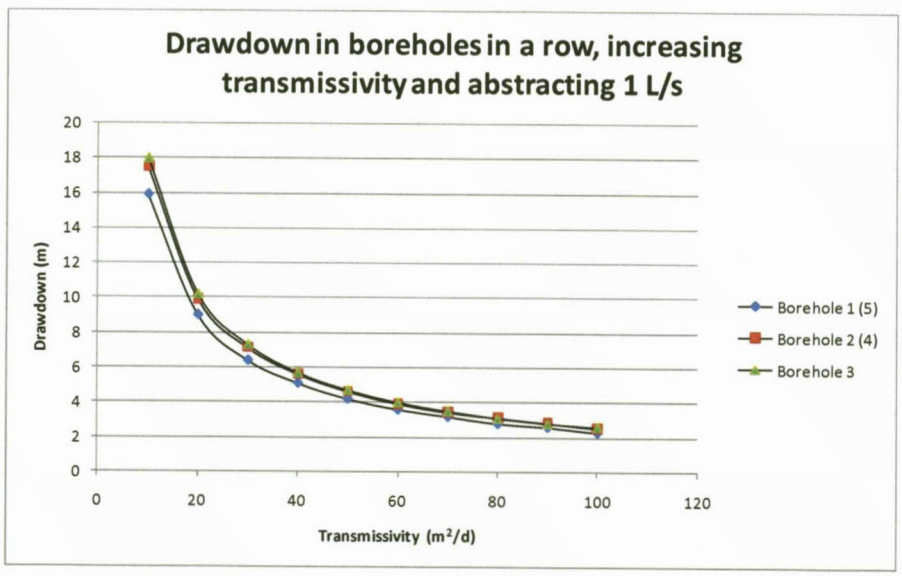

Figure 53. Drawdown in five boreholes placed 500 m apart in a row, with a constant abstraction (1 L/s) and increasing transmissivity

The results of running the model are as expected, illustrating that the higher your transmissivity, the lower the resultant drawdown. It is not viable to pump boreholes greater than 1 L/s in a very low transmissivity area, but where the area has a higher transmissivity value (from 5 – 10 m^2/d) the resultant drawdown may be more acceptable. Examples of this are listed below:

- When T = 1 m^2/d, every abstraction increase of 1 L/s results in a further 120 m drawdown
- When T = 5 m^2/d, every abstraction increase of 1 L/s results in a further 30 m drawdown
- When T = 10 m^2/d, every abstraction increase of 1 L/s results in a further 15 m drawdown

Scenario 2: With a no-flow boundary

This design is the same as Design 1, but with the presence of a no-flow boundary located 500 m from Borehole 1 (Figure 54). The effect of the boundary on the boreholes was observed as transmissivity values were increased and while abstraction was held constant at 10 L/s in all boreholes.

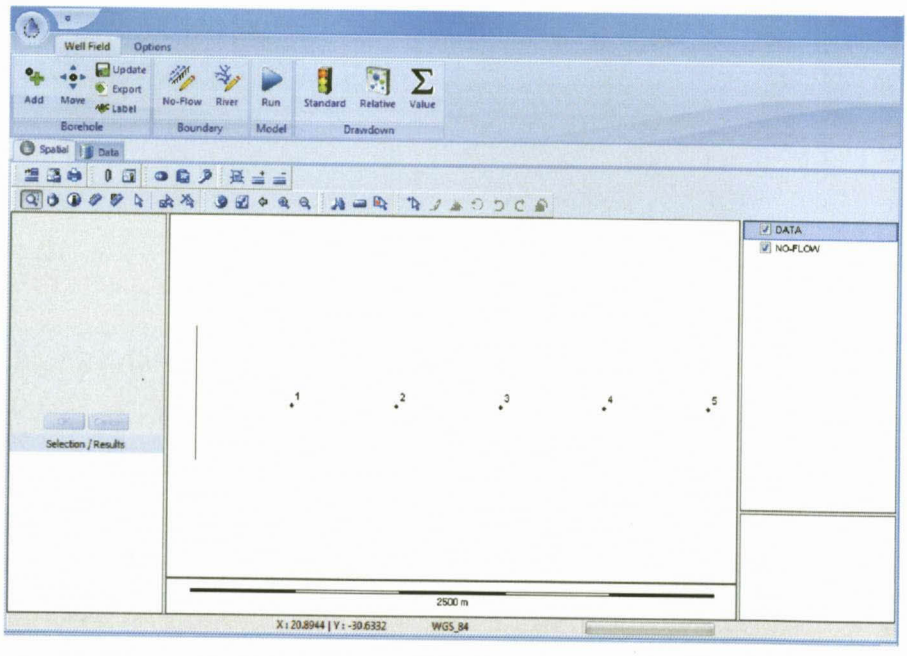

Figure 54. An image of the Wellfield Model displaying the positions of the boreholes relative to the no-flow boundary.

The effect of the no-flow boundary on the boreholes as the transmissivity value was increased from 10 – 100 m^2/d and where abstraction was set at 10 L/s from all boreholes is as follows:

- Borehole 1, located 500 m from the boundary is affected by 3 – 8 m as the transmissivity value is increased from 10 - 100m^2/d
- Borehole 2, located 1 km from the boundary is affected by 0.7 – 2.3 m as the transmissivity value is increased from 20 - 100m^2/d. At a transmissivity value of 10 m^2/day, the boundary had no effect on the drawdown in this borehole.
- Borehole 3, located 1.5 km from the boundary is affected by 0.5 – 1 m as the transmissivity value is increased from 50 – 100 m^2/d. At transmissivity values of 10 and 20 m^2/day, the boundary had no effect on the drawdown in this borehole.
- Borehole 4, located 2 km from the boundary is affected by 0.2 m as the transmissivity value is increased from 80 - 100 m^2/d. At transmissivity values of 10, 20 and 50 m^2/day, the boundary had no effect on the drawdown in this borehole.
- Borehole 5, located 2.5 km from the boundary is not affected.

The presence of no-flow boundaries results in an increase in drawdown in pumped boreholes. This is most noticeable in boreholes closest to a boundary and where transmissivity values are high (50 – 100 m^2/d). In designing a wellfield, and particularly in areas of high transmissivity, one must take care when siting boreholes so as to consider the additional drawdown from no-flow boundaries. As a guide, boreholes should be sited more than 1 km from no-flow boundaries if your transmissivity value is reasonably high (above 20 m^2/d) as the effect of a boundary is substantially less than at 500 m from a boundary. A borehole located 2 km from a boundary displays negligible drawdown effects and a borehole 2.5 km from a boundary shows no drawdown effect at all. As a guide based on the simple scenario presented above, a borehole located more than 2 km from a boundary will not be affected by a no-flow boundary.

6.5.2 Establishing spacing between two boreholes with different allowable interference between boreholes

The Wellfield Model was tested with various scenarios in order to determine optimum placing of boreholes and pumping rates. Two boreholes were placed adjacent to one another with varying transmissivity values, abstraction rates and allowable drawdown interference between them, and all possible combinations were carried out. The model was run for 360 days. The values used for each parameter are given in Table 11.

Table 11: Parameters and values used in determining borehole spacing

Parameter	Values tested
Abstraction (L/s)	1, 2.5, 5, 10
Transmissivity (m^2/d)	5, 10, 20, 50, 100, 200
Allowable interference (m)	2, 5, 10

Transmissivity graphs (Figures 55 – 60) have been produced whereby ranges of parameter values (Table 11) were tested to establish optimum spacing between boreholes when an allowable interference restriction exists.

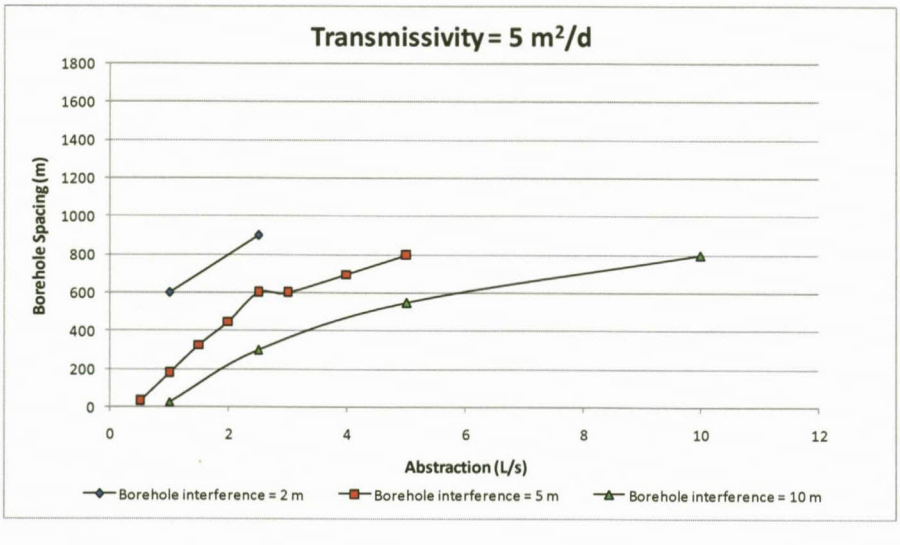

Figure 55. Borehole spacing with abstraction where transmissivity is 5 m^2/d.

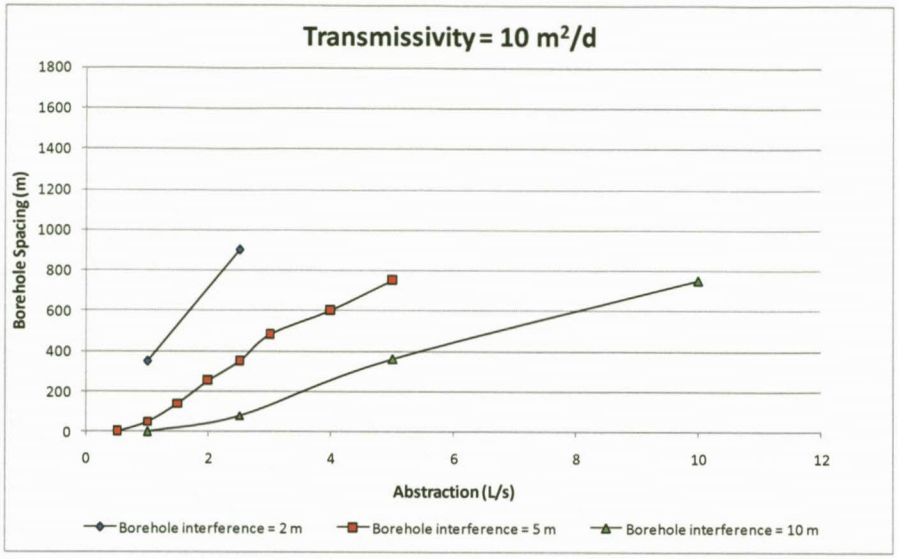

Figure 56. Borehole spacing with abstraction, where transmissivity is 10 m^2/d.

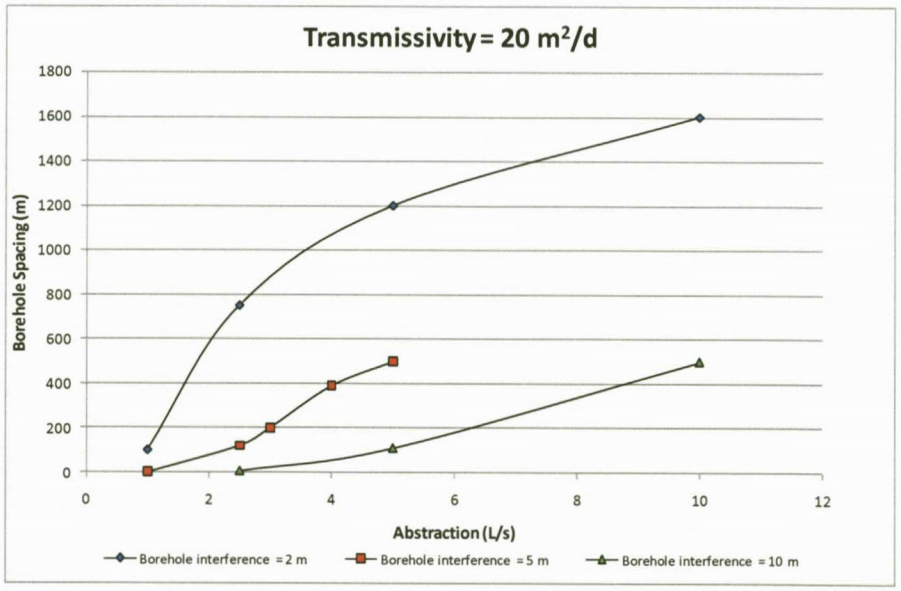

Figure 57. Borehole spacing with abstraction, where transmissivity is 20 m^2/d.

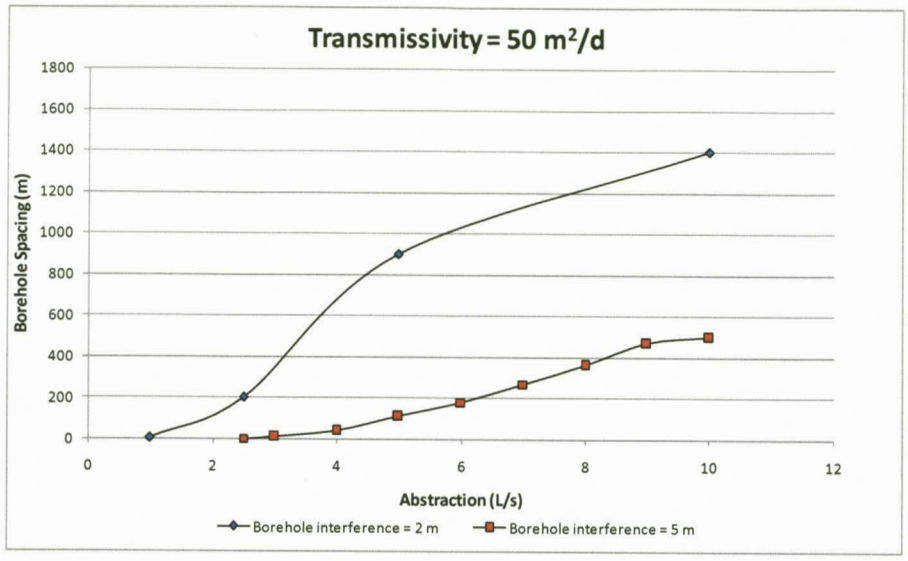

Figure 58 Borehole spacing with abstraction, where transmissivity is 50 m^2/d.

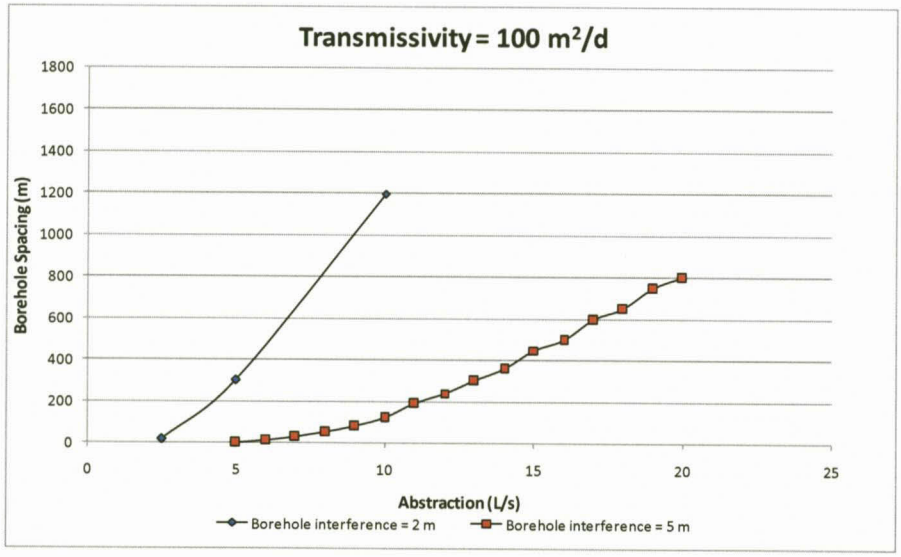

Figure 59. Borehole spacing with abstraction, where transmissivity is 100 m^2/d.

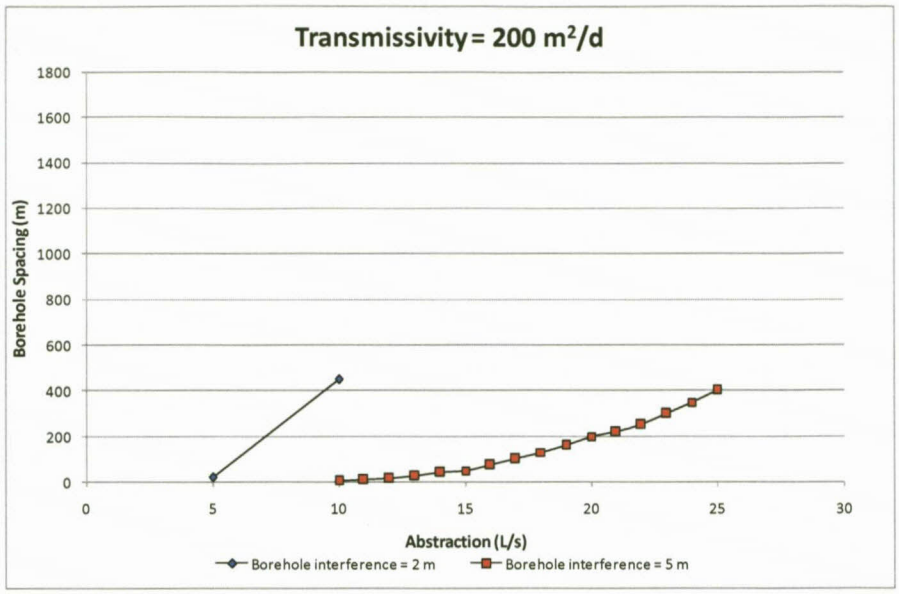

Figure 60. Borehole spacing with abstraction, where transmissivity is 200 m^2/d.

The examples presented in the scenarios above again show that with increasing transmissivity values (and constant abstraction rate) boreholes can be located closer together. The model is based on the Cooper-Jacob equation which assumes that an aquifer is of infinite extent, thus in a highly transmissive aquifer, the radius of influence is extensive, abstraction rates can be high and drawdowns low. For example, using a borehole interference of 5 m and an abstraction rate of 5 L/s, with a transmissivity value of 10 m^2/day the boreholes would have to be located 750 m apart, whereas with a transmissivity value of 50 m^2/day they could be positioned 100 m apart, and with a transmissivity value of 100 m^2/day or more, they could be situated adjacent to one another. These graphs can thus be used as a rough guideline for spacing two boreholes apart when the transmissivity of the study area (or dyke) is known. Bearing this in mind, however, the presence of a no-flow boundary would limit the volume of water available for abstraction. Thus, in reality, it may be necessary to increase your initial borehole spacing calculated if a no-flow boundary is present.

6.5.3 Establishing and comparing borehole spacing between two and three boreholes

Further testing of the model was carried out to determine the spacing of boreholes required for different transmissivity values. The tests were done with both two and three boreholes (the third borehole being placed in a line with the other two) to compare the difference in required borehole spacing. In these scenarios, an additional drawdown of 5 m as a result of interference was allowed. A wide range of transmissivity values were tested, with a minimum of 5 m^2/d and maximum of 200

m^2/d. Testing was carried out on scenarios until drawdowns in individual boreholes became unrealistic (exceeding ~40 m). In the case of three boreholes present, the middle borehole was monitored to ensure borehole interference did not exceed 5 m. Thus if the drawdown at a borehole was say 38 m and the additional drawdown caused by borehole interference was 5 m, leading the total drawdown to be 43 m, this was discarded – only total drawdown values up to ~40 m were accepted. As a rough guide for this limit, the maximum thickness of the weathered zone of Karoo Formations was used (~40 m). Below this zone storage coefficients generally decrease and consequently the risk of borehole failure with long-term drawdown below this level should be high.

Optimum borehole spacing

Different transmissivity and abstraction values were used to establish the distance required between boreholes in order to not exceed 5m interference. Figures 61 and 62 illustrate the borehole spacing required for both two boreholes and three boreholes, all of which are pumping simultaneously at the rate shown on the X-axis.

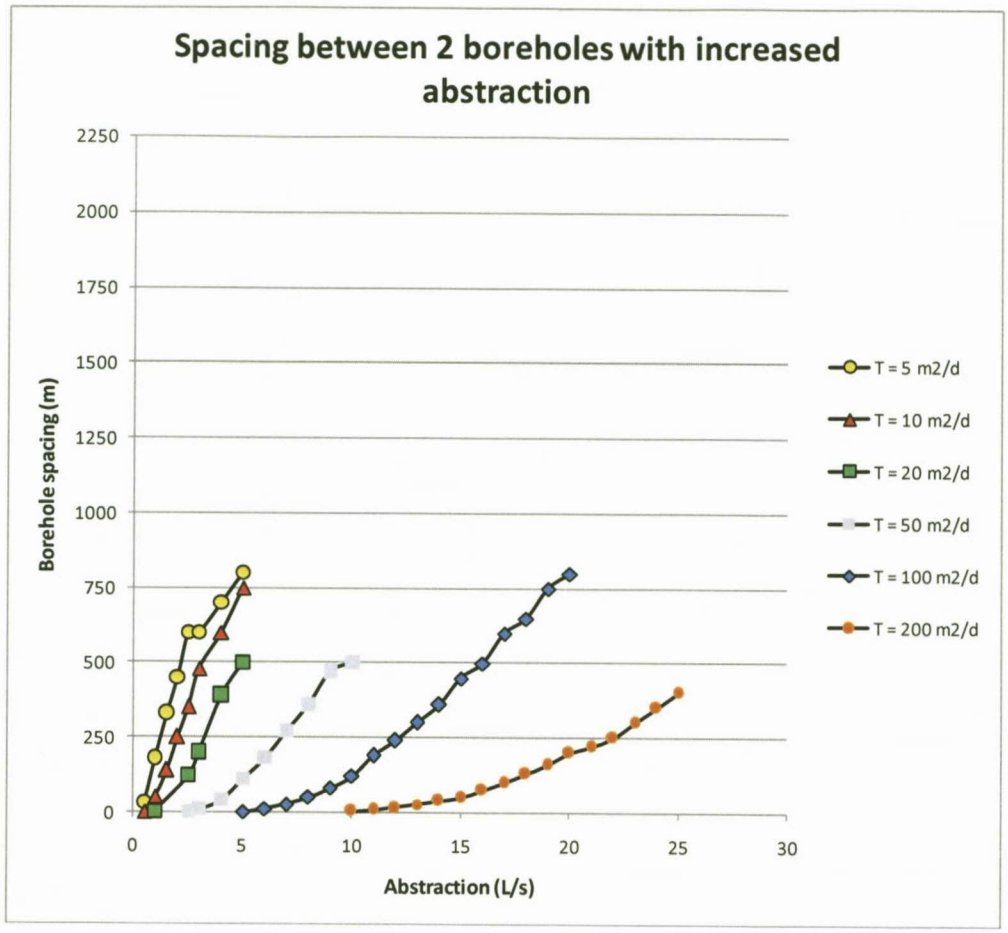

Figure 61. Borehole spacing required between two boreholes to limit interference to 5 m.

Figure 61 shows, for example that with a T-value of 20 m^2/day and an abstraction rate of 5 L/s, two boreholes would have to be placed 500 m apart in order to restrict their interference to 5 m over a year of abstraction.

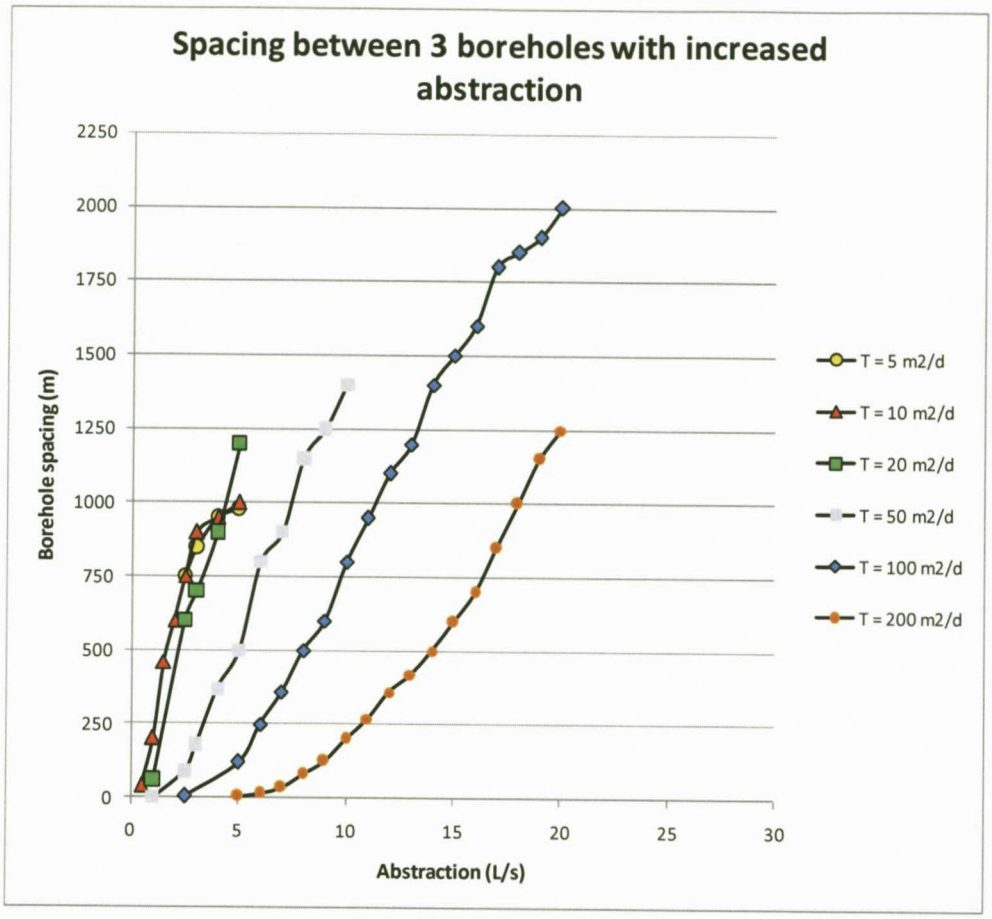

Figure 62. Borehole spacing required between each borehole when three are present to limit interference to 5 m.

Figure 62 shows that borehole spacing between all boreholes should be increased significantly when a third borehole is added. This is clear when comparing to Figure 61 above, with a T-value of 20 m^2/day and an abstraction rate of 5 L/s, three boreholes would have to be placed 1240 m apart in order to restrict their interference to 5 m over a year of abstraction. Taking this example, it can be seen that the borehole separation distance increased remarkably by 740 m, from 500 m with two boreholes to 1240 m with three boreholes.

Comparison of spacing between a 2 borehole scenario and a 3 borehole scenario

Slopes of both scenarios (two and three boreholes) were then compared for each transmissivity value. A few examples are shown in Figures 63 – 65.

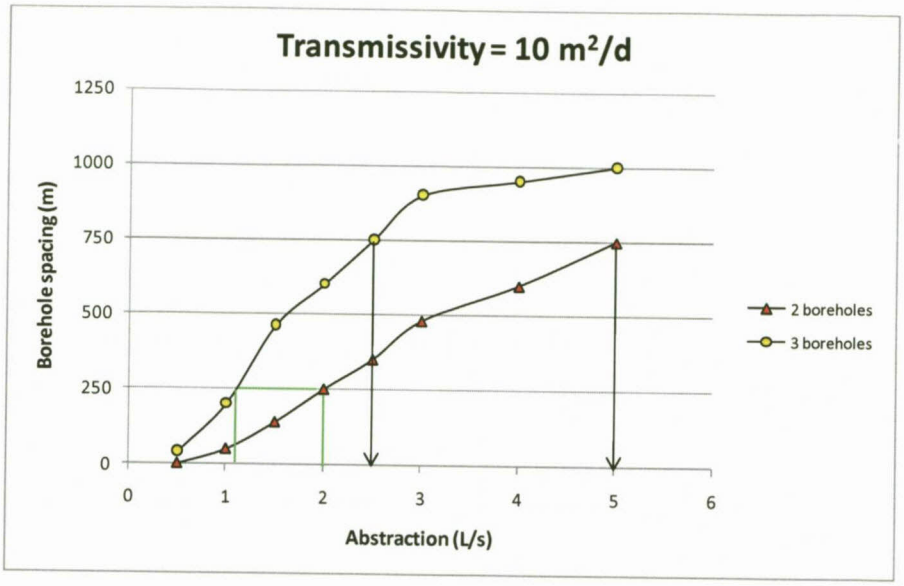

Figure 63. A comparison of borehole spacing required between two and three boreholes to limit interference to 5 m with a transmissivity of 10 m^2/d.

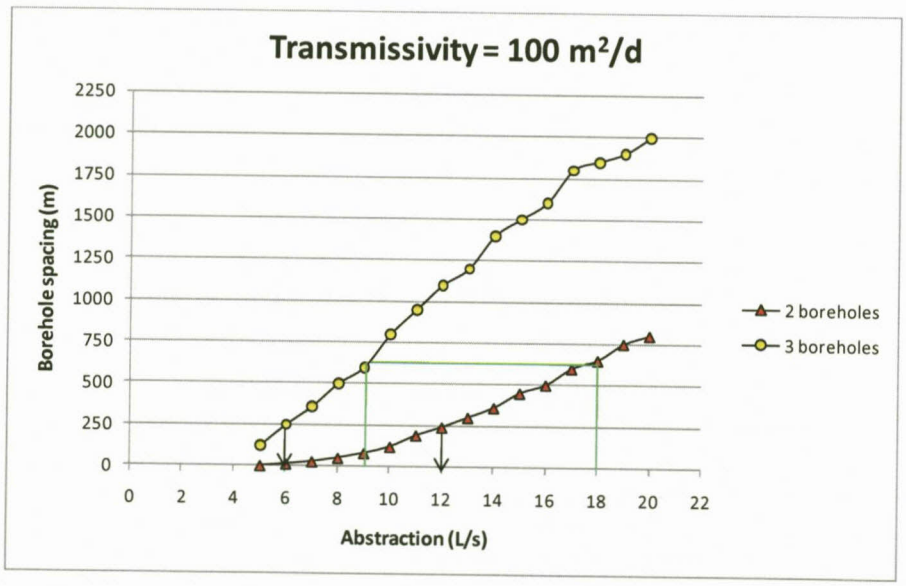

Figure 64. A comparison of borehole spacing required between two and three boreholes to limit interference to 5 m with a transmissivity of 100 m^2/d.

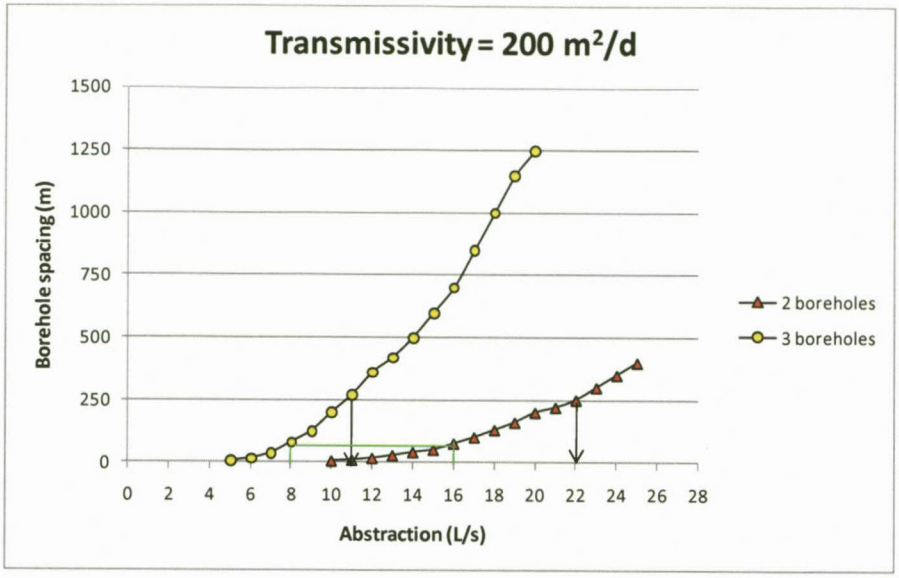

Figure 65. A comparison of borehole spacing required between two and three boreholes to limit interference to 5 m with a transmissivity of 200 m^2/d.

Figures 63 – 65 compare spacing requirements with abstraction between two boreholes and three boreholes. It appears that in order to add a third borehole to a two boreholes scenario and at the same distance apart, the pumping rate of all three must be half of the rates of each of the two boreholes. For example, in an environment where transmissivity is 10 m^2/d, with two boreholes both pumping at 5 L/s for 360 days of the year, if another borehole is to be added, keeping the same spacing between each borehole, the pumping rates for each borehole must be reduced in all boreholes to 2.5 L/s in order for no further drawdown to occur. This can be observed in all graphs, demonstrated by the black arrows and green lines joining the relevant points of abstraction rates with the two and three borehole slopes. It would therefore be more productive to site two abstraction boreholes rather than three, as the addition of a third, if placed the same distance away as the first two, will require all boreholes to be pumped at half of the initial abstraction rate. The results from Figure 63 – 65 thus indicate that for areas with a wide range of transmissivity values (10 – 200 m^2/d) borehole interference plays a large role in restricting the rate at which each borehole can be pumped. Thus one must consider carefully the transmissivity of the area of interest and the rate of water required from the area in order to determine the most optimum borehole design.

Relationship between 2 and 3 borehole scenarios regarding borehole spacing

This section explores the relationship between the spacing of two boreholes and the further spacing required when a third borehole is added in a line to the first two boreholes whilst maintaining a maximum interference between boreholes of 5 m. This was done using a number of transmissivity and abstraction values (see Table 12), and the results are shown in Figure 66.

Table 12: Abstraction rates applied for different transmissivity values when determining required borehole spacing with an interference limit of 5 m.

Transmissivity = 5 m^2/d											
Abstraction rate (L/s)	0.5	1	1.5	2	2.5	3	4	5			
Transmissivity = 10 m^2/d											
Abstraction rate (L/s)	0.5	1	1.5	2	2.5	3	4	5			
Transmissivity = 20 m^2/d											
Abstraction rate (L/s)	1	2.5	3	4	5						
Transmissivity = 50 m^2/d											
Abstraction rate (L/s)	2.5	3	4	5	6	7	8	9	10		
Transmissivity = 100 m^2/d											
Abstraction rate (L/s)	5	6	7	8	9	10	11	12	13	14	15
Transmissivity = 200 m^2/d											
Abstraction rate (L/s)	10	11	12	13	14	15	16	17	18	19	20

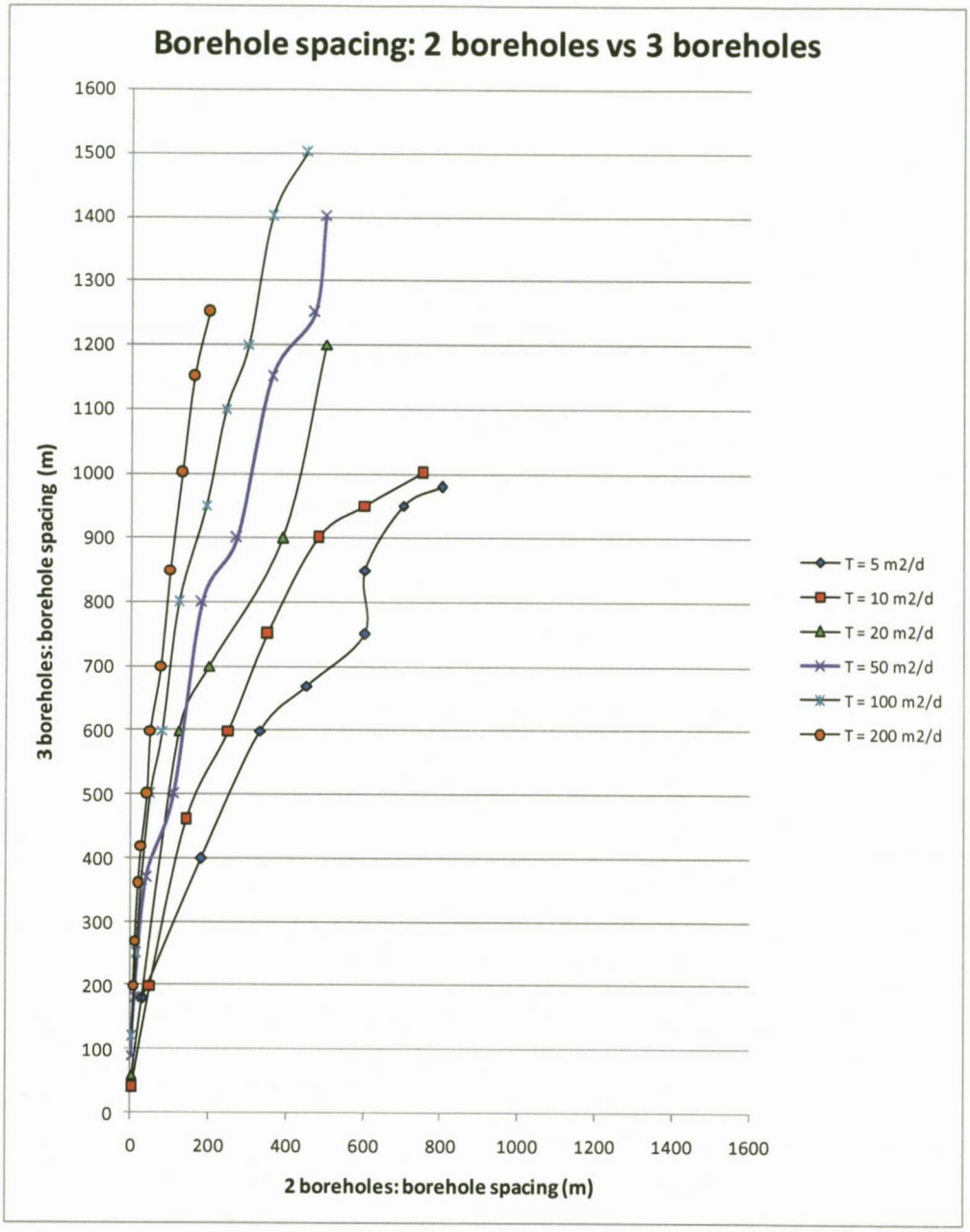

Figure 66. A comparison of borehole spacing required between two and three boreholes with different transmissivity values and abstraction rates applied and an interference limit of 5 m (Note that the increasing points along the slopes refer to increasing abstraction rates as listed in Table 12).

Figure 66 shows that borehole spacing must be increased significantly when a third borehole is added in line to two other boreholes (and pumped at the same rates as the others) in order to have no increase in drawdown. With transmissivity values less than 20 m^2/d, the increase in spacing from two to three boreholes is not as dramatic as when transmissivities are greater (from 50 – 200 m^2/d).

The increase in required borehole spacing is more sensitive to increased abstraction at higher transmissivity rates, thus care must be taken when spacing boreholes in a wellfield in higher transmissivity areas.

Extensive testing was carried out to compare the borehole spacing required when two boreholes are sited in a certain transmissivity environment (and pumped at the same rate) to when three boreholes are sited in the same transmissivity environment and with the same pump rate. Linear trend lines were fitted to the slopes above in Figure 66, equations obtained for each slope were in the form:

$y = mx + c$ Equation 15

Where:

y = borehole spacing in a three borehole scenario

x = borehole spacing in a two borehole scenario

m and c = variables

Two examples of the Equation 15 obtained can be seen below, for the lowest and highest transmissivity values implemented:

- For $T = 5\ m^2/d$ $y = x + 200$ Equation 16
- For $T = 200\ m^2/d$ $y = 5x + 270$ Equation 17

The two equations illustrate the diversity of the equations obtained, which is primarily due to the large number of variables that require testing. Thus a generalised relationship for all transmissivity and abstraction values might not exist. If more extensive work is carried out to model a larger number of scenarios perhaps a more complex, but more widely applicable, relationship may be developed.

6.5.4 Comparing the Cooper-Jacob equation to a linear flow equation (the Boonstra-Boehmer equation)

Before a conclusion can be decided upon drawdown regarding borehole spacing, a different equation should be considered when dealing with flow in dykes. This flow differs from regular, matrix flow as it involves preferential flow through single vertical dykes in country rock aquifers which is one of the primary targets in the Karoo Basin.

Background

Contrary to previous beliefs, dykes may largely be considered as highly permeable geological features due to the presence of joints and fractures as a consequence of cooling and shearing respectively during emplacement in colder country rock. Through experience it has become more apparent that higher yielding boreholes can be sited in and adjacent to dolerite dykes in the Karoo. The standard well flow equations are therefore not applicable for this analysis (Kruseman & de Ridder, 1992; Murray, 2008).

A pumped borehole, situated in dyke with a high transmissivity positioned within a low transmissivity aquifer, will produce a *trough* of depression instead of the typical cone of depression. The extent of this trough will be dependent on a number of pump rate and duration, transmissivity and storativity (see equation below) (Kruseman & de Ridder, 1992).

This variation in hydraulic behaviour resulted in the development of Boonstra and Boehmer's drawdown equation for early and medium pumping times. This equation applies to a dyke with an infinite length, but definite width and hydraulic conductivity values. The permeability of the dyke is a consequence of uniformly distributed fractures and the water within these fractures is confined above and below by weathering and impermeable basement rock respectively (Kruseman & de Ridder, 1992).

During pumping of a well placed in the dyke, three gradually transitioning time phases can be distinguished. Early time is characterised by parallel flow within the dyke from the fracture system,

medium time by parallel flow from the aquifer, and late time by pseudo radial flow within the aquifer (Kruseman & de Ridder, 1992).

Analysis of pump tests is based on the following assumptions and conditions:

- "The dyke is vertical and of infinite extent over the length influenced by the test;
- The width of the dyke is uniform and does not exceed 10 m;
- The flow through the fracture system in the dyke is laminar, so Darcy's equation can be used;
- The uniformly fractured part of the dyke can be replaced by a representative continuum to which spatially defined hydraulic characteristics can be assigned;
- The fractured part of the dyke is bounded above by an impermeable weathered zone and below by solid rock;
- The well fully penetrates the fractured part of the dyke and is represented by a plane sink: flow through the dyke towards the well is parallel;
- The country-rock aquifer, which is in hydraulic contact with the fractured part of the dyke, is confined, homogeneous, isotropic, and has an apparently infinite aerial extent;
- All water pumped from the well comes from storage within the composite system of dyke and aquifer;
- The ratio of the hydraulic diffusivity of the dyke to that of the aquifer should not be less than 25;
- Well losses and well-bore storage are negligible." (Kruseman & de Ridder, 1992)

<u>Boonstra-Boehmer's curve-fitting method (1986)</u>

This equation is applicable for early and medium pumping times to analyse drawdown in observation wells along a pumped dyke.

$$s(x,t) = \frac{Q}{3.75\sqrt{T_d ST/S_d}} F(\chi,\tau)$$

Equation 18

S (x,t) = Drawdown in the dyke, distance (x in m) away from the borehole after time (t in days)

S = Storativity of the aquifer

S_d = Storativity of the dyke

T = Transmissivity of the aquifer (m^2/d)

T_d = Transmissivity of the dyke (m^2/d)

W_d = Width of the dyke (m)

An additional assumption requires flow in the aquifer as near parallel to parallel thus pumping time should be considered as:

$t < 0.28\ S(W_d T_d)2/4T^3$ Equation 19

(Kruseman & de Ridder, 1992)

Methodology

The Boonstra-Boehmer equation was implemented noting the increase in drawdown in a borehole while increasing the abstraction rate, at varying transmissivity values. In addition, the Cooper-Jacob approximation (Equation 12) was applied in the same sense, making the drawdown observations. The Cooper-Jacob equation made use of the transmissivity and storativity values used for the dyke (not matrix) in the Boonstra-Boehmer equation. All remaining parameters (pump duration, rate and distance from well) were the same for both equations.

Comparison of the Cooper-Jacob equation with the Boonstra-Boehmer equation

Due to an assumption of the Boonstra-Boehmer equation ("The ratio of the hydraulic diffusivity of the dyke to that of the aquifer should not be less than 25"), transmissivity values had to be kept reasonably high in order to provide realistic results. An additional requirement (Equation 19), limited

the duration of pumping to 0.3 days. This process was carried out using a number of transmissivity and abstraction values (Table 13), and the results are shown in Figures 67 - 70.

Table 13: Abstraction rates and transmissivity values applied to each equation when noting drawdown

Transmissivity (m^2/d)	25	50	100	200
Pumping rate (L/s)	1	2	4	10

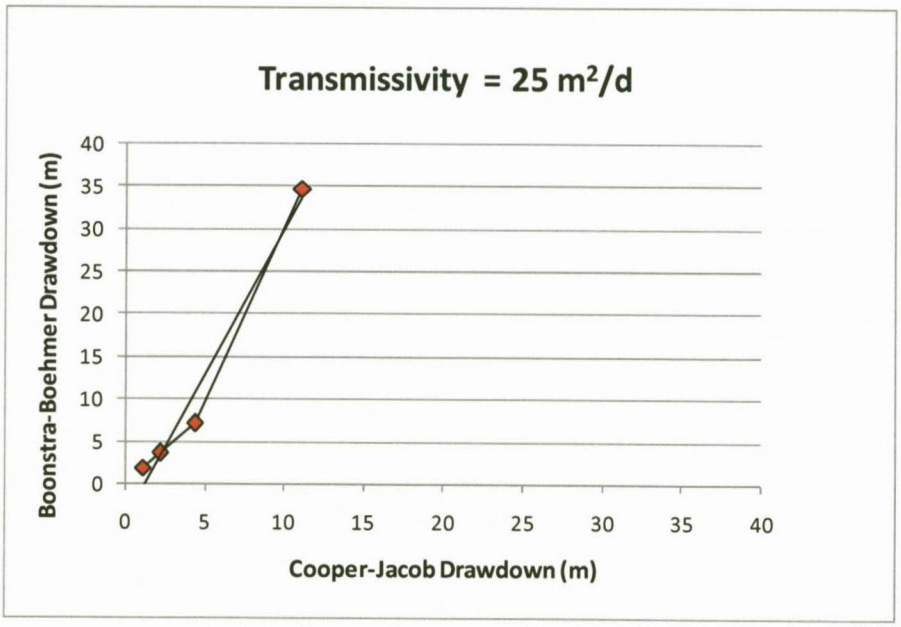

Figure 67. Comparison of Boonstra-Boehma and Cooper-Jacob drawdown with abstraction, where transmissivity is 25 m^2/d (Note that the increasing points along the slopes refer to increasing abstraction rates as listed in Table 13).

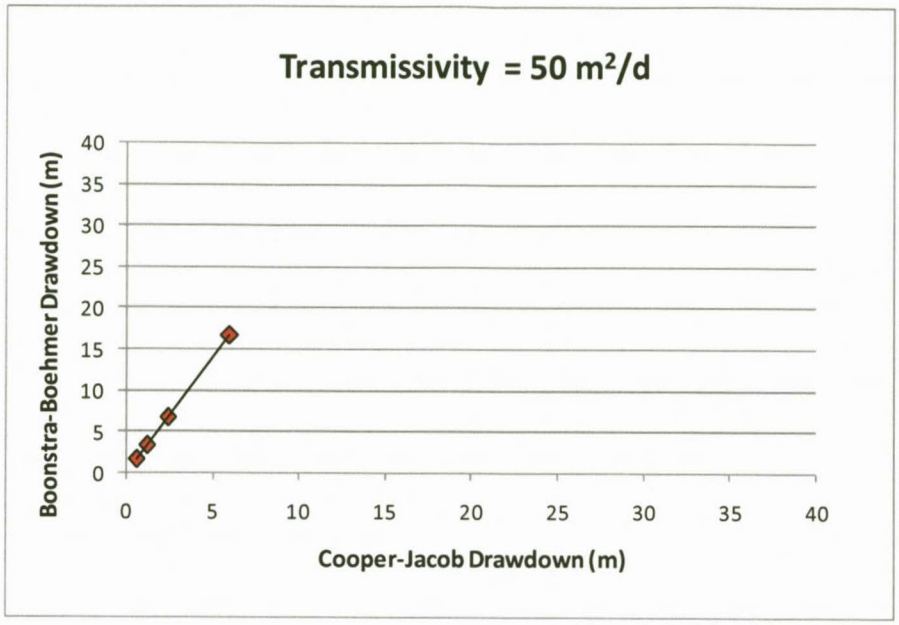

Figure 68. Comparison of Boonstra-Boehma and Cooper-Jacob drawdown with abstraction, where transmissivity is 50 m^2/d (Note that the increasing points along the slopes refer to increasing abstraction rates as listed in Table 13).

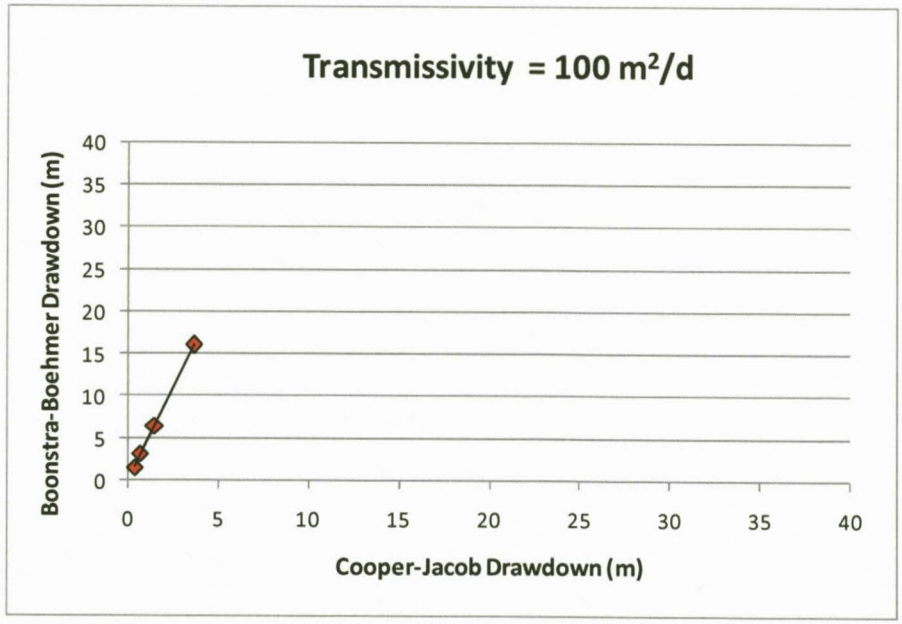

Figure 69. Comparison of Boonstra-Boehma and Cooper-Jacob drawdown with abstraction, where transmissivity is 100 m^2/d (Note that the increasing points along the slopes refer to increasing abstraction rates as listed in Table 13).

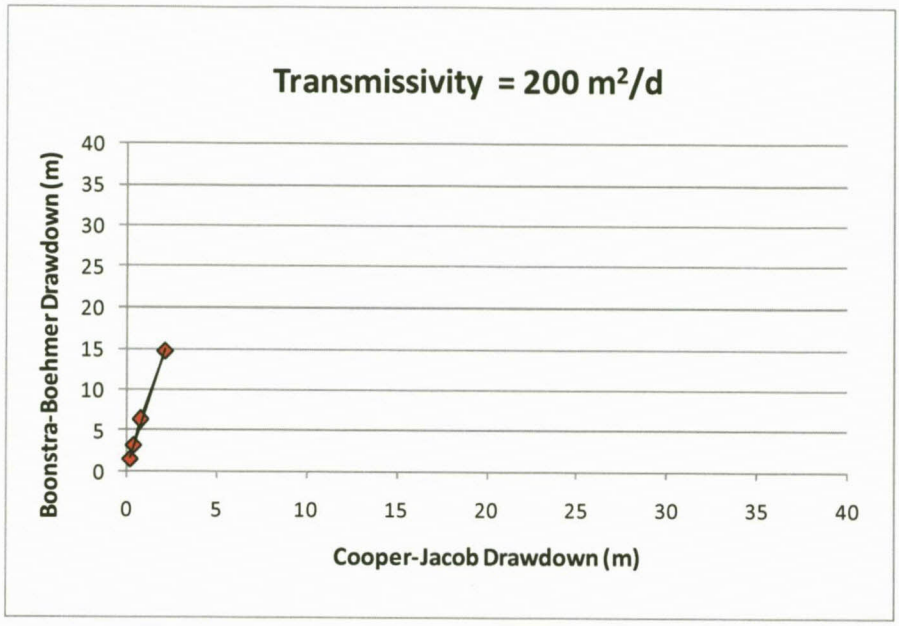

Figure 70. Comparison of Boonstra-Boehma and Cooper-Jacob drawdown with abstraction, where transmissivity is 200 m^2/d (Note that the increasing points along the slopes refer to increasing abstraction rates as listed in Table 13).

Observations

The Boonstra-Boehmer equation behaves in a similar way to the Cooper-Jacob equation whereby drawdown increases with increased abstraction, and/or decreased transmissivity. A significant difference, however, is the amount of drawdown that occurs. The drawdown calculated from the Boonstra-Boehmer equation is more sensitive to abstraction, increasing more rapidly in comparison to the Cooper-Jacob calculated drawdown. This may be due to the limited extent of the high transmissivity zone (i.e. the dyke) in the Boonstra- Boehmer equation, whereas in the Cooper-Jacob, the transmissivity value is applied to an infinite area.

A possible relationship was investigated between the spacing of two boreholes using the Cooper-Jacob equation and the further spacing required when the boreholes are positioned on a dyke, thus using the Boonstra-Boehmer equation. Linear trend lines were fitted to the graphs producing the following equations, where y is the "BB drawdown" and x is the "CJ drawdown":

- $T = 25\ m^2/d$ $y = 3.4x - 4$
- $T = 50\ m^2/d$ $y = 3x$
- $T = 100\ m^2/d$ $y = 4.5x$
- $T = 200\ m^2/d$ $y = 7x$

The above equations can provide a rough guideline regarding the additional drawdown that could be expected over and above predicted CJ drawdowns, and in turn, may be used to provide guidance on the increase in borehole spacing required from the Cooper-Jacob calculation, when boreholes are sited on a dyke. As can be observed, the drawdown in boreholes calculated from the Cooper-Jacob equation must be increased significantly if considering the linear flow in dykes instead of radial flow, thus boreholes should be sited a larger distance apart when sited in a row along a dyke. Furthermore, the increase required between boreholes when dealing with linear over radial flow is larger in an area with high transmissivity values compared to an area with low transmissivity values. Thus when working in an area with a high transmissivity (~200 m^2/d) value and siting boreholes on a dyke, if the Cooper-Jacob equation is used as an initial estimate regarding borehole spacing, it is recommended that the calculated drawdowns are multiplied by ~7 in order to gain a more accurate estimate of drawdown in abstraction boreholes.

6.6 Conclusion

This chapter aimed to assist in the designing of a wellfield by testing a number of borehole abstraction and spacing scenarios. Different scenarios were run to evaluate the effect of groundwater abstraction on drawdown, and from this the most optimum theoretical wellfield design was established. Furthermore, a rough guideline on the required increase in borehole spacing when siting three boreholes compared to two boreholes was developed, as well as when boreholes are sited on a dyke, potentially experiencing linear, and not radial, flow.

Chapter 7

7 Case Studies

7.1 Introduction

The purpose of the case studies is to apply the groundwater yield assessment methods that have been developed during the project in areas with known aquifer parameters and yields. The yield assessment methods are compared with other existing yield assessment tools and with field data. The approach adopted firstly takes the aquifer yield, or the groundwater yield of the larger area into account, then the wellfield yield, and finally individual borehole yields.

This component of the project aims to address aquifer and wellfield yield estimations by the application of these various methods to case study areas and comparing the results from each method in terms of accuracy and practicality. More specifically, the groundwater balance model (AAYM and Wellfield Model) results may be compared to the HP (Baron *et al.,* 1998) and GRAII (DWAF, 2006) databases which will assist in drawing conclusions on the model feasibility in assessing groundwater potential and its application in project planning. Future users of these methods must have adequate knowledge and experience of the study area on which the parameter estimations will be based.

7.2 Methodology

7.2.1 Reports

Previous work done at certain localities in the Karoo Basin provided the basis upon which both case study areas were selected. Reports on the areas were supplied by Groundwater Africa, these reports include a brief reconnaissance of the area and the processes carried out in the groundwater supply scheme. The previous knowledge and experience acquired were essential in these study areas in order to validate certain assumptions necessary in this investigation. Additionally, experience will provide a good sense of the reliability of the results found from the models.

7.2.2 Geology of each Case Study

The regional geology of each case study is included in the reports supplied by Groundwater Africa, and on the 1:250 000 geological maps provided by the Council for Geoscience office in Bellville. Understanding the underlying geology as well as the geological structures present in the areas provides a good indication of the type of aquifers present as well as the nature of the targets for borehole siting.

7.2.3 Existing Data

Borehole data obtained from the Groundwater Africa reports will be used for further borehole siting and in the estimation of aquifer parameters. Relevant information provided from these borehole datasets includes that of the method of siting, water strikes and borehole depths, as well as yields and aquifer parameters estimated by pump tests carried out on these boreholes. Borehole coordinates are also provided enabling the mapping of their positions on Google Earth.

7.2.4 Delineate Area

The relevant data-sets used to delineate the study area include:

- Geological Maps, Scale of 1:250 000
- Arcview GIS (Geological Map 1:250 000, Topographical Maps 1:50 000, Aerial Photography)
- Google Earth

The delineation typically combines topography, air or satellite photos and geological maps. Once the area is delineated as a polygon, it must be converted into a KML file to be imported into Google Earth where the area size can be calculated.

7.2.5 Aquifer Yields

Once the study area has been delineated and the quaternary catchment in which the area lies established, yields from databases HP and GRAII (AGEP) can be obtained. The databases provide approximate figures which the AAYM, Wellfield Model and individual borehole yields can be measured against and evaluated. The values must be proportioned according to the ratio of the size of the delineated area to the total quaternary catchment size.

7.2.6 Identify Drilling Targets

This approach involves a process of identifying areas with potential for high yielding boreholes. This is carried out in a series of steps using different data-sets, each of which incorporates an increased level of detail.

The following resources are used in this step:

- Transmissivity map (Chapter 4)
- Geological map 1:250 000 (Arcview GIS)
- Google Earth
- Aerial Photographs (not available for all case studies)

The following symbols are presented on Google Earth for the various borehole siting methods involved:

250G – boreholes sited using 1:250 000 geological maps

GE – boreholes sited using Google Earth

DP – boreholes sited using aerial (digital) photographs

7.2.7 Assigning Aquifer Parameters Values

Three processes are presented for establishing borehole and aquifer yields from the identified groundwater targets: 1) Assured Yield Model Assessment, 2) Wellfield Model Assessment and 3) Borehole Yield Assessment. They all require using various aquifer parameters, of which default values are presented below.

7.2.8 Assured Yield Model Assessment

The aquifer parameters that are required for the Aquifer Assured Yield Model (AAYM) are presented in Table 14 below:

Table 14: Default values or their sources provided for the application of AAYM

Parameter	Default Value
Extinction Depth (m.bgl)	1, 2 or 4*
Baseflow (mm/a)	Mean Annual Baseflow: Pitman
Maximum Allowable Waterlevel Drawdown (m)	5 **
Recharge (% MAP)	From GRAII
Threshold (mm)	MAP/12 (initially used)***

*Depending on MAP
**GRAII, DWAF, 2006
*** Bean, 2003

7.2.9 Wellfield Model Assessment

Different scenarios have been tested whereby existing data was used (obtained from the reports) as well as lower and upper ranges of theoretical parameters. Each scenario went through a trial and error process to determine the optimum pumping rate of each borehole considering its position in relation to the other boreholes. The available drawdown for each borehole was known (or a "theoretical" value was used) which was the main factor to consider when increasing the pumping rate. This is done to test the credibility of the wellfield model and to determine whether or not any factors should be taken into consideration when designing a wellfield system.

7.2.10 Borehole Yield Assessment

It is widely accepted that the Cooper-Jacob approximation of the Theis (1935) transient state radial flow equation (referred hereafter as the Cooper-Jacob equation) gives a reasonable estimate of borehole yields in Karoo aquifers (Murray, 1996; Sami and Murray, 1998; Van Tonder *et al.*, 1998). The two aquifer parameter values required for use in this equation are transmissivity and storativity, and in addition to these, the boreholes' available drawdown is needed to obtain a yield. In order to calculate the maximum pumping rate which would maintain a drawdown (s) above a specific point, after a long duration of pumping, the Cooper-Jacob equation can be defined as:

$$Q = \frac{4\pi Ts}{2.3log\frac{2.25Tt}{r^2S}}$$ Equation 20

Where:

Q = sustainable yield (m^3/day)

T = transmissivity (m^2/day)

s = available drawdown (m)

t = pumping time (days)

r = radius of the borehole (m)

S = storativity

It is evident from the Cooper-Jacob equation that the only sensitive parameters are T and s.

Transmissivity values

The transmissivity value can first be obtained from Transmissivity maps, Figure 1 & 2 below display the middle and upper ranges, which were used for the study areas. The Transmissivity map provides a range of values that reflect the conductivity of the various aquifer types with the lower values representing the matrix and the higher values representing what are considered to be permeable geological structures such as dolerite dykes. If transmissivity values are known from site-specific data, then they should be used.

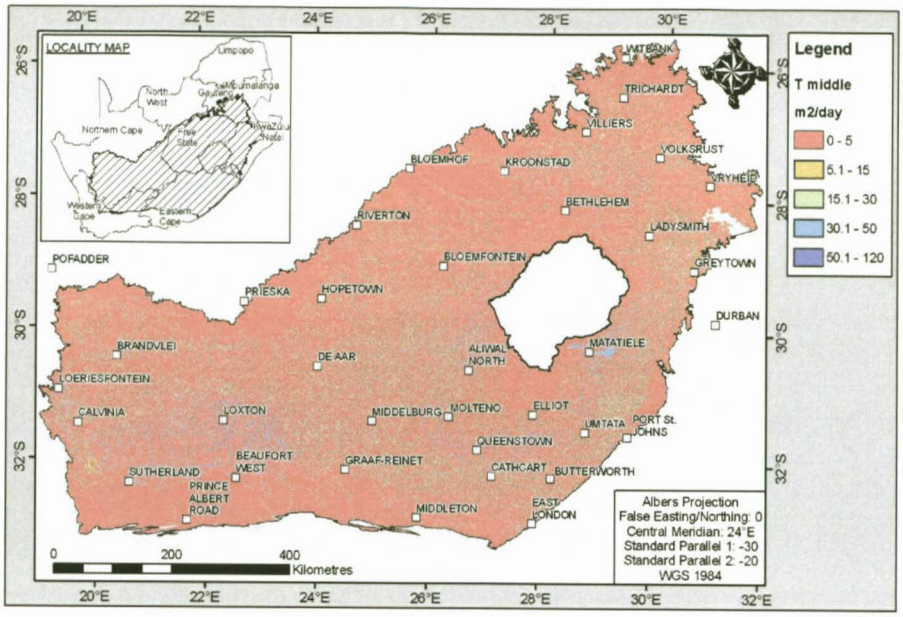

Figure 71. T-middle map of the Main Karoo Basin.

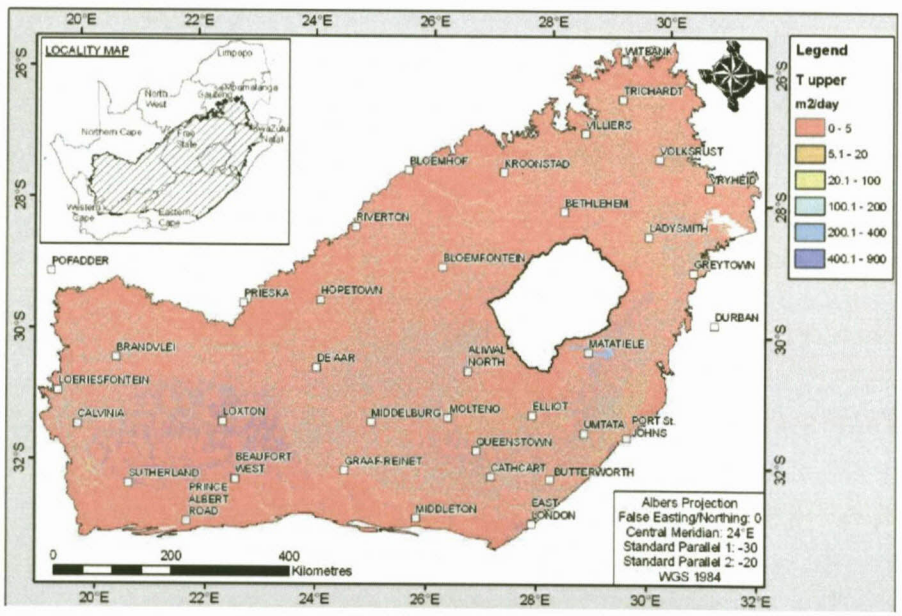

Figure 72. T-upper of the Main Karoo Basin.

Drawdown values

Local experience should govern the s-values used. As a guide the inflection point in typical drawdown curves should be used (Murray, 1996). If no such data is available, then the maximum value should not exceed the thickness of the weathered zone of Karoo Aquifers, which is estimated to be on average 18 m in the Eastern Karoo Basin. This value was calculated using the average saturated thicknesses (obtained from water strike frequency analyses (Dondo *et al.*, 2010)) of the weathered zone of each lithological domain in the Eastern Karoo Basin, which are presented in Table 15 (Dondo *et al.*, 2010).

Table 15: Average depth and saturated thickness of lithological domains.

Lithological Domain	Weathered/Jointed Zone	
	Depth Base (mbgl)	Saturated Thick (m)
Basalt	12.0	0.0
Clarens	40.0	28.1
Elliot	45.0	21.9
Molteno	30.0	11.3
Burgersdorp	52.0	34.5
Katberg	45.0	28.7
Adelaide	37.0	19.3
Tarkastad Subgroup	65.0	41.2
Normandien	55.0	30.9
Fort Brown (South)	30.0	12.4
Ripon (South)	33.0	13.3
Prince Albert (South)	22.0	6.0
South Zone	30.0	12.3
Ecca (Central)	27.0	7.5
Volksrust (North)	40.0	21.0
Vryheid (North)	33.0	8.1
Pietermaritzburg (North)	33.0	12.1
Dwyka	45.0	13.2
Msikaba	27.0	0.0
Metamorphosed Basement	50.0	30.0

Storativity or specific yield values

Table 16 (Dondo *et al.*, 2010) provides a reasonable first estimate of S-values that can be used.

Table 16: Specific Yield values per lithological unit in upper Karoo Aquifer layers

Lithological Unit	'Average' Specific Yield (*Sy*)
Basalt	0.0080
Clarens Sandstone	0.0300
Fine-grained Sandstone	0.0080
Coarse-grained Sandstone	0.0100
Mudstone	0.0025
Siltstone	0.0050
Tillite	0.0020
Shale	0.0009
Quartzite	0.0070

7.2.11 Calculation of Individual Borehole Yields

The desktop sited boreholes require the estimation of certain parameters in order for their potential theoretical yields to be determined, referred to as 'Theoretical Yield Values'. The theoretical yield values were determined using a range of transmissivity and drawdown values based on previous studies estimated from pumping tests, as well as the knowledge of the underlying geology (Table 17). Smaller dykes are associated with low transmissivity values and larger dykes with high transmissivity values. Individual borehole yields were calculated and tabulated using the Cooper-Jacob equation with a range of transmissivity and available drawdown values, r and S values of 0.165 mm and 0.002, respectively over the duration of one year (365 days) to demonstrate the possible range of yield values. The quality of this step thus depends on the knowledge, judgment and experience of the user.

Table 17: Range of transmissivity and drawdown values implemented in the Cooper-Jacob equation to determine theoretical yield values.

Parameter values		Yield for year-long abstraction	
T (m^2/d)	s (m)	Q (m^3/d)	Q (L/s)
10	5	34.1	0.4
20	5	65.8	0.8
40	5	127.0	1.5
10	10	68.3	0.8
20	10	131.6	1.5
40	10	254.0	2.9
10	20	136.6	1.6
20	20	263.2	3.1
40	20	508.0	5.9

2.9 Comparison of the various yields

In reality, an aquifer's yield is greater than a wellfield's yield, which in turn is greater than an individual borehole's yield. These yields need to be compared and where this is found not to be the case, the assumptions that governed the estimates need to be re-examined and modified. In some cases an aquifer's ability to allow water to flow through it (its transmissive capacity) is greater than the recharge potential. In such circumstances, the borehole yields could be theoretically higher than the aquifer yields. If this is the case, the borehole yields would need to be reduced to (at best) match the aquifer's yield.

7.3 Makhoba Village Case Study

7.3.1 Introduction

A groundwater exploration and resource assessment was undertaken in 2004 in the village of Makhoba to assess the possibility of expanding the existing surface water supply scheme by incorporating groundwater. Makhoba lies roughly north-east of Matatiele neighboring the Lesotho border (Figure 73). The aim of the project was to identify potential groundwater sites in close proximity to the existing pipe lines (Murray, 2004). The area surrounding this village was chosen as a case study because of the previous work carried out of this area. Data provided by the reports can be used to test the credibility of the various results obtained from the models.

Figure 73. The position of the study areas Makhoba and Outspan/Hebron in relation to Matatiele.

7.3.2 Geology

The underlying geology of the area surrounding Makhoba village comprises the Tarkastad Subgroup of the upper Beaufort Group and the Molteno Formation of the Drakensberg Group, which outcrops a further distance from the village. The Tarkastad consists of predominantly red, purple and green mudstone and fine to medium grained yellow and grey sandstone as well as dolerite dyke and sill intrusions. The Molteno Formation outcrops in the upper areas and is predominantly made up of coarse grained sandstones with occasional thin shale beds (Johnson *et al.*, 2006; Murray, 2004).

7.3.3 Existing Borehole Data

Information from the Groundwater Africa report was gathered and tabulated (Table 18) including relevant data on the existing boreholes in the study area (Murray, 2004). The location of existing boreholes is shown in Figure 74.

Table 18: Existing data

Borehole	Siting Method	Depth (m)	Water Strikes (mbgl)	Cumulative Q (L/s)	T (m^2/d)	Available Drawdown (m)	Recommended Q: Year-long abstraction (L/s)
GWA1	Geological Mapping and Air Photos	96	41 66 84 96	0.6 0.7 5.0 5.6	14	25	1.3
GWA3	Magnetics	101	27 31 38	1.5 1.7 2.9	16	5	0.4

Figure 74. Previously sited and drilled boreholes in the area surrounding Makhoba Village

7.3.4 Delineated Study Area

Figures 75 – 78 show the delineated study area surrounding Makhoba village upon which the groundwater resource estimation was undertaken. The area was delineated using topographic and geological boundaries.

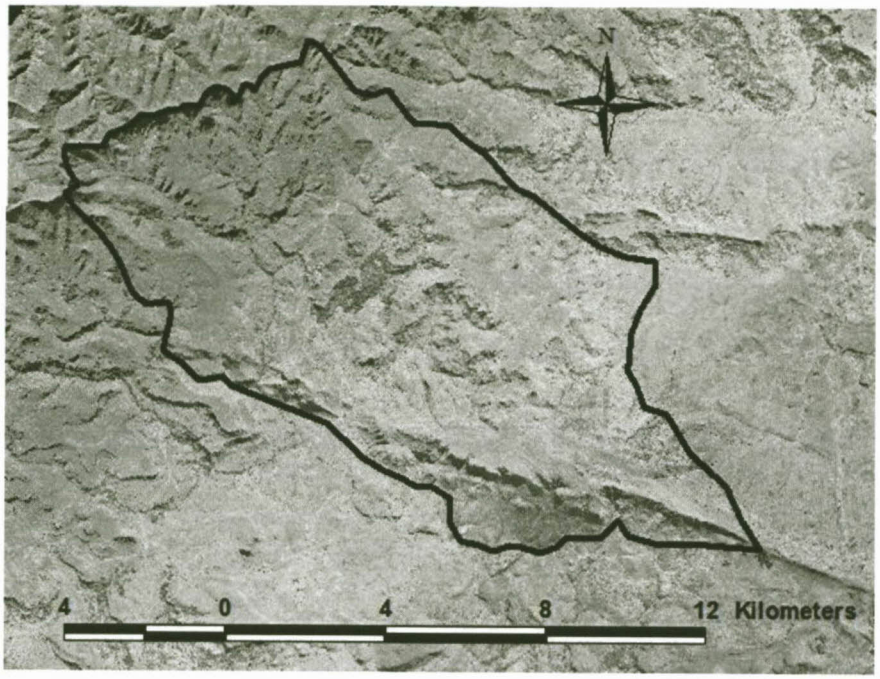

Figure 75. Satellite image of the delineated area around Makhoba Village.

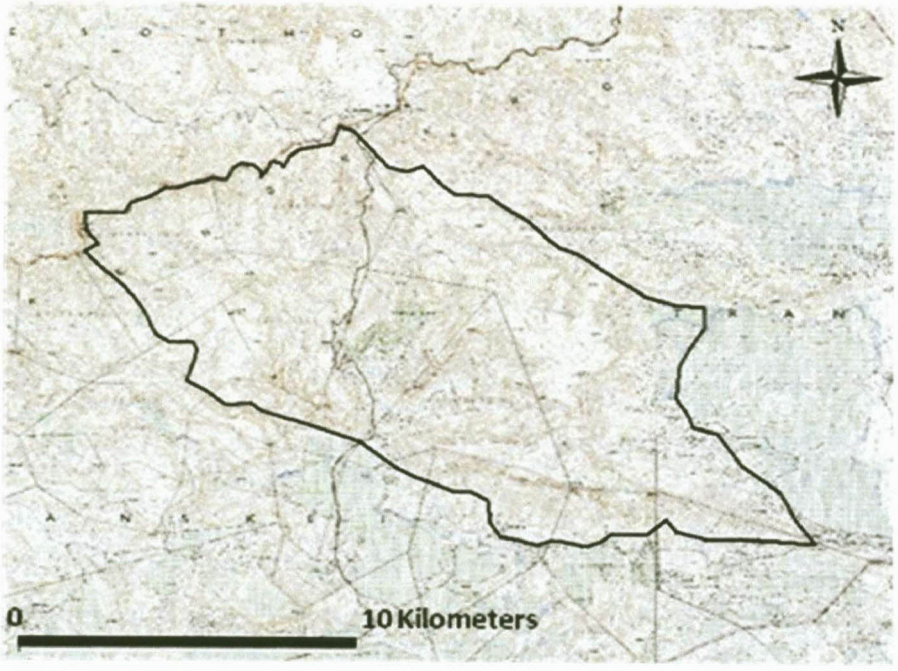

Figure 76. Topographic image of the delineated area around Makhoba Village

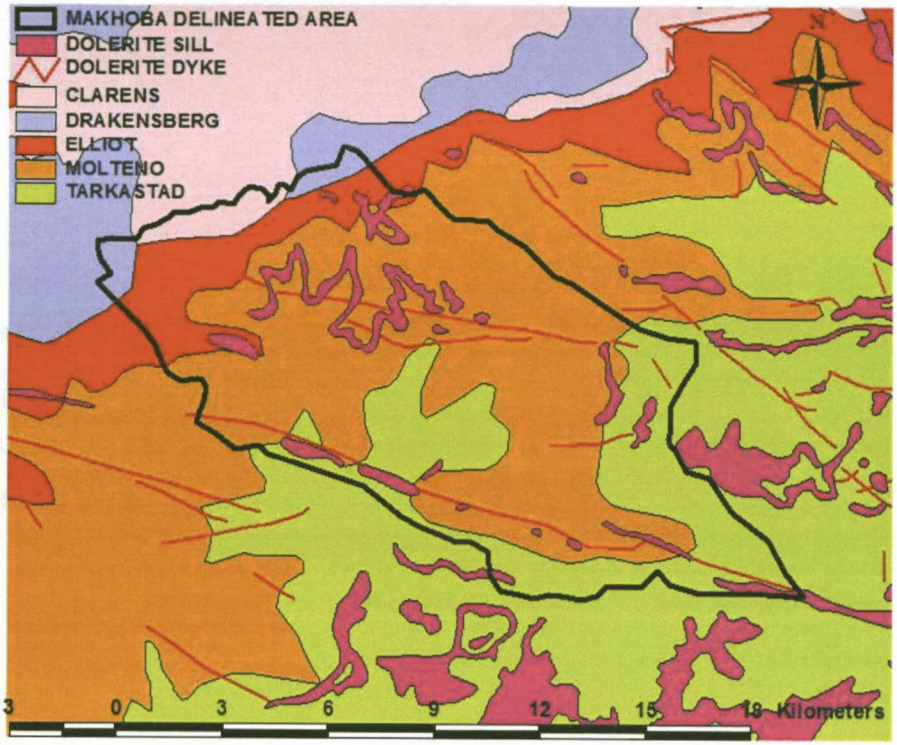

Figure 77. Geological image of the delineated area around Makhoba Village.

Figure 78. Google Earth image of the delineated around Makhoba Village. The calculated size is approximately 113 km^2.

7.3.5 Aquifer Yield Assessments

In determining AAYM yields, certain parameter values need to be specified which include a recharge threshold value and a recharge factor. The upper and lower limit of AAYM yields were obtained by using threshold values of 10 mm and 20 mm respectively. GRAII recharge factors are provided as default values for each quaternary catchment and these values appeared adequate for the area under investigation. Table 19 shows how the AAYM values compare to previous methods.

Table 19: Aquifer yields

Database/ Model	Measured parameter	T31C Q (L/s) Proportioned	T31E Q (L/s) Proportioned	Total Q Delineated Area (L/s)
HP		16.2	42.9	59.1
GRAII	AGEP normal	22.2	54.4	76.6
	AGEP Drought	17.2	41.5	58.7
AAYM (ver. 1.0.77)	Upper Limit	17.1	36.1	53.2
AAYM (ver. 1.0.77)	Lower Limit	11.3	21.4	32.7

AAYM values from the older version 1.0.77 are conservative when compared with other aquifer yield approaches. The Upper Limit of AAYM is similar to the AGEP Drought and the Harvest Potential, but the Lower Limit is appreciably lower.

7.3.6 Wellfield Yield Assessment

Potential borehole sites

Potential boreholes sites were identified using the following data sources: Transmissivity map; Geological map and Google Earth. Borehole siting was carried out in a step wise manner firstly taking the Transmissivity Map and Geological map into account, and then pinpointing sites using Google Earth. With the satellite imagery from Google Earth one can identify major dykes, easily extrapolate dykes marked on the geological and Transmissivity Maps, and accommodate the accessibility of these targets to drilling rigs and conveyance infrastructure. The potential borehole sites can be seen in Figures 79 - 81. Transmissivity values taken from the Transmissivity maps are listed in Table 20.

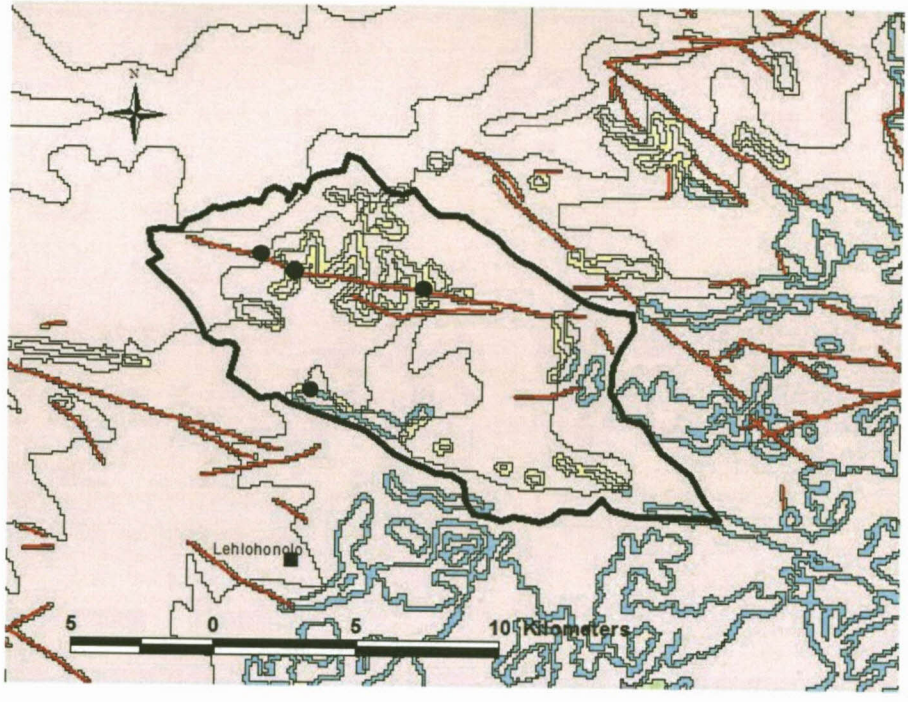

Figure 79. Newly sited boreholes on the Transmissivity Map.

Table 20: Transmissivity values obtained from the Transmissivity Map(Chapter 4)

Molteno	**Lower (using T-middle values) (m^2/d)**	**Upper (using T-upper values) (m^2/d)**
Matrix	1.5	11
Dyke	20.5	139

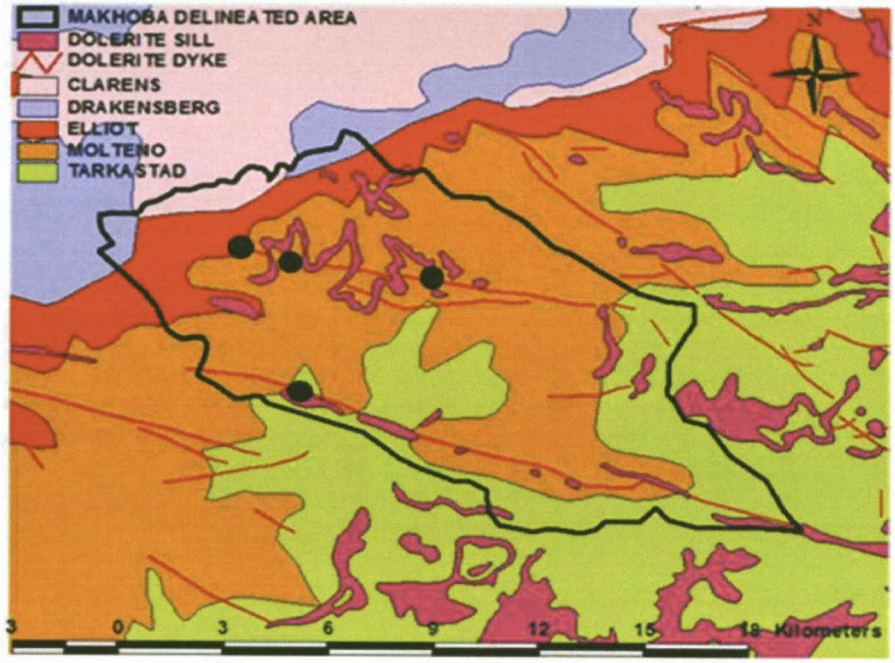

Figure 80. Newly sited boreholes on the 1:250 000 Geological map.

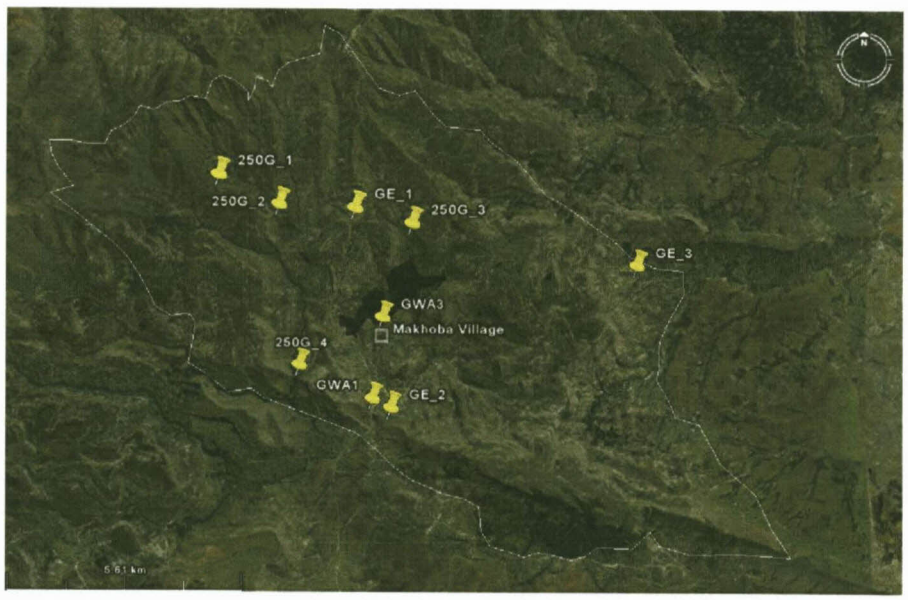

Figure 81. Existing and potential borehole sites on Google Earth imagery

7.3.7 Aquifer parameter values

The existing boreholes GWA1 and GWA3 are located on a large dyke situated in the Molteno Formation and a small dyke situated in the Tarkastad Formation respectively (Figure 74). Regardless of their different positions, the transmissivity values determined from pump tests yield similar

results. The difference in the amount of available drawdown however is significant. These values can be seen below in Table 21.

Table 21: Transmissivity and drawdown values from previous experience and the values to be used in theoretical calculations

Formation	# Bhs Drilled	# Bhs Newly Sited	Theoretical T Value* (m^2/d)	T from data** (m^2/d)	Theoretical Available s*** (m)	Available s from data** (m)
Molteno	1	4	20 – 30	14	10	25
Tarkastad	1	3	20 – 30	16	35	5

* Transmissivity Map (Chapter 4)
* *Murray, 2004
***Table 15 (Dondo *et al.*, 2010)

7.3.8 Wellfield yield assessment

Scenario 1

The availability of existing data obtained from previous pump test data enabled a scenario to be run using real parameter values. These parameters were then applied to the newly sited boreholes. The values used can be seen below in Table 22.

Table 22: Parameter values implemented in the wellfield model

Borehole	Transmissivity (m^2/d)	Available Drawdown (m)
GWA 1	14	25
GWA 3	16	5
Newly sited	15	Up to 25

Firstly, no abstraction from newly sited boreholes was simulated, only abstraction of 1.3 and 0.4 L/s from GWA 1 and GWA 3 respectively. This caused drawdown in GWA 1 of 13.8 m and in GWA 3 of 4.2 m, suggesting the possibility of further abstraction. Each newly sited borehole therefore was assigned an initial abstraction rate of 0.6 L/s, and this value was slowly increased in each borehole (up to 2.9 L/s) in order to determine the optimum rates for each. The final abstraction rates are below in Table 23 followed by Figure 82 of the scenario illustrating the drawdown of each borehole as a consequence of the abstraction rates applied.

Table 23: Optimum abstraction rates for each newly sited borehole in the study area

Borehole	Transmissivity (m^2/d)	Abstraction rate (L/s)	Drawdown (m)
GWA1	14	1.3	16.1
GWA3	16	0.4	4.6
250G_1	15	2.3	24.1
250G_2	15	2.3	24.1
250G_3	15	0.6	6
250G_4	15	0.6	7.5

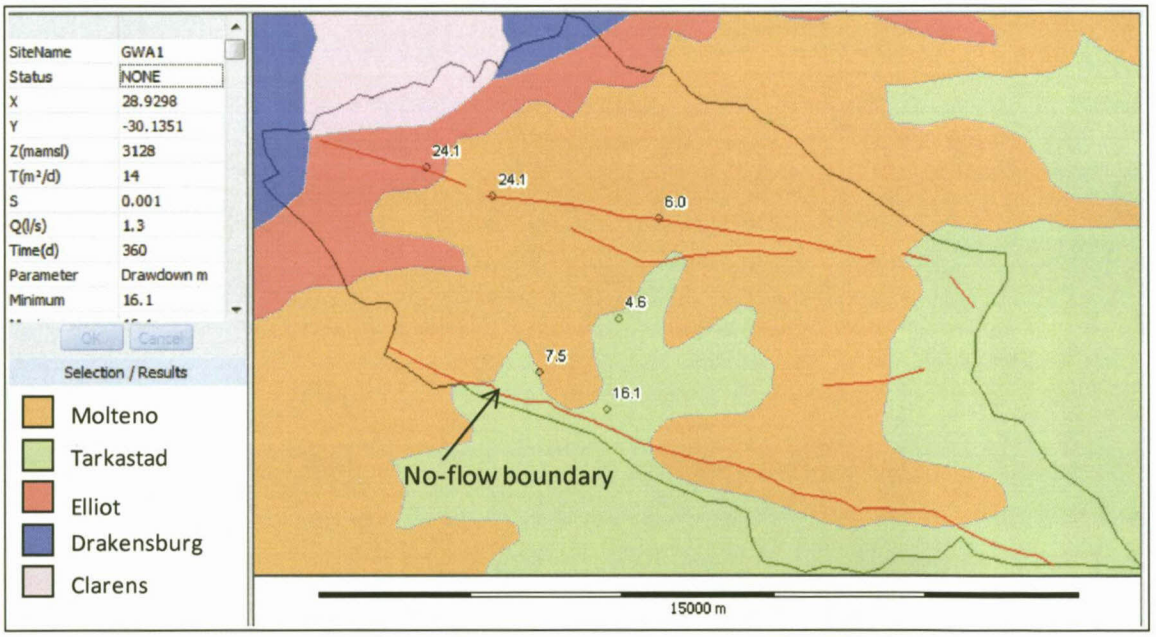

Figure 82. Image from the wellfield model with boreholes and their subsequent drawdown after abstraction.

- The total abstraction rate is 7.5 L/s
- The no-flow boundary causes a significant increase in drawdown in boreholes close to the boundary, including GWA1, GWA3 and 250G_4
- The abstraction rate of 250G_4 could not be increased as the drawdown of GWA 3 was already 4.6 m (max drawdown is 5 m)

- The abstraction rate of 250G_3 could not be increased as it had a further effect on the drawdown of GWA3.

Scenario 2

Assuming no data was available and the user has limited experience in the area, the tools developed were tested using theoretical values. Table 24 illustrates the theoretical parameter values that were assigned to the boreholes, using the recently developed Transmissivity map (Chapter 4) and the saturated thickness of the weathered/jointed zone in the Molteno Formation (Table 15, Dondo *et al.,* 2010) as the available drawdown. In this "Lower estimate" the average values were taken from the Transmissivity Map.

Table 24: Theoretical transmissivity and drawdown values based on Dondo et al., 2010

Borehole Position	**Transmissivity (m^2/d)**	**Available drawdown (m)**
Matrix (Molteno)	1.5	11.3
Dyke (on Molteno)	20.5	11.3

Each borehole was assigned an abstraction rate of 0.5 L/s, and this value was slowly increased in each borehole to determine the individual optimum pumping rates. The final abstraction rates are below in Table 25.

Table 25: Abstraction rates for each newly sited borehole in the study area

Borehole	**Transmissivity (m^2/d)**	**Abstraction rate (L/s)**	**Drawdown (m)**
GWA1	20.5	1	10.5
GWA3	1.5	0.1	9.7
250G_1	20.5	1.4	11.1
250G_2	20.5	1.4	11.2
250G_3	20.5	1.5	11
250G_4	1.5	0.1	10.4

- The total abstraction rate is 5.5 L/s

- The presence of a no-flow boundary significantly increases the drawdown in the boreholes close to the boundary, including GWA3 and 250G_4
- When the initial abstraction of 0.5 L/s was implemented, GWA3 and 250G_4 displayed drawdown around 45 m. Their abstraction was thus reduced to 0.1 L/s. The question arises as to whether or not they should be pumped.
- Due to the higher transmissivity on the dykes (20.5 m^2/d), the increased abstraction rate on GWA 1 has negligible effect on the drawdown of 250G_4.
- It appears that when boreholes are sited on the dykes, the limiting factor regarding the maximum abstraction rates is the available drawdown. In the matrix, however, it is the transmissivity.

Scenario 3

Table 26 shows the theoretical parameter values that were assigned to the boreholes, using the Transmissivity map and same available drawdown values as before. This scenario represents the higher scenario and used the "upper" values from the new Transmissivity Map.

Table 26: Theoretical transmissivity and drawdown values based on Dondo et al., 2001

Borehole Position	**Transmissivity (m^2/d)**	**Available drawdown (m)**
Matrix (Molteno)	11	11.3
Dyke (on Molteno)	139	11.3

Each borehole was assigned an abstraction rate of 0.5 L/s, and this value was slowly increased in each borehole in order to determine the optimum rates for each. The final abstraction rates are below in Table 27.

Table 27: Abstraction rates for each newly sited borehole in the study area

Borehole	Transmissivity (m^2/d)	Abstraction rate (L/s)	Drawdown (m)
GWA1	139	2.3	5.2
GWA3	11	0.7	10.9
250G_1	139	2	3.2
250G_2	139	1.5	2.8
250G_3	139	1.6	2.9
250G_4	11	0.6	11.3

- The total abstraction rate is 8.7 L/s
- The presence of a no-flow boundary significantly increases drawdown in borehole 250G_4. 250G_2 had an effect on 250G_4.
- 250G_4 limited the rates of abstraction in surrounding boreholes due to the presence of the no-flow boundary.

7.3.9 Borehole yield assessment

If the yields of all boreholes are assessed on an individual basis, that is, if it is assumed that there is no interference between boreholes as is predicted by the wellfield model, then the total yield from all boreholes range from 4.1 – 20.3 L/s assuming a T-value of 15 m2/day and a range of s-values from 5 to 25 m (Table 28).

Table 28: Total yield of individual boreholes

Parameter	Value
T value (m^2/d)	15
Available s range (m)	5 to 25
Minimum Q single Bh (L/s)	0.6
Maximum Q single Bh (L/s)	2.9
Minimum Total Q (L/s)	4.1
Maximum Total Q (L/s)	20.3
Mean Q (L/s)	12.2

7.3.10 Comparison of all Yields

Table 29 below shows all yields determined from the databases HP and GRAII, the model AAYM and the total borehole yield.

Table 29: Comparison of aquifer, wellfield and individual borehole yields

	Range definition	Lower Range (L/s)	Upper Range (L/s)	
Aquifer Yield				
HP		59.1		
AGEP	Lower = Drought, Higher = Normal	58.7	76.7	
AAYM (Ver. 1.0.77)	Lower = 20 mm Recharge Threshold, Higher =10 mm Recharge Threshold	32.7	53.2	
Wellfield Yield				
Theoretical	Lower = Middle values from T-map, Higher = Maximum values from T-map	5.5	8.7	
From data		7.5		
Individual Borehole Yield				
Total Borehole Yield		4.1	12.2	20.3

In conclusion the following points can be made:

1. The AAYM version 1.0.77 values, particularly the Lower range, are conservative when compared with other aquifer yield assessment methods. The HP, AGEP Drought and the Upper range AAYM all produce similar yields.

2. Wellfield model estimates are all conservative in comparison to the other aquifer yield methods. The values from actual data, however, fall within the range determined using the theoretical data. It therefore seems that there is potential to site more boreholes in the area to fully utilize the groundwater potential. If there is no data available, it appears the theoretical values are adequate.

3. Borehole yields fall within the aquifer yields and suggest that the area is currently under-pumped. The existing boreholes give a combined yield of 1.7 L/s. It is feasible that if the newly identified borehole sites were drilled, that an additional 10.5 L/s could be obtained, and potentially as much as 18.6 L/s (if the upper borehole yield values are used as opposed to the mean).

7.4 Matatiele

7.4.1 Introduction

In 2009, Maluti GSM assigned Groundwater Africa the task of determining the potential for groundwater development in the greater Matatiele area. A total rate of 50 L/s was required from this scheme. This project is still, at present, proceeding with geophysics, borehole siting and borehole drilling. Tools developed in the WRC project K1763, and in this thesis can now be implemented and their validity determined almost immediately. Values provided by the reports from projects carried out in earlier years will be compared with default values from the tools, and both will be implemented in the models for further comparison of results.

7.4.2 Geology

The study area is underlain by the Beaufort and Drakensberg Group of the Karoo Supergroup. The Beaufort Group occurs in the lower areas and consists of mudstone and fine grained sandstone. The Molteno Formation of the Drakensberg Group outcrops in the upper areas and is predominantly made up of coarse grained sandstones with occasional thin shale beds. It is within this formation that boreholes were primarily sited as the coarse grained nature of the sandstone could potentially yield large quantities of groundwater (Murray, 2004/2005).

7.4.3 Existing Borehole Data

Information was gathered and tabulated for Matatiele (Table 30) as well as additional borehole data from the nearby village, Outspan/Hebron (Figure 73; Table 31). Both tables include relevant data on the existing boreholes in the study area (Murray, 2004, 2005). The location of existing boreholes is shown in Figure 83.

Table 30. Data from existing boreholes in the Matatiele area.

Borehole	Siting Method	Lithology	Depth (m)	T (m^2/d)	Available Drawdown (m)	Daily yield (m^3)
Bh MT1	Geological maps, satellite imagery	Molteno	65.8	$T_E = 50.8$ $T_L = 8.1$	25	288
Bh ML1	Geological maps, satellite imagery	Molteno	91.5	$T_E = 224$ $T_L = 36.7$ (poor recovery!)	2	216
Bh ML2	Geological maps, satellite imagery	Molteno	9.5	$T_E = 101$ $T_L = 10.6$	24	432
Bh MLB1	Geological maps, satellite imagery	Molteno	164.2	$T_E = 73$ $T_L = 9.5$	16	432

Table 31: Data from existing boreholes in Outspan/Hebron.

Borehole	Siting Method	Depth (m)	Water Strike (mbgl)	T (m^2/d)	Available s (m)	Recommended Q (L/s)	Maximum Q (L/s)
3B	Geological Maps, Air Photos, Magnetics	94	56 62 64 73 78 82 87 92	22	6	0.6	6
5A	Magnetics	71	43 54 58 60 62 65	27	7	1.75	3.5
6	Magnetics	101	58 66	4.7	26	0.7	2
7C	Geological maps, magnetic	110	37 47 59 77 105	130	1.5	1.2	3
8	Geological maps, magnetic	120	86 92 97	160	3	2	5
10	Geological maps, magnetic	100	29 34 47 50 67	180	5	3.5	10
Total						9.75	29.5

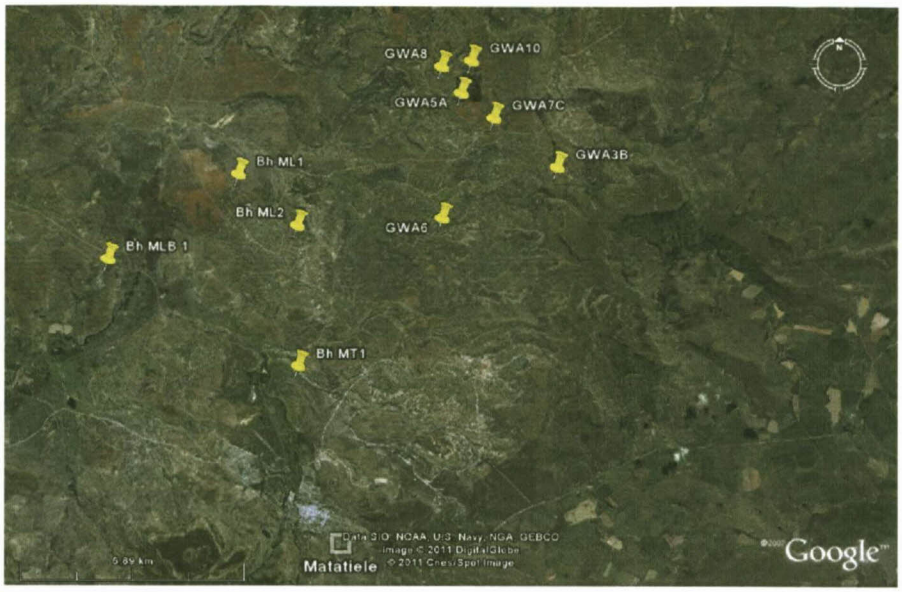

Figure 83. Image of existing boreholes in the greater Matatiele area.

7.4.4 Delineated Study Area

Figure 84 shows the delineated study area surrounding Matatiele upon which the groundwater resource estimation was undertaken. Due to the sheer size of the study area, four wellfields have been delineated (Figure 85). Both the outer area and the wellfields were delineated using topographic and geological boundaries. A perennial river runs through the area and is underlain by significant alluvial deposits. Due to the size of this river and its different hydraulic properties, the river's potential yield will be calculated separately and thus was buffered and delineated independently (Figure 86). Over the years, the river has changed its path which has resulted in the development of a significant alluvial basin. Three major dykes cut through the study area, dykes 1 and 2 more north of the area and dyke 3 through the central part of the alluvial basin (Figure 87). It is on or near to these dykes that boreholes have been sited. The optimum sites will be determined as experience is gained from drilling in these areas.

Figure 84. The outer delineated study area surrounding Matatiele.

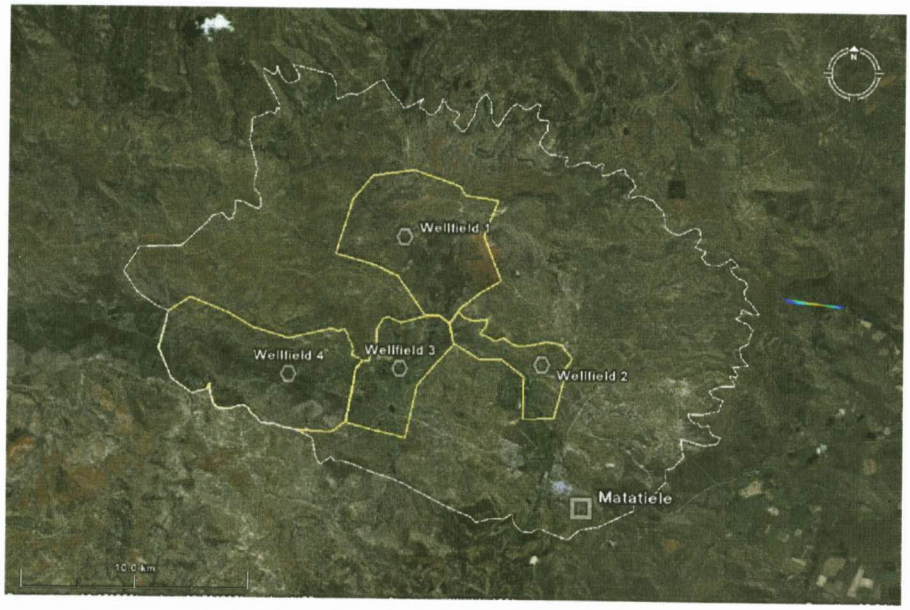

Figure 85. The four wellfields within the study area.

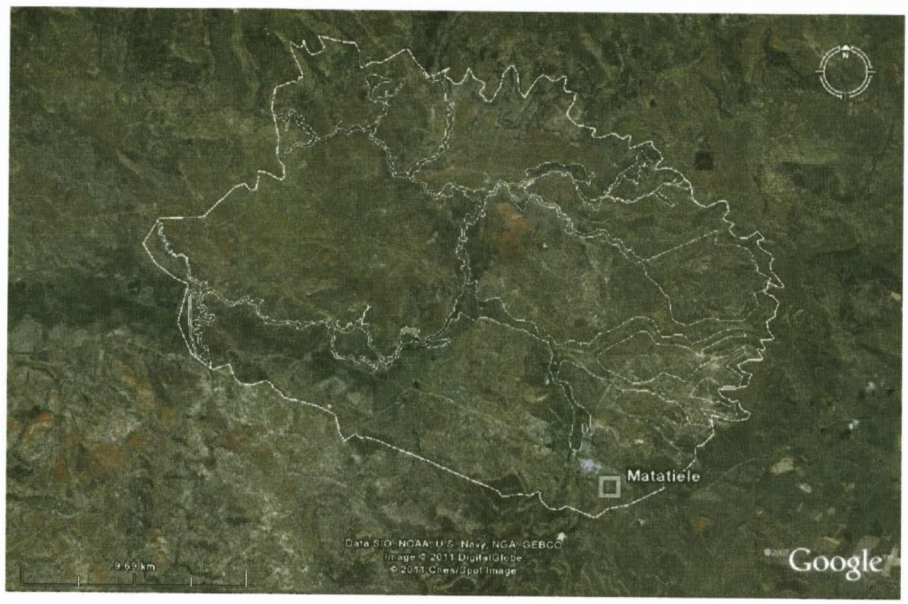

Figure 86. The perennial river that has been delineated separately from the study area.

Figure 87. The three major dykes running through the area, dykes 1 and 2 lying north and dyke 3 cutting through the more central part of the alluvial basin.

Table 32 below provides the approximate sizes for each delineated area as well as existing boreholes within these areas. These values will be used when proportioning the assured yields obtained from the AAYM. Other boreholes that are not listed in the table fall just outside of the delineated area, but were included in this study in order to have a larger set of data upon which initial parameter estimations can be made.

Table 32: The size of all Wellfields and separated areas within the study area.

Wellfield	Size (km^2)	Existing Boreholes
Wellfield 1	30.3	
Wellfiled 2	9.5	Bh MT1
Wellfield 3	14.8	
Wellfield 4	32.8	
Buffered River	45	GWA 6
Matatiele Basin	346.6	Bh MLB1, Bh ML1, Bh ML2,

7.4.5 Aquifer Yield Assessments

In determining AAYM yields, certain parameter values need to be specified which include a recharge threshold value and a recharge factor. The upper and lower limit of AAYM yields were obtained by using recharge threshold values of **0 mm** and **10 mm** respectively. GRAII recharge factors are provided as default values for each quaternary catchment and these values appeared adequate for the area under investigation. The differing hydraulic properties of the buffered river suggested a separate calculation of a potential aquifer yield. Parameters MAWD and aquifer recharge were increased and applied in different orders to determine the best suited conditions applicable for this area (Table 33). The values obtained for the Lower and Upper Yield of the Matatiele Basin (excluding the buffered river) are 112.7 and 177.4 L/s respectively. Table 34 show how the AAYM values compare to previous methods.

Table 33: The list of values tested for MAWD and recharge to obtain the most suitable combination to represent the buffered river.

MAWD (m)	Recharge (% MAP)	River Buffer Yield (L/s)	Total Basin Yield Lower (L/s)	Total Basin Yield Upper (L/s)
5	13	91.1	203.8	268.5
10	**6.5**	**51.9**	**164.6**	**229.3**
10	13	106.1	218.8	283.5
15	13	110.2	222.9	287.6
20	6.5	49.9	162.6	227.3
20	13	110.2	222.9	287.6

A MAWD of 10 m and a recharge value of 6.5 % MAP were used to represent the buffered river. The separate yields of the buffered river and remaining Matatiele basin were then added together to form the total delineated area.

Table 34: Aquifer yields

Database/Model	Measured Parameter	Total Q delineated area (L/s), T33A
HP		153.4
GRAII	AGEP Normal	204.6
	AGEP Drought	153.9
AAYM (Ver. 1.0.77)	Upper Limit = 0 mm recharge threshold	229.3
	Lower Limit = 10 mm recharge threshold	164.6

7.4.6 Wellfield Yield Assessment

Potential Borehole Sites

Wellfield 3 through which dyke 3 runs roughly NW-SE, and which is likely to be developed in the near future, was investigated in this study. Potential boreholes sites were identified using the following data sources: aeromagnetic survey results, magnetic traverse results, Transmissivity map; Geological map and Google Earth.

Aeromagnetic data

Magnetic traverses were determined from the aeromagnetic results, seen below in Figure 88. The aeromagnetic data was obtained during the Regional Bulk Implementation Study (source: Alfred Nzo District Municpaliy).

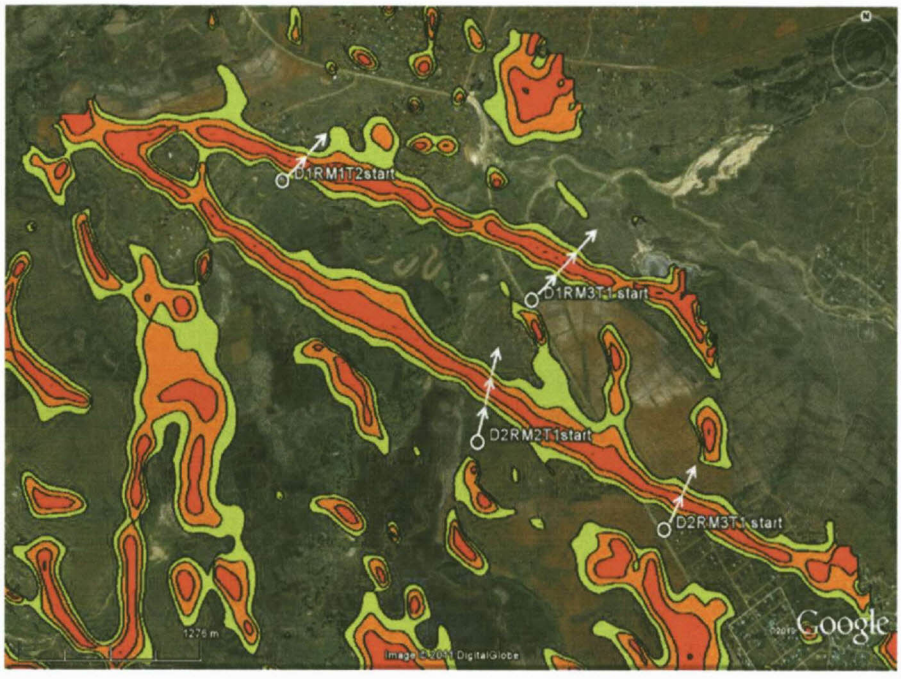

Figure 88. Aeromagnetic and satellite imagery used to identify dolerite dykes in Matatiele

The image above displays how aeromagnetic data overlying satellite imagery can aid in the identification of geological structures in the study area. The dolerite dykes can clearly be seen, running roughly NW-SE. From this data, the direction of magnetic traverses were defined.

Magnetic traverse data

The magnetic traverses and modelled data can be seen below in Figures 89 - 92. The data was modelled by Mr M. de Klerk (Cape Geophysics) to determine the centre and trend of the dykes over which the traverses were walked. Boreholes were sited primarily on the centre of the dyke. The traverse graphs below were obtained from walking the traverses laid out above.

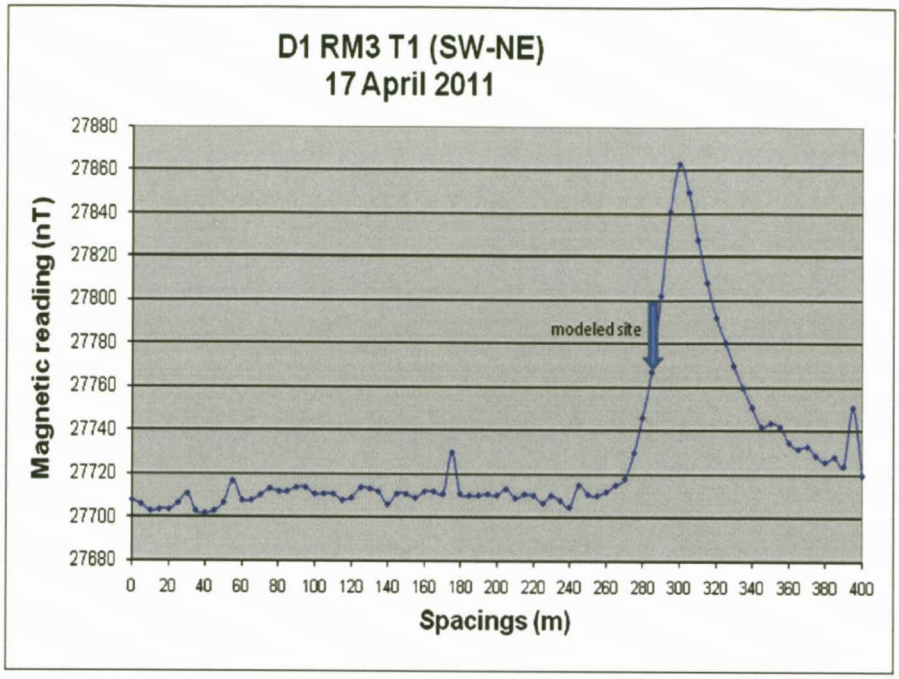

Figure 89. Magnetic profile, showing the position of RM3 on dyke 1.

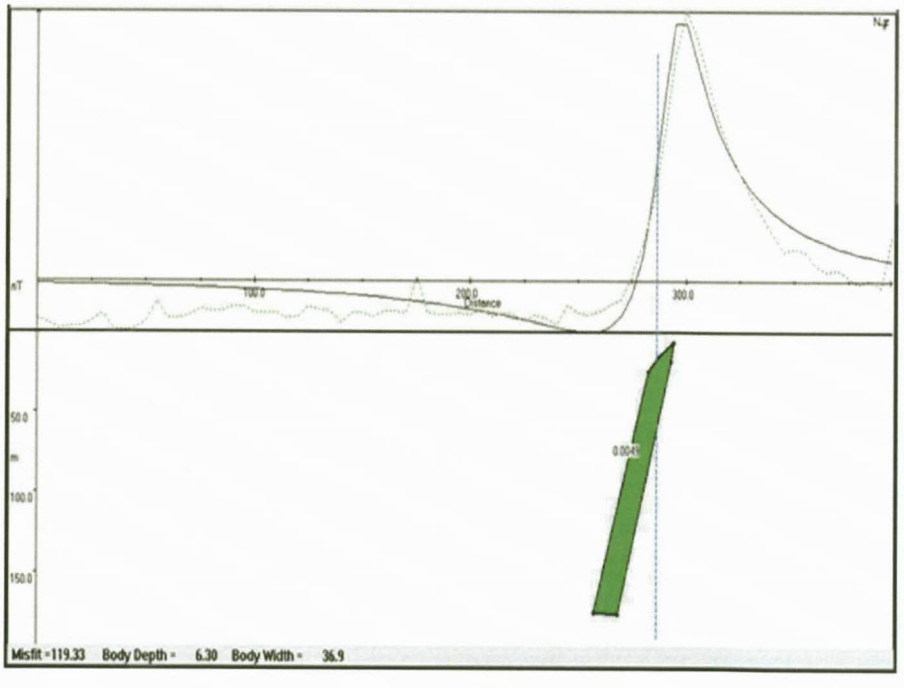

Figure 90. The modeled traverse of D1RM3 showing the centre of the dyke.

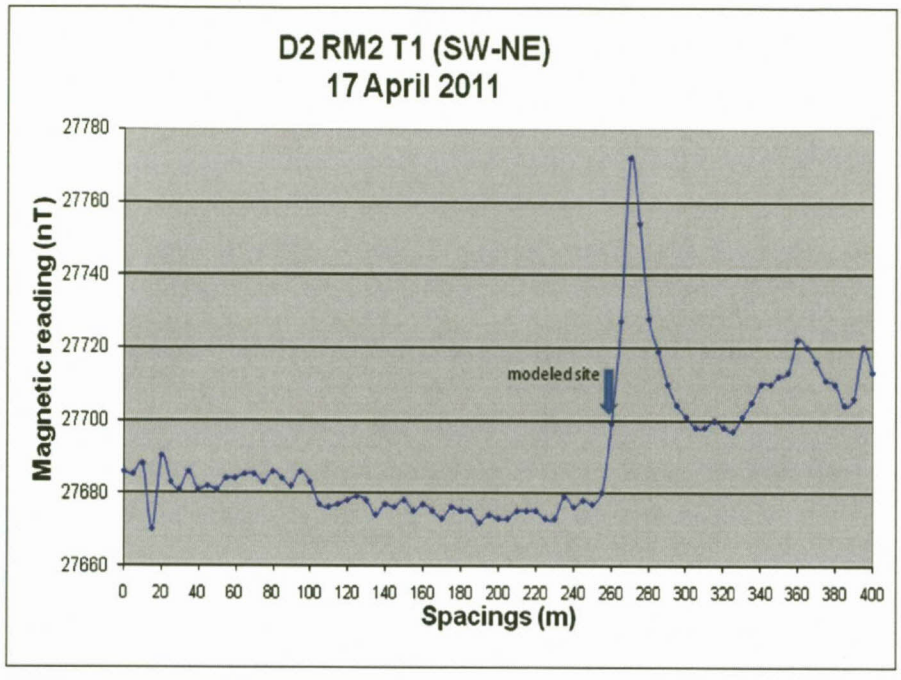

Figure 91. Magnetic profile showing the position of RM2 on dyke 2.

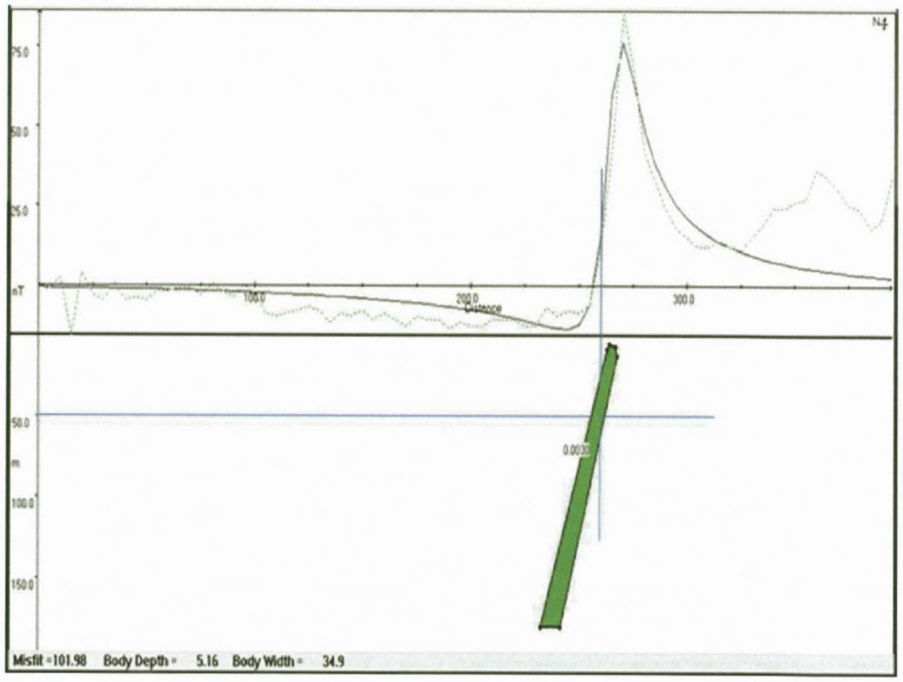

Figure 92. The modeled traverse of D2RM2 showing the centre of the dyke.

From the models presented above, it appears the centre of the dyke is approximately 10 m to the left of the peak of the magnetic traverse. The model has also illustrated that both dykes are dipping

slightly towards the north east. From this information, additional boreholes were sited on the centre of the dykes and Figures 93 and 94 below shows the position of these sites.

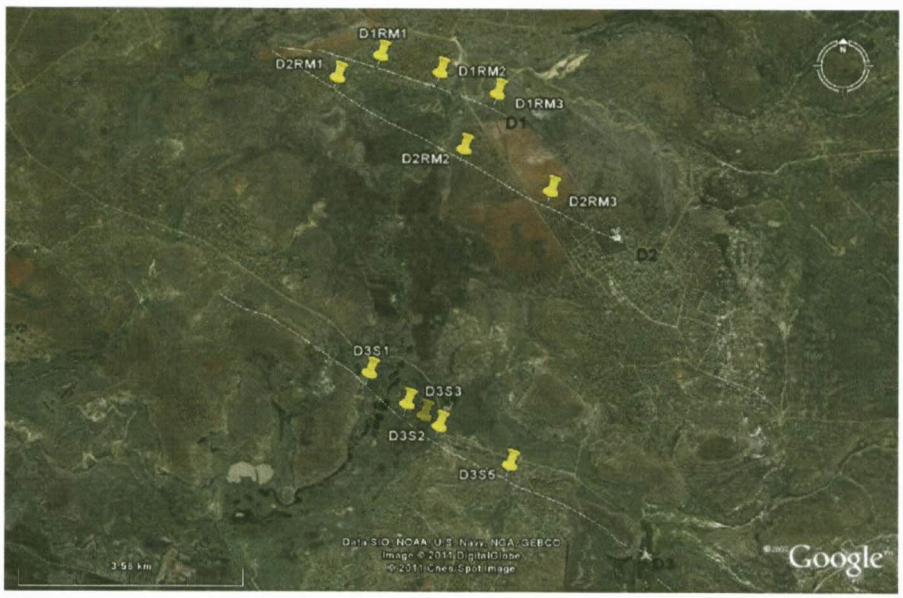

Figure 93. Potential borehole sites in the greater Matatiele area and their position in relation to the three major dykes.

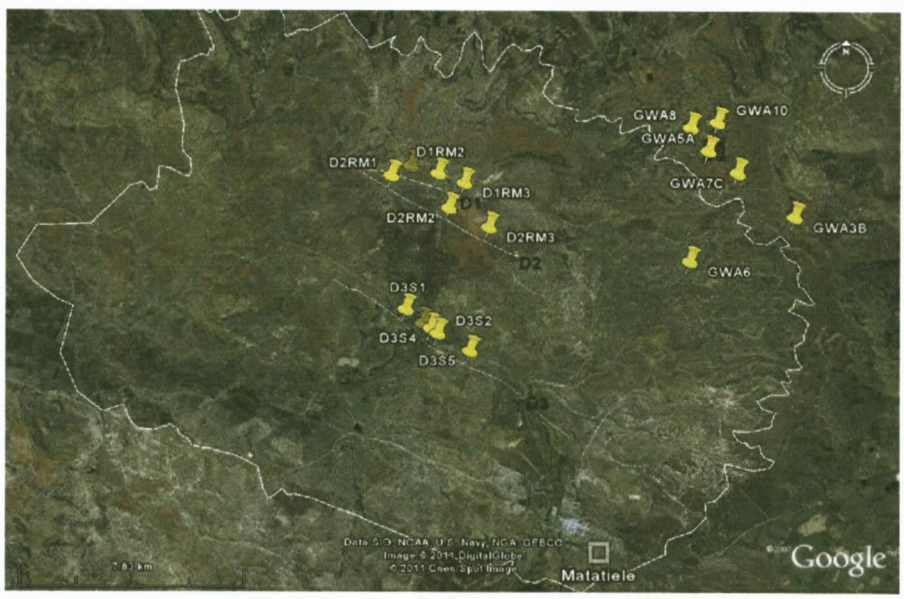

Figure 94. Potential borehole sites and existing boreholes in the greater Matatiele area.

A total of 15 boreholes have been drilled to date as part of this project, 5 of which were specifically drilled as monitoring boreholes (GWA6, GWA7, GWA13, GWA14 and GWA15). Boreholes GWA1, GWA8 and GWA10 were not high yielding and are therefore not considered as potential production

boreholes. The position of borehole GWA8 was shifted 10 m to the south west, where GWA9 was drilled.

7.4.7 Drilling results: Borehole logs

The newly drilled boreholes are listed below with their positions and a brief overview of the borehole logs. Boreholes GWA13, GWA14 and GWA15 were very shallow, monitoring holes drilled into alluvium and thus were not logged (Tables 35 - 46).

Table 35: Borehole log – GWA1

Borehole GWA1	**-30.29073: 28.74551**
Depth (m)	Description
1 – 13	Soil, overburden
14 – 35	Dolerite and sandstone gravel, 4 cm pebbles.
36 – 57	Sand, minor dolerite gravel, 6 cm pebbles.
58 – 79	Fresh, fine grained dolerite.
80 – 101	Shale, fresh and brittle.

Table 36: Borehole log – GWA2

Borehole GWA2	**-30.28505: 28.75777**
Depth (m)	Description
1 – 37	Clay and sand
38 – 48	Sand with dolerite gravel, 1 cm chippings.
49 – 80	Weathered shale becoming fresh at 54 m.
81 – 93	Fine grained sandstone. Chip size 0.5 – 1 cm.
94 – 120	Fresh and slightly weathered dolerite, quartz

Table 37: Borehole log – GWA3

Borehole GWA3	**-30.29051: 28.76943**
Depth (m)	Description
1 – 24	Sand and mud
25 – 30	Subangular dolerite pebbles, 0.5 – 2 cm.
31 – 40	Olive green shale
41 – 52	Mud with sandstone pebbles, 1 cm chips.
53 – 58	Dark and light grey fresh shale.
59 – 61	Fine to medium grained sandstone, 0.5 cm.
62 – 84	Blue and green shale, sandstone from 76 – 82 m.
85 – 98	Very fine grained sandstone with shale lenses,
99 – 120	Dark grey shale with thick sandstone lenses, 0.5

Table 38: Borehole log – GWA4

Borehole GWA4	**-30.28348: 28.75522**
Depth (m)	Description
1 – 15	Mud, clay and sand
16 – 20	Sand with few pebbles of sandstone and
21 – 30	Large dolerite pebbles, minor smaller fragments
31 – 60	Same as above, smaller pebbles.

Table 39: Borehole log – GWA5

Borehole GWA5	**-30.28174: 28.7526**
Depth (m)	Description
1 – 16	Mud and clay
17 – 62	Weathered dolerite, chips size ranges from 0.5 –
63 – 90	Fresh and weathered shale, with a few metres of

Table 40: Borehole log – GWA6

Borehole GWA6	**-30.28335: 28.75539**
Depth (m)	Description
1 – 16	Mud and sand.
17 – 26	Dolerite, 0.5 – 2 cm, with smaller chippings of

Table 41: Borehole log – GWA7

Borehole GWA7	**-30.28299: 28.75581**
Depth (m)	Description
1 – 15	Sand, mud and clay.
16 – 24	Sand and sandstone pebbles (2 cm) from 21 m.

Table 42: Borehole log – GWA8

Borehole GWA8	**-30.27747: 28.74635**
Depth (m)	Description
1 – 3	Sand and mud.
4 – 11	Weathered dolerite and sandstone, chip: 1-3cm.
12 – 16	Sand and mud, minor dolerite chips.
17 – 27	Mud and small dolerite chips <0.5 cm.
29 – 30	White, powdery sand.
31 – 41	Mud and small dolerite chips, <0.5 cm.
42 – 44	Weathered dolerite and white sand.
45 – 76	Fresh and weathered shale, chips <0.5 – 1.5 cm.

Table 43: Borehole log – GWA9

Borehole GWA9	**10 m SW of GWA 8**
Depth (m)	Description
1 – 3	Sand and mud.
4 – 19	Weathered dolerite. Chips size reaches 2.5 cm.
20 – 27	Same as above, but in mud. Chips reach 4 cm.
28 – 44	Weathered dolerite. Chips size 0.5 – 2 cm.
45 – 59	Fresher, light grey dolerite. Chip size 1 – 1.5 cm.
60 – 74	Orange weathered dolerite. Chip size 0.5 – 2 cm.
75 – 80	Small fresh dolerite chips.
81 – 83	Large orange dolerite chips, reaching 4 cm.
84 – 110	Fresh dolerite, <0.5 cm chips. Larger chips from

Table 44: Borehole log – GWA10

Borehole GWA10	**-30.27345: 28.74921**
Depth (m)	Description
1 – 14	Mud and sand
15 – 18	Mud with weathered dolerite and sandstone.
19 – 24	Blue shale.
25 – 37	Dark grey, hard shale.
38 – 41	Shale with medium grained sandstone, in sand.
42 – 44	Dark grey, hard shale
45 – 50	Medium grained sandstone, in sand

Table 45: Borehole log – GWA11

Borehole GWA11	**-30.2459: 28.76183**
Depth (m)	Description
1 – 4	Mud
5 – 14	Sand and mud with weathered dolerite and
15 – 59	Weathered dolerite.
60 – 69	Coarse grained sandstone and sand.

Table 46: Borehole log – GWA12

Borehole GWA12	**-30.23804: 28.76725**
Depth (m)	Description
1 – 6	Mud
7 – 12	Sand with quartzite chips
13 – 23	Fine powder with chips of hard, weathered shale
24 – 38	Weathered sandstone, minor shale
39 – 47	Weathered dolerite
48 – 53	Fresh and weathered shale
54 – 63	Weathered dolerite
64 – 70	Coarse grained sand
71 – 87	Weathered orange and grey shale
88 – 93	Sandstone and medium grained sand
94 – 122	Fresh and weathered dolerite.

7.4.8 Pump Test Results

Welltek Services, from East London, were contracted to conduct the pump tests. Below are the results of the step test (Figure 95) and Constant Rate Test (Figure 96) carried out on GWA4. The step test was carried out for a period of 60 minutes, followed by 80 minutes of recovery measurements. The constant rate test was conducted 15 L/s for 40 hours.

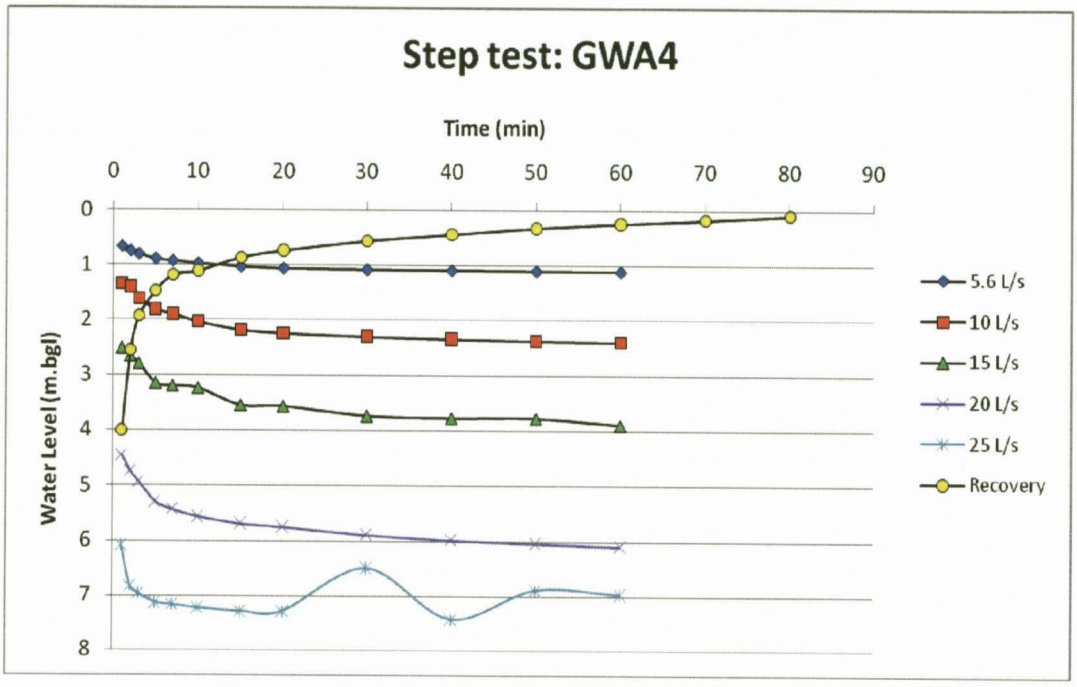

Figure 95. Step test results – GWA4.

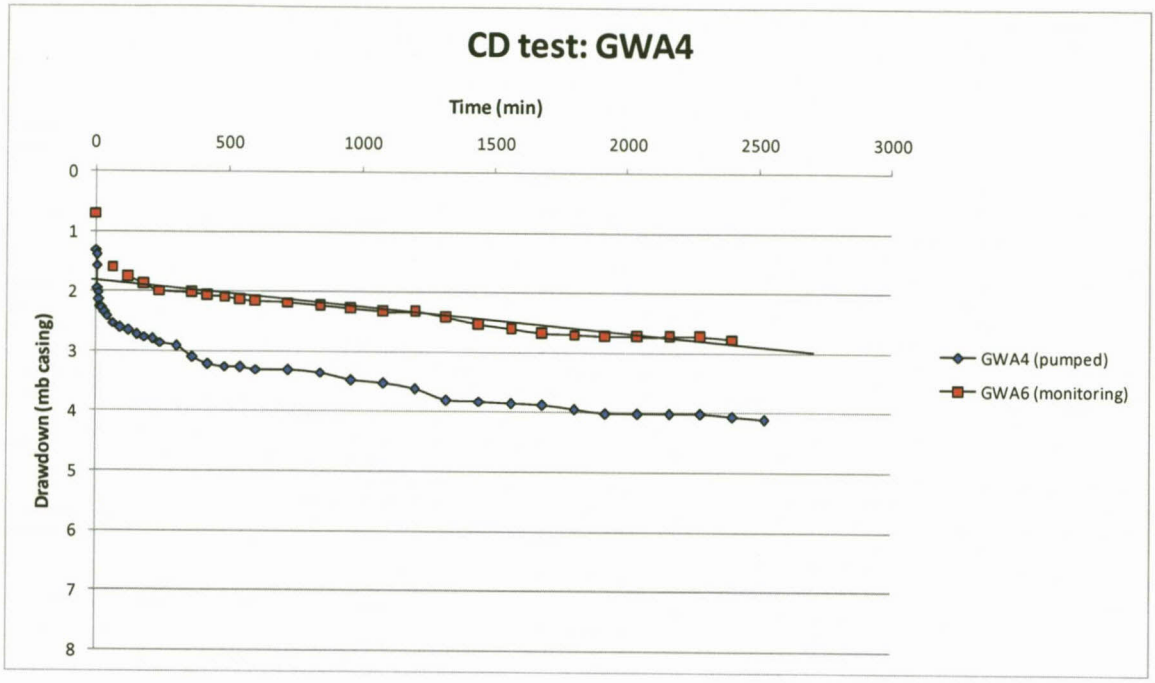

Figure 96. Constant rate test results – GWA4

A best fit line can be place along the slope of the monitoring borehole, GWA6. From this slope, a transmissivity value of 440 m^2/d was determined.

7.4.9 Aquifer Parameter Values

The transmissivity values of boreholes located in the Molteno Formation from Outspan/Hebron are clustered in two groups, a lower group ranging from 22 – 27 m^2/day and a higher group ranging from 130 – 180 m^2/day (Table 31). The Matatiele boreholes also have a wide range of transmissivity values, a lower around 60 m^2/d and a higher reaching 224 m^2/d (Table 30), and the transmissivity value obtained from the constant rate test carried out on the newly drilled borehole, GWA4, is approximately 440 m^2/d. Furthermore, theoretical transmissivity values can be obtained from the Transmissivity map seen below in Figure 97 (for further detail see Chapter 4). Between the two areas, there is a large range of available drawdown, from 1.5 to 25 m.

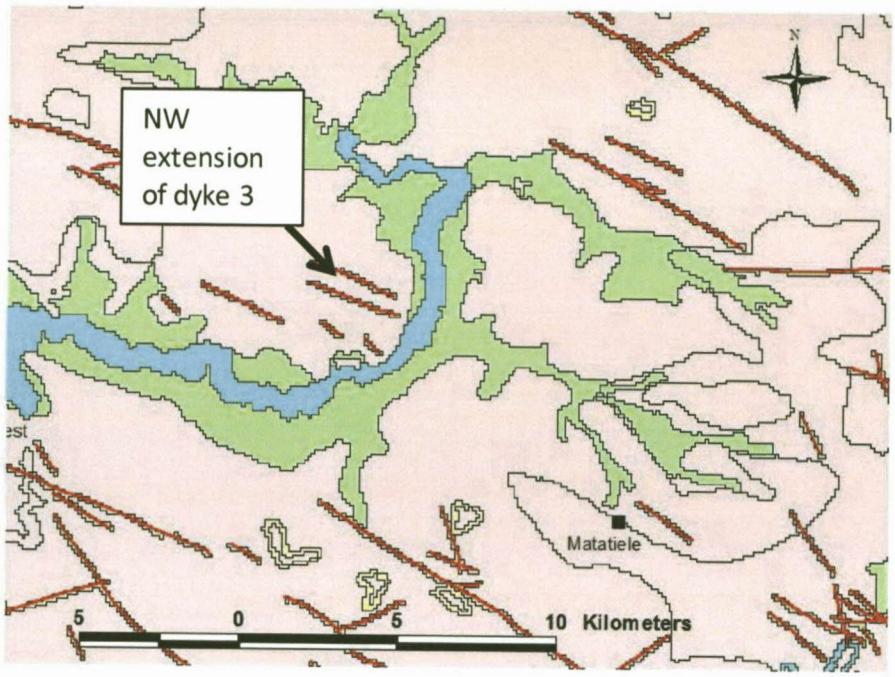

Figure 97. Transmissivity Map of the area surrounding Matatiele.

The image above illustrates the different transmissivity values in the area surrounding Matatiele. The basin through which dyke 3 runs is visible in blue and green and the north-west extension of the dyke can be seen in red. The ranges of possible transmissivity values are presented below in Table 47.

Table 47: Theoretical transmissivity values

T-Lower (Molteno) (m^2/d)		T-Middle (Molteno) (m^2/d)		T-upper (Molteno) (m^2/d)	
Alluvium	**Dyke**	**Alluvium**	**Dyke**	**Alluvium**	**Dyke**
11	1.8	33	19	255	128

The available drawdown values were taken from a depth just above the first water strikes of the two highest yielding boreholes, GWA4 and GWA5. These boreholes are potential abstraction boreholes for the area (Table 48).

Table 48: Water strike depths of new boreholes

Borehole	Depth of first water strike (m)
GWA4	20
GWA5	20

In order to accommodate for the thick alluvium upon which these boreholes are positioned, the available drawdown will be increased. Since the theoretical available drawdown of the Molteno formation is ~10 m (Table 15), this value was doubled to allow a drawdown of 20 m. This value seemed suitable as GWA4 and GWA5 both reached their first water strikes by 20 m (Table 48).

From Figure 97 above, dyke 3 appears to run through the alluvial basin in the south, thus the transmissivity values obtained for a dyke must be added to the transmissivity values of the alluvium (from the Transmissivity Map) to determine the estimated, theoretical transmissivity value of this zone as a number of boreholes have been drilled in this area. From the Transmissivity map, this zone has a transmissivity value of 383 m^2/d. This value compares well with the transmissivity value obtained from the constant rate test, which is approximately 440 m^2/d. In addition, if the theoretical available drawdown value is increased, it is very similar to the value provided by the most recent drilling (depth of first water strike) (Table 49).

Table 49: Transmissivity and drawdown values from previous experience and the values to be used in theoretical calculations

Formation	# Bhs Drilled	# Bhs Newly Sited	Theoretical T value* (m^2/d)	T from data (m^2/d)	Theoretical Available s*** (m)	Available s from data** (m)
Dyke and alluvium	5 (O/H)+ 4 (Mata)	11 (Matat)	383	440	10	20

* Transmissivity Map (Chapter 4)
** Murray, 2004/2005
***Table 15 (Dondo *et al.*, 2001)

7.4.10 Wellfield Yield Assessment

The wellfield model was run for Wellfield 3, which is intersected by dyke 3 along which 3 potential production boreholes were sited and drilled, and near to which a further 5 monitoring boreholes were drilled. These boreholes were drilled as part of the water supply project currently being undertaken in Matatiele. The Wellfield model will be implemented to assist in assigning pump rates to the abstraction boreholes by monitoring the drawdown in the surrounding boreholes. As Table 49 above illustrates, the theoretical transmissivity values are very similar to the transmissivity value

obtained for GWA4, thus the latter will be used in the model. Boreholes MT1 (-30.3036:28.8025) and MLB1 (-30.2740:28.7413) are positioned on the same dyke and their recommended abstraction rates (Table 30) will be implemented. Furthermore the transmissivity values obtained from these two boreholes will be applied to GWA9 as no pump test data is available for this borehole to date.

Results

The transmissivity values and abstraction rates can be seen below in Table 50. Transmissivity values were not necessary for monitoring boreholes as the drawdown in these boreholes is calculated using the transmissivity values of the adjacent, abstraction boreholes. A storativity value of 0.002 was used for all boreholes. The positions of the boreholes can be observed below in Figure 98. An approximate position of the dyke can be seen along which all abstraction boreholes were sited.

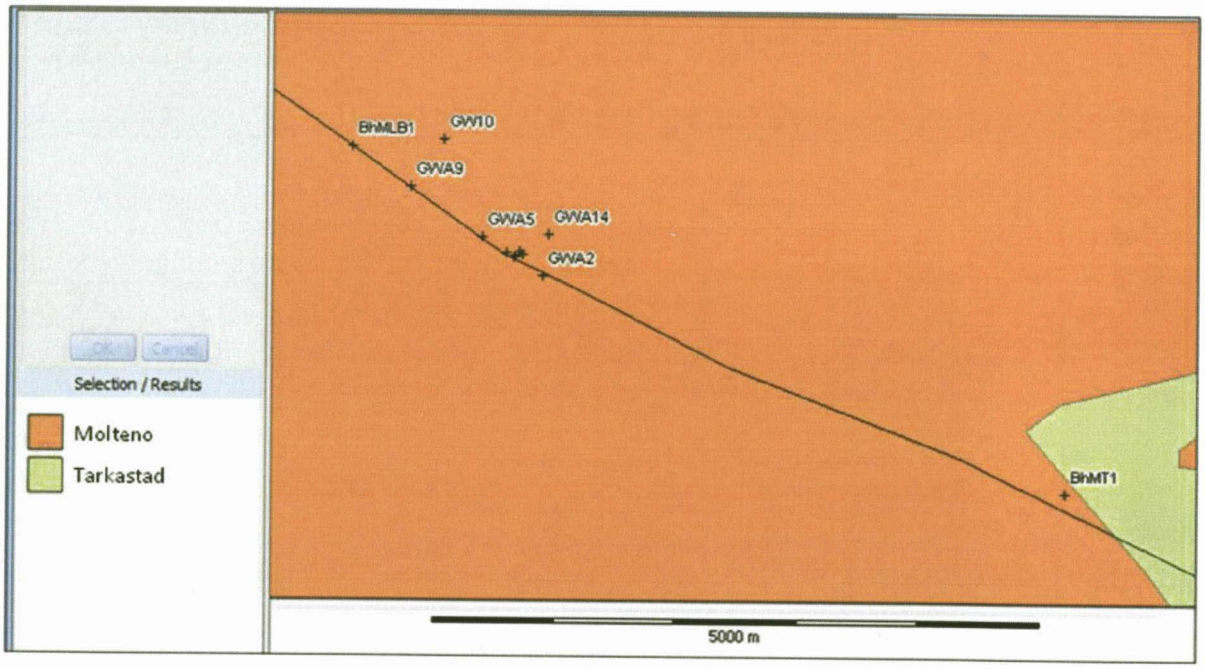

Figure 98. The positions of boreholes in the Matatiele basin.

Table 50: Parameter values assigned to the existing and newly sited boreholes in wellfield 3.

Borehole	T (m^2/d)	Abstraction (L/s)
BhMT1	50.8	6
BhMLB1	73	3.5
GWA2	50	Monitoring
GWA4	440	23
GWA5	200	18
GWA6	-	Monitoring
GWA7	-	Monitoring
GWA8	-	Monitoring
GWA9	100	5
GWA10	-	Monitoring
GWA13	-	Monitoring
GWA14	-	Monitoring
GWA15	-	Monitoring

Although the boreholes in Matatiele are a significant distance apart (minimum ~200 m), the high transmissivity values result in significant drawdown interference between the boreholes when the abstraction boreholes are pumped. The abstraction rate of GWA9 could not be increased due to the interference caused by abstraction from boreholes BhMLB1, GWA5 and GWA4.

A total abstraction rate of 55.5 L/s can be obtained from the scenario outlined above, which meets the future water requirements of Matatiele (this value is used in the upper estimation of the wellfield yield, Table 52 below). This abstraction, however, causes a notable drawdown in nearby monitoring boreholes, including GWA6, GWA7, GWA14 and GWA15. The alluvial nature of the aquifer in which these abstraction boreholes were sited results in possible environmental limitations. The dyke 3 is cutting through the basin which yields significantly high transmissivity values. The area, however, has a number of wetlands which will restrict the amount of allowable water level drawdown. Thus a number of monitoring boreholes were drilled in order to monitor the water level drawdown when water is abstracted. If the abstraction rates listed above were to be implemented, this would cause significant drawdown throughout the basin, with a water level drawdown of 10.5 m in GWA15, which was sited in between the two abstraction boreholes and a wetland. In an attempt to protect this area, a drawdown restriction of 2 m was put into place for GWA15. The positions of GWA4, GWA5 and GWA15 can be seen below in Figure 99.

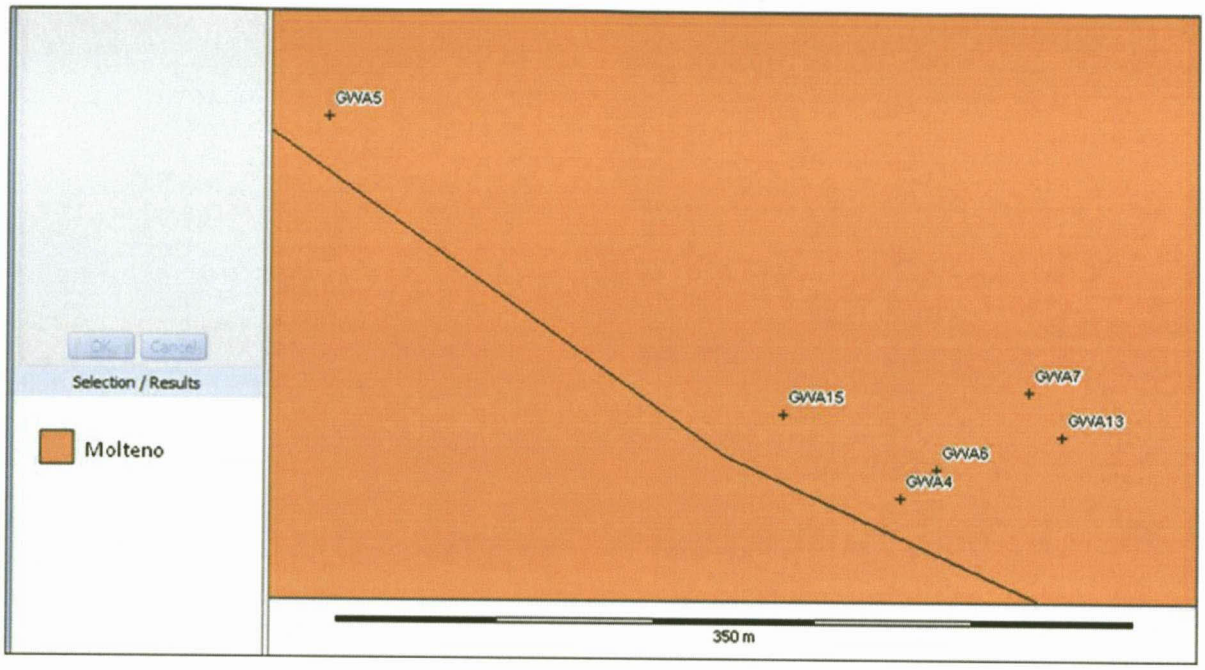

Figure 99. Positions of the newly drilled boreholes in the Matatiele basin.

With the transmissivity value of 60 m^2/d applied to GWA9 from existing transmissivity data (boreholes MT1 and MLB1, because it is close to MLB1), an abstraction rate of 1 L/s from GWA9 causes drawdown in nearby boreholes, including GWA4. Thus in order to abstract a productive volume of water annually from GWA4 and GWA5, no abstraction should be implemented in GWA9 when a drawdown limitation due to the wetland exists.

Due to the very high transmissivity of the area surrounding GWA4 and an only slightly lower transmissivity value of GWA5, the cones of depression caused by abstraction in both boreholes is very wide reaching, having a significant effect on the drawdown occurring in GWA15. Various scenarios of pump rates were therefore tested in order to determine the most optimum setup.

- Pumping both GWA4 and GWA5 at 3 L/s, abstraction = 6 L/s
- Pumping only GWA4, abstraction = 8 L/s (causing 1.7 m drawdown in GWA5)
- Pumping only GWA5, abstraction = 5 L/s (causing 1.8 m drawdown in GWA4)

Therefore, although GWA4 is significantly closer to the GWA15 (see Figure 99 above), the higher transmissivity does allow for a greater rate of abstraction (8 L/s) when compared to GWA5 (5 L/s). The total abstraction in this wellfield is the sum of GWA4, BhMT1 and BhMLB1, which is approximately 17.5L/s (this value will be used in the lower estimation of the Wellfield yield, see Table 52 below). Thus when assigning abstraction rates to these boreholes two things should be considered, firstly, it appears more productive to abstract from only one borehole to obtain the highest rate of abstraction in this scenario, and secondly the highest abstraction rates should be applied to the boreholes in the highest transmissivity zones. Although the high transmissivity values suggest a potentially high rate of abstraction, the rates of abstraction are limited due to the close proximity of boreholes and subsequent well interference.

7.4.11 Borehole Yield Assessment

If the yields of all boreholes are assessed on an individual basis, that is, if it is assumed that there is no interference between boreholes as is predicted by the wellfield model, then the total yield from all boreholes range from 8 – 53 L/s assuming a T-value range of 60 – 440 m^2/day and an available drawdown of 20 m (Table 51).

Table 51: Total yield of individual boreholes.

Parameter	Value
T value (m^2/d)	60 – 440
Available s range (m)	20
Minimum Total Q (L/s)	8
Maximum Total Q (L/s)	53
Mean Q (L/s)	31

7.4.12 Comparison of all Yields

Table 52 below shows all yields determined from the databases HP and GRAII, the models AAYM and Wellfield Model, and the total borehole yield.

Table 52: Comparison of aquifer, wellfield and individual borehole yield.

	Range definition	Lower Range (L/s)		Upper Range (L/s)
Aquifer Yield				
HP		153.4		
AGEP	Lower = Drought, Higher = Normal	153.9		204.6
AAYM Assured Yield (Ver. 1.0.77)	Lower = 10 mm Threshold, Higher = 0 mm Threshold	129.4		203.6
Wellfield Yield				
Only for wellfield 3 (multiplied by 4 for all wellfields)	Lower = middle T-map values, Higher = upper T-map values	17.5 (70)		55.5 (222)
Individual Borehole Yield				
Total Borehole Yield for wellfield 3 (multiplied by 4 for all wellfields)	Lower = mean of the min range, Upper = mean of the max range	8 (32)	31 (124)	53 (212)

- AAYM version 1.0.77 yield values that are very similar to the GRAII AGEP values. Both upper ranges are almost exactly the same. The HP value is very similar to the AGEP drought value.
- The wellfield values provided are firstly the values only for wellfield 3. These values are low in comparison to the assured yield and AGEP values. The values were then multiplied by 4 (seen in the brackets) as there are four delineated wellfields. The upper value (222 L/s), although high, still lies only slightly higher than GRAII and AAYM lower estimations and falls below the upper AAYM yield.
- The Borehole yields were also multiplied by 4 to represent the four delineated wellfields. The maximum value of the borehole yields reaches a value of 212 L/s, which is very close to the upper wellfield approximation (where the wetland was not considered), and slightly higher than GRAII and AAYM lower yields.
- From the case study provided above, it seems that the Transmissivity Map was useful in identifying the dyke 3 by displaying this structure as a high transmissivity zone (Figure 97). It

was not successful, however, in identifying dykes 1 and 2. Aeromagnetic data was fortunately available in this area and this data was successful in identifying structures of interest, which were determined to be dolerite dykes.

7.5 Discussion and Conclusion

The aim of the case studies is to assess the new tools being developed for groundwater resource planning. These tools include the AAYM, the wellfield model and an approach to identifying potential wellfield areas using merged geological maps, Transmissivity Maps and Google Earth imagery. Both case studies assessed with all tools are near Matatiele in the Eastern Cape Province. Thus far, the AAYM version 1.0.77 appears to provide reasonable and at times somewhat conservative estimates of an aquifer's potential yield. The theoretical transmissivity and available drawdown values (from the Transmissivity Maps and Table 15) for borehole yield estimates are reasonable in both areas. In addition, it appears the Wellfield Model produces adequate values in the Matatiele area, but somewhat conservative values in comparison with the assured yield estimates in Makhoba. Using theoretical parameter values (from the Transmissivity map and calculations of the available drawdown from the weathered zone) provide values that are consistent with the existing data. The case studies did show that the newly produced geological maps and the Transmissivity Map can be easily used with Google Earth to identify new potential borehole and wellfield areas.

Chapter 8

8 Conclusion

The aims of this thesis include:

1. Identify and delineate areas in the Main Karoo Basin with high groundwater yield and development potential

2. Provide relevant groundwater resource information and integrate it into existing water resource planning frameworks.

The project achieved the following objectives:

- Produced a Transmissivity Map for the Main Karoo Basin to aid in the identification of groundwater development areas
- Described the process by which tools such as the geological GIS coverages and the Transmissivity Maps are to be used in the identification of these areas
- Tested the credibility of the newly developed models Aquifer Assured Yield Model (AAYM) and Wellfield Model
- Developed and recommended a process for the identification of high groundwater potential areas, and the quantification of groundwater in these areas
- Provided case studies demonstrating the functionality of existing and newly developed tools and models

From this thesis, a guideline has been developed which included the process of identifying and delineating areas in the Main Karoo Basin with potential for high groundwater yields. In addition, relevant groundwater resource potential information was produced as well as an approach to integrate this into existing water resource planning frameworks. The high groundwater potential areas were identified based upon spatial variability of geology, aquifer transmissivity, and assured aquifer yield which are favourable for groundwater development. Throughout this thesis the tools and models implemented in this process have been described, tested and their credibility assessed.

There are a number of major outcomes of this thesis, which include: development of a Transmissivity Map of the Main Karoo Basin, critically reviewing the Aquifer Assured Yield Model (AAYM) and Wellfield Model, and providing guidelines for optimum wellfield design. Finally, the methodology incorporating the tools developed and/or assessed in this thesis was produced by which areas of high groundwater potential can be identified, and the volume of groundwater quantified for water planning purposes.

In order to use/apply the Transmissivity map in the correct manner, the process by which it was developed must be properly understood. The approach took both existing borehole yields and geology into account, and provides a range of possible transmissivity values presented both in tables and maps. The ranges are provided for each hydrogeological domain (based on lithologies and in some cases, sub-divided lithologies), dolerite dykes and sills, fractured margins of sills and areas of thick alluvium. Woodford's method was used whereby numerous pump test data was analysed taking the relationship between borehole yield and transmissivity into account (with the use of the Cooper-Jacob equation), and various equations were applied to the lithological domains (Dondo *et al.,* 2010). This method was then extrapolated across the Main Karoo Basin. The Transmissivity Map developed in this thesis is the most detailed map produced of the Main Karoo Basin and from the case studies presented appears to provide a reasonable estimate of transmissivity values. The map does, however, require improvements which would entail interpreting hundreds to thousands of pump test data and developing new relationships between yield and transmissivity for the various structures and lithologies in the Karoo Basin.

The AAYM was run for a large number of quaternary catchments spread across the Karoo Basin to test the model's credibility, as well as to propose parameter values to be used per region or drainage basin. The AAYM compared well with other databases, namely the HP and GRAII AGEP. There is no apparent relationship between MAP and parameter input/output values for quaternary catchments as each catchment is different and therefore must be treated individually. The work presented is pioneering (in that it appears to be the first documented approach to quantifying groundwater with levels of assurance), and thus should be considered "work-in-progress", as is it requires an iterative process of development, testing, modifying and re-testing. Furthermore, additional testing is still needed in order to expand on the findings presented in this thesis.

The Wellfield Model was successfully developed on the basis of the Cooper-Jacob equation (Cooper & Jacob, 1946). Through the testing of the model, relationships of borehole spacing with transmissivity values were investigated in an attempt to provide a guideline on the design of a wellfield with certain borehole interference limitations. In addition to this, the distinct nature of groundwater flow in dykes was considered by referring to the Boonstra-Boehmer equation (Kruseman & de Ridder, 1992) whereby a certain increase in borehole spacing is required when a borehole is sited on a dyke. This model enables the designing and manipulation of a wellfield and the effect of groundwater abstraction on drawdown can be evaluated thereby aiding in the most optimum design.

The methodology applied to case studies demonstrates the practical application of these tools (Geological and Transmissivity maps) and models (AAYM and Wellfield Model) described above. The purpose of the case studies was to apply the groundwater yield assessment methods in areas with known aquifer parameters and yields. The yield assessment methods were evaluated in terms of their accuracy and practicality by comparing the results with other existing yield assessment tools and with field data. The case studies showed that the newly produced geological maps and the Transmissivity Map can be easily used with satellite imagery to identify new potential borehole and wellfield areas. Both the AAYM and Wellfield Model appear to provide reasonable and occasionally somewhat conservative estimates of an aquifer's potential yield compared to previous approaches such as GRAII and the Harvest Potential. The application of this method in project planning seems suitable for estimating the groundwater potential of an area and in siting boreholes in the area.

Overall, this thesis provides a step by step methodology to identify and delineate high groundwater potential areas in the Main Karoo Basin, and quantify the groundwater that is available in these areas. In order for groundwater resources to be accurately quantified, it must be presented with levels of assurance of supply and from these volumes, a wellfield can be developed whereby guidelines should be followed to obtain an optimum design in order to avoid over abstraction. Recommendations have been provided regarding further work and expansion to be undertaken in each of these tools and models.

9 References

- Alley, W.M., Reilly, T.E. & Franke, O.L. (1999). Sustainability of ground-water resources, U.S Geological Survey, Denver, Colorado.
- Baker, K.V. & Murray, E.C. (2009). Deliverable 14. Progress Report No. 2. The identification and delineation of high-yielding well-field areas in Karoo aquifers as future water supply options to local authorities. WRC Report No. K5/1763, Pretoria, South Africa.
- Baker, K.V. & Murray, E.C. (2010). Deliverable 21. Case studies: Identify and quantify favourable groundwater development zones. The delineation of high-yielding wellfield areas in Karoo Aquifers as future water supply options to local authorities. WRC Report No. K5/1763, Pretoria, South Africa.
- Balleau, W.P. (1988). Water appropriation and transfer in a general hydrogeologic system, Natural Resources Journal, Volume 28, No. 2, pp. 269 – 291.
- Baron, J., Seward, P. & Seymour, A. (1998). The groundwater harvest potential map of the Republic of South Africa. Technical Report Gh 3917. Directorate Geohydrology, Department of Water Affairs and Forestry, Pretoria.
- Bean, J.A. (2003). A critical review of recharge estimation methods used in southern Africa. PhD (unpubl.) Faculty of Natural and Agricultural Sciences , Department of Geohydrology, University of the Free State, Bloemfontein, South Africa.
- Cole, D. (2005). Prince Albert Formation. Catalogue of South African lithostratigraphic units. Volume 8. Council for Geoscience. Edt: M.R. Johnson.4 pp.
- Conrad, J. (2005). Preparation and production of a series of GIS-based maps to identify areas where groundwater contributes to baseflow. Report No. G2005/02-1, GEOSS, Stellenbosch, South Africa.
- Cooper, H.H. & Jacob, G.E. (1946). A generalized graphical method for evaluating formation constants and summarising well field history. Am. Geophys. Union Trans., 27, pp. 526 - 934.
- Dennis, S.R. (2011). Deliverable 16: Aquifer Assured Yield Model, Version 2. The identification and delineation of high-yielding well-field areas in Karoo aquifers as future water supply options to local authorities. WRC Report No. K5/1763, Pretoria, South Africa.

- Department of Water Affairs and Forestry (2006). Groundwater Resource Assessment II – Groundwater Planning Potential, Technical Report 2C, Project No. 2003-150, DWAF, Pretoria.
- Department of Water Affairs (2010). Groundwater Resource Determination Method (GRDM), Version 4.
- Dondo, C., Chevallier, L., Woodford, A.C., Murray, E.C., Nhleko, L.O., Nomnganga, A. & Gqiba, D. (2010). Flow conceptualisation, recharge and storativity determination in Karoo aquifers, with special emphasis on Mzimvubu – Keiskamma and Mvoti-Umzimkulu water management areas in the Eastern Cape and Kwazulu-Natal Provinces of South Africa. WRC Report No. 1565/1/10, Pretoria, South Africa.
- Enslin, J.P. (1970). Die grondwaterpotensiaal van Suid-Afrika. Convention: Water for the Future, November 1970.
- Freeze, R.A. & Cherry, J.A. (1979). Groundwater, Prentice Hall, Inc., United States of America.
- Heath, R.C. (2004). Basic ground-water hydrology, U.S. Geological Survey Water-Supply Paper 2220, Denver.
- Hughes, D., Parsons, R. & Conrad, J. (2007). Quantification of the groundwater contribution to baseflow. WRC Report No. 1498/1/07, Pretoria, South Africa.
- Johnson, E.E. (1975). Ground water and wells, 4th ed. Johnson Division, UOP Inc., Minnesota.
- Johnson, M.R., Van Vuuren, C.J., Visser, J.N.J., Cole, D.I., Wickens, H. de V., Christie, A.D.M., Roberts, D.L., and Brandl, G., (1997). The foreland Karoo Basin, South Africa. In: R.C. Selley (Ed.), African Basins. Sedimentary Basins of the World, 3. Elsevier, Amsterdam.
- Johnson, M.R., van Vuuren, C.J., Visser, J.N.J., Cole, D.I., Wickens, H. de V., Christie, A.D.M., Roberts, D.L. & Brandl, G. (2006). The geology of South Africa. Geological Society of South Africa, Johannesburg/Council for Geoscience, Pretoria, 461-501.
- Kirchner, J. and Van Tonder, G.J. (1995). Proposed guidelines for the execution, evaluation and interpretation of pump tests in fractured-rock formations. Water SA, 21 (3), pp. 87-200.
- Kirchner, J., Van Tonder, G.J. and Lukas, E. (1991). Exploitation potential of Karoo Aquifers. WRC Report No. 170/1/91. Pretoria, South Africa.

- Kruseman, G.P. & de Ridder, N.A. (1992). Analysis and evaluation of pumping test data, International Institute for Land Reclamation and Improvement, The Netherlands.
- Meinzer, O.E. (1920). Quantative methods of estimating groundwater supplies: Bulletin of the Geological Survey Water Supply Paper 494.
- Midgley, D. C., Pitman, W. V. & Middleton, B. J. (1994). Surface water resources of South Africa 1990, vols I–VI. WRC Reports no's 298/1.1/94–298/6.1/94, Pretoria, South Africa.
- Murray, E.C. (1996). Guidelines for assessing single borehole yields in secondary aquifers, unpubl. Msc. Thesis, Rhodes University, Grahamstown.
- Murray, E.C. (2004). Makhoba groundwater exploration and resource assessment, unpubl. Report, Groundwater Africa, Somerset West.
- Murray, E.C. (2004/2005). Outspan/Hebron groundwater exploration and resource assessment PHASE 1 and PHASE 2, unpubl. Report, Groundwater Africa, Somerset West.
- Murray, E.C. (2008). Tasks 2Gii, 2Ji and 2Jiii, Dykes report. Groundwater characteristics of major dolerite dykes of the eastern Karoo Basin. WRC Report No. K5/1565, Pretoria, South Africa.
- Murray, E.C., Woodford, A., Ravenscroft, P., Chevalier, L. & Behrmann, D. (2008). Deliverable 1: Inception Report. The delineation of high-yielding well-field areas in Karoo aquifers as future water supply options to local authorities. WRC Report No. K5/1763, Pretoria, South Africa.
- Odling, N.E. (1993). An investigation into the permeability of a 2D natural fracture pattern. In: Proceedings of the hydrogeology of hard rocks. Memoirs of the XXIVth Congress of the IAH. S. B. & D. Banks (eds.) (Oslo), Norway. Vol 1 International Association of Hydrogeologists.
- Rosewarne, P.N. (2008). Aquifer transmissivity, document prepared as part of the Water Resources of South Africa 2005 Study (WR2005). WRC Report No. K5/1491. Pretoria, South Africa.
- Rowsell, D.M. & de Swardt, A.M.J., (1976). Diagenesis in Cape and Karoo sediments, South Africa and its bearing on their hydrocarbon potential. Trans. geol. Soc. S. Afr., pp. 81-145.

- Sami, K. & Murray, E.C. (1998). Guidelines for the evaluation of water resources for rural development with an emphasis on groundwater. WRC Report No. 677/1/98, Pretoria, South Africa.

- Schultze, R.E. (1997). South African agrohydrology and climatology, WRC Report No. TT82/96, Pretoria, South Africa.

- Schutte, L.C. (1993). Die geologie van gebied Kronstaad. Explanation of sheet 2726 at 1 : 250 000. Geological Survey.

- Sophocleous, M. (1998). On the elusive concept of safe yield and the response of interconnected stream-aquifer systems to development, Kansas Geological Survey, Bulletin 239, Kansas.

- Theis, C.V. (1935). The relationship between the lowering of the piezometric surface and the rate and duration of discharge of a well using groundwater storage. Am. Geophys. Union Trans., 16, pp 519-524.

- Van Tonder, G.J., Kunstmann, H. & Xu, Y. (1998). Estimation of the sustainable yield of a borehole including drawdown derivatives, boundary information and error propogation. IGS Report, UFS, Bloemfontein.

- Van Tonder, G.J., Kunstmann, H. & Xu, Y. (2001). FC-Program Version 3.0, programming by Jin-hui Zhang, IGS, UFS, Bloemfontein.

- Van Vuuren, C.J. & Cole, D.I. (1979). The stratigraphy and depositional environments of the Ecca Group in the northern parts of the Karoo basin. In: Anderson A.M. and Van Biljon, W.J. (Eds.). Some sedimentary basins and associated ore deposits of South Africa. Special Publication Geological Society of South Africa, Vol.6, pp.103-111.

- Veevers, J.J., Cole, D.I. and Cowan, E.J. (1994). Southern Africa: Karoo Basin and Cape Fold Belt. In: Veevers, J.J. & Powell, C. McA. (Eds.), Permian-Triassic Pangean Basins and Foldbelts Along the Panthalassan Margin of Gondwanaland. Mem. Geol. Soc. Am., 184, 223–279.

- Vegter, J.R. (1995). Groundwater Resources of South Africa: An explanation of a set of national groundwater maps. WRC Report No. TT 74/95, Pretoria, South Africa.

- Viljoen, J.H.A (2004). Piroklastiese afsettings van perm-ouderdom in die hoof-Karoomkom met special verwysing na die collingham formatsie, Ecca groep. Memorie No 94. Council for Geoscience, 145pp.

- Viljoen, J.H.A. (2005). Tierberg Formation. Catalogue of South African Lithostratigraphic Units. Volume 8. Council for Geoscience. Edt: M.R. Johnson.4 pp.
- Visser, J.N.J., von Brunn, V. & Johnson, M.R. (1990). Dwyka Group. Catalogue of South African Lithostratigraphic Units. Volume 2. Council for Geoscience. Edt: M.R. Johnson.3 pp.
- Vivier, J.J.P. (1996). The influence of geology on the geohydrology of Karoo aquifers. Master of Science. 1-81.
- Witthueser, K.T. (2006). Geohydrological software development for decision support: Phase 1. Activity 28: Surface-groundwater interaction methodologies literature study. Institute for Groundwater Studies, Bloemfontein.
- Woodford, A.C. (1988). The exploration and evaluation of groundwater units in the Van Rynevelds Pass Dam basin, north of Graaff-Reinet Cape Province, unpubl. Msc. Thesis, Rhodes University.
- Woodford, A.C., Ravenscroft, P. & Murray, R. (2008). Deliverable 4, Task 4a: Proposed methodology for quantifying the assured yield of Karoo fractured-rock aquifers. The identification and delineation of high-yielding well-field areas in Karoo aquifers as future water supply options to local authorities. WRC Report No. K5/1763, Pretoria, South Africa.
- Woodford, A.C. (2010). Deliverable 4, Task 4f: Description of the Assured Aquifer Yield Model. The identification and delineation of high-yielding well-field areas in Karoo aquifers as future water supply options to local authorities. WRC Report No. K5/1763, Pretoria, South Africa.